Altered growth-mediated signaling in the hearts of NFATc2 null mice

Patrick Sin-Chan

A Thesis

in

The Department

of

Chemistry and Biochemistry

Presented in Partial Fulfillment of the Requirements

for the Degree of Master of Science (Chemistry) at

Concordia University

Montreal, Quebec, Canada

November 2010

CONCORDIA UNIVERSITY

School of Graduate Studies

This is to certify that the thesis prepared

By: Patrick Sin-Chan

Entitled: Altered growth-mediated signaling in the hearts of NFATc2 null mice

and submitted in partial fulfillment of the requirements for the degree of

Master of Science (Chemistry)

complies with the regulations of the University and meets the accepted standards with respect to originality and quality.

Signed by the final examining committee:

Dr. Christine Dewolf Chair

Dr. Paul Joyce Examiner

Dr. Joanne Turnbull Examiner

Dr. Robin Michel Supervisor

Approved by

Chair of Department or Graduate Program Director

December 13th, 2010

Dean of Faculty

Altered growth-mediated signaling in the hearts of NFATc2 null mice

Patrick Sin-Chan

An abnormality associated with all forms of cardiovascular diseases is cardiac hypertrophy, which is an overall increase in heart mass without improved contractile function. Prolonged cardiac hypertrophy eventually leads to heart failure, in which the heart can no longer supply adequate amounts of blood to meet the body's hemodynamic demands, resulting in cardiac dilatation, thinning of the myocardial walls, decrease in contractile effectiveness, organ failure and death.

The Ca^{2+}- dependent phosphatase, calcineurin (Cn) and its downstream target, nuclear factor of activated T-cells (NFAT), are major intracellular modulators of cardiac hypertrophy. In young 1-2 month old mice, the NFATc2 transcription factor has been identified as the major NFAT isoform responsible for Cn-mediated cardiac hypertrophy. We observed that adult 6-9 month old NFATc2-/- mice were more prone to sudden death, suggesting that the loss of NFATc2 was detrimental at later stages of life. Using histology, we showed that adult NFATc2-/- mice display left ventricular dilatation and thinning of the ventricular walls, characteristic of failure. Western blot and immunofluorescene results showed that NFATc2-/- mice displayed alterations in the signaling of growth pathways, which predisposed these mice to heart failure. Furthermore, angiotensin II-induced cardiac growth revealed that the hearts of NFATc2-/- mice displayed changes in contractile protein gene expression and an inactivation of both transcriptional and translational mechanisms. Our collective findings propose an uncharacterized role of NFATc2 for normal heart function and biochemical signaling in adult mice, providing further evidence that normal Cn-signaling is crucial in the heart.

Acknowledgements

There are many individuals I would like to acknowledge for helping me during my studies at Concordia University.

First and foremost, I would like to thank my family and friends for everything they've done for me, their encouragement and support. Thanks to Dr. Robin Michel for providing me the opportunity to pursue research in his laboratory, his help with angiotensin II-infusions and allowing me to present our work at conferences and meetings. To my lab mates, most notably Ewa Kulig, Mohammad Al Khalaf, Mathieu St-Louis, Manal Al Zein, Michal Solecki and Sarah Slater, I thank all of you for your help, understanding, friendship, and for keeping me grounded. I am grateful to have met you all and wish you the best of luck and success in whichever paths you choose to pursue. To my thesis committee members, Dr. Paul Joyce and Dr. Joanne Turnbull, and the graduate program director, Dr. Heidi Muchall, for their advice and support throughout my time as a graduate student in the Chemistry and Biochemistry department. In addition, I would like to acknowledge Dr. Andreas Bergdahl for teaching me gelatin infusions in the heart and Aileen Murray for her help with the animals.

Table of Contents

List of Figures

List of tables

List of Abbreviations

Ang II: Angiotensin II

ANP: Atrial Natriuretic Peptide

BNP: Brain Natriuretic Peptide

CaM: Calmodulin

CK: Casein Kinase

Cn: Calcineurin

DAPI: 4',6-diamidino-2-phenylindole

eIF2α: Eukaryotic Initiation Factor 2α

ERK: Extracellular-Regulated-Signal Kinases

GAPDH: Glyceraldehyde-3-Phosphate Dehydrogenase

GSK3-β: Glycogen Synthase Kinase 3-β

HW/BW ratio: Heart weight-to-body weight ratio

JNK: Janus N-Terminal Kinase

MyHC: Myosin Heavy Chain

NFAT: Nuclear Factor of Activated T-cells

Chapter 1: Literature Review

The structure of cardiac muscle cells

The capacity for cells to utilize biochemical energy to generate both mechanical force and movement of the human body is a dominant feature found in muscles. There exist three distinct categories of muscle tissue, each differing by specific structural and functional properties. These categories include smooth muscle, skeletal muscle and cardiac muscle. Smooth muscles are involuntarily contracting, non-striated muscles that surround the inside walls of hollow organs such as the urinary bladder, reproductive organs, and both the gastrointestinal and respiratory tracts. Its contraction enables and regulates the progression of liquid content, such as food, urine and blood, along the internal passageways (1). Skeletal muscles are voluntarily contracting, striated muscles that attach to bones of the skeleton. The contractions of skeletal muscles are primarily responsible for the movement of the skeleton, but also have roles in heat production and protection of internal organs (1). Cardiac muscles are an involuntarily contracting, striated muscle found exclusively in the walls of the heart, more specifically in the myocardium. Contractions of cardiac muscles propel oxygenated blood into the circulatory system to deliver oxygen and nutrients to the body and also regulate blood pressure (1).

Cardiac muscle tissue is composed of a network of individual cardiac muscle cells, called cardiomyocytes. Cardiomyocytes are small in size, averaging 10-20 μm in diameter and 50-100 μm in length, have a single centrally positioned nucleus and connect

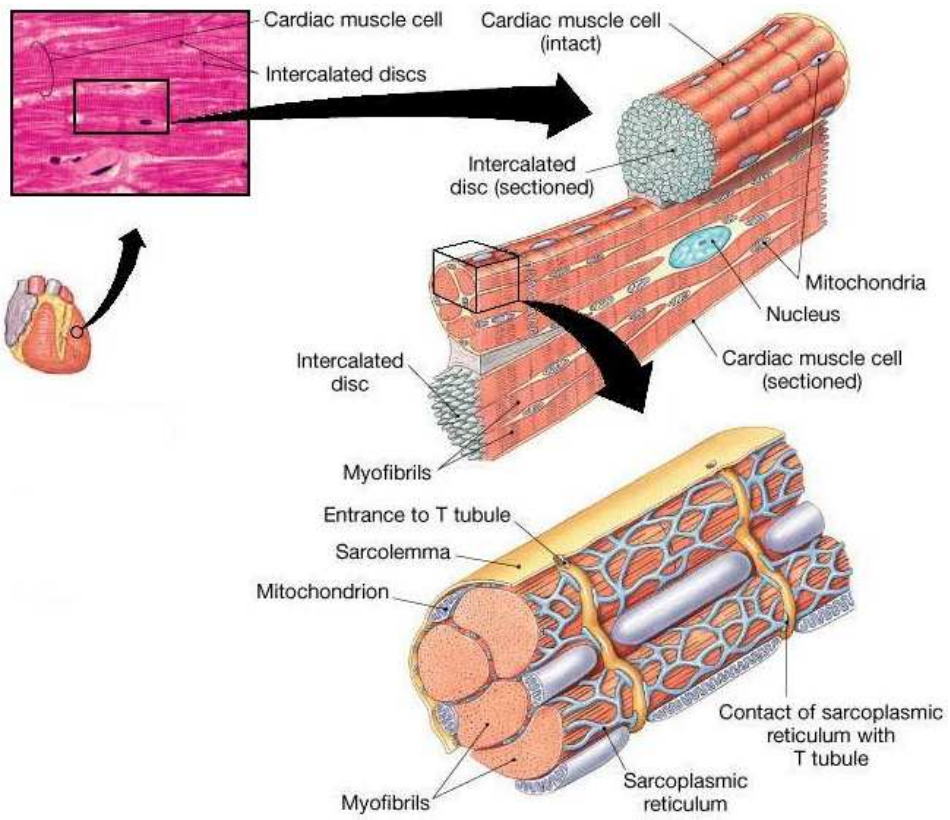

Figure 1.1: A schematic representation of the structure of cardiomyocytes. Adapted from Martini, F. et al. (2009) (1).

to adjacent cells in a branched manner through specialized sites known as intercalated discs (1). Two structures that are found within the intercalated discs are desmosomes and gap junctions. Desmosomes are specialized structures involved in cell-to-cell adhesion and gap junctions are intercellular channels that connect the cytoplasms of adjacent cells, allowing the free passage of molecules, ions and electrical signals.

Within the cytoplasm of striated muscle cells are long, cylindrical organelles termed myofibrils [Figure 1.1]. With a diameter of 1 to 2 μm and numbering between hundreds to thousands in a cell, myofibrils are enveloped and grouped together by connective tissue called the fasciculus, which forms bundles of myofibrils that span the

length of the cell (2). Individual myofibrils can be further divided into two types of contractile filaments: thin filaments and thick filaments [Figure 1.2]. These filaments are composed primarily of actin and myosin proteins. The thin and thick filaments are aligned in a manner where they form repeating structural units along the myofibril. Among these structures is the sarcomere, which is a Ca^{2+}-dependent contractile unit responsible for muscle contraction and relaxation (2). An increase in cytoplasmic Ca^{2+} influx causes the thin and thick filaments to overlap each other, causing a shortening of the sarcomere, leading to a muscle contraction. Alternatively, a decrease in cytoplasmic Ca^{2+} levels causes the thin and thick filaments to pull away from each other, triggering muscle relaxation. The specific arrangement of the thin and thick myofilaments is responsible for the striated appearance of both skeletal and cardiac muscle tissue.

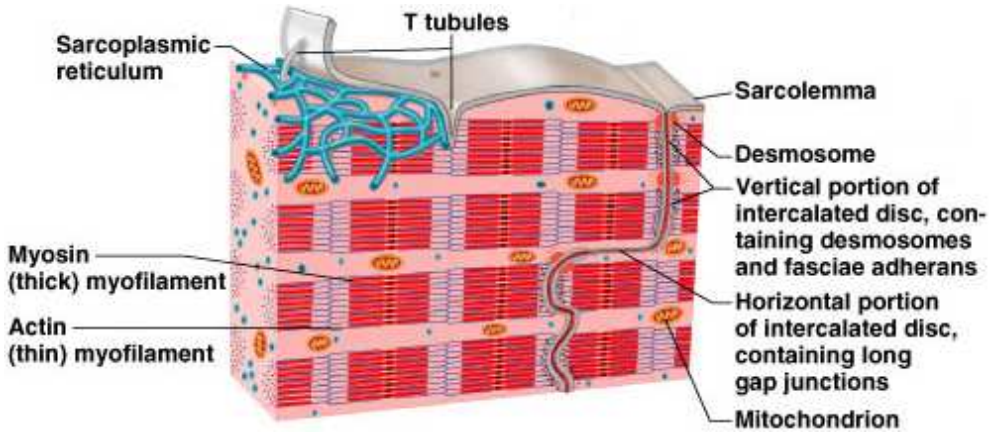

Figure 1.2: A detailed view of the muscle cell myofibrils. Taken from Marieb, E. et al. (2007) (3).

Electrical stimuli, called action potentials, are required for striated muscle cell contraction. In skeletal muscles, action potentials are derived from neurons in the brain and spinal cord that transmit the signal through the nervous system and innervate muscle fibers, causing contraction. However, unlike skeletal muscles, the contraction of cardiac

muscles occurs without neural stimulation, a property called automaticity (1). This is because the heart contains pacemaker cells, which are specialized cells that have no contractile function; rather having the ability to initiate and conduct action potentials to neighboring cardiomyocytes. Cells which have pacemaker activity constitute 1% of cardiac muscle cells, whereas the other 99% are contractile cells (4). The cardiac action potential propagates across cardiomyocytes through gap junctions, allowing the cells to contract in tandem, which enables the heart to contract as one muscle.

The conversion of an electrical stimulus into a mechanical response is performed through a physiological process known as excitation-contracting coupling (ECC). This phenomenon has a critical role in muscle cells as it allows a propagating action potential to cause shortening of the sarcomere, leading to muscle cell contraction. When action potentials are produced by pacemaker cells, they conduct across the heart by traveling along the length of the myofibril on the muscle sarcolemma. An action potential will transmit on the sarcolemma until it reaches a transverse-tubule (T-tubule). T-tubules are deep invaginations of the sarcolemma that contact the cisternae of the sarcoplasmic reticulum (SR), an organelle that functions as a Ca^{2+} storing body. Resting within the T-tubules are many ion transporters such as voltage-gated L-type Ca^{2+} channels and Na^{+}/Ca^{2+} exchangers (5). Upon penetrating the T-tubules, the action potential will open and activate these Ca^{2+}-transporters, prompting the entry of extracellular Ca^{2+} into specific microdomains in the cytosol and cause a net depolarization of the membrane voltage potential (6). An elevation of cytoplasmic Ca^{2+} levels will trigger the opening of ryanodine receptors (RyR), which are intracellular Ca^{2+} channels present on the membrane of the SR, allowing stored Ca^{2+} to exit the SR and enter the cytosol. The

mechanism of how Ca^{2+} ions trigger Ca^{2+} release from the SR was identified by several groups in the 1960s, and appropriately termed 'Ca^{2+}-induced- Ca^{2+}-release' (7,8).

An overall increase in intracellular Ca^{2+} levels causes Ca^{2+} to bind and induce a conformational change in Troponin C, a protein present on actin filaments. This conformational change causes a displacement of Tropomyosin, which prevents the interaction of myosin protein with actin filaments, thereby allowing myosin to contact actin, promoting contraction of the sarcomere. Alternatively, Ca^{2+} sequestration from myofilaments and cytoplasmic depletion prompts a relaxation of the sarcomere. Ca^{2+} depletion from the cytoplasm occurs either by re-entering the lumen of organelles, such as the SR and mitochondria, or cellular export by Ca^{2+} pumps and Na^{+}/Ca^{2+} exchangers on the sarcolemma (5). An overview of the ECC process is summarized below [Figure 1.3].

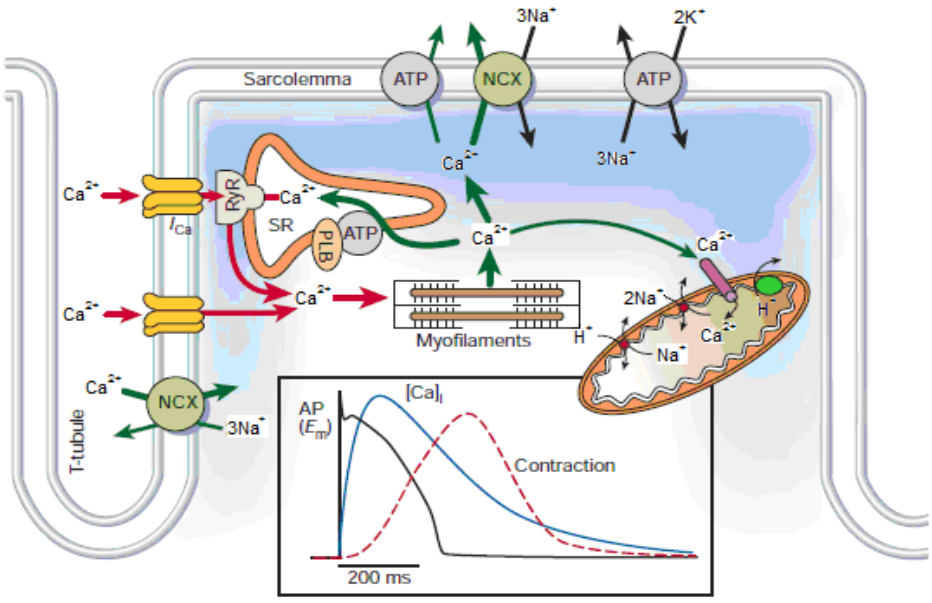

Figure 1.3: Overview of muscle cell excitation-contraction coupling process. Adapted from Bers, D. (2002) (5).

The efficiency of muscle contraction is partly depicted by the type of myosin heavy chain (MyHC) that the cell expresses. MyHC are enzymes, found on the head of myosin proteins, which catalyze the hydrolysis of ATP. The rate at which MyHC can hydrolyze ATP ultimately defines the speed at which the myofilaments contract, as well as the overall energy efficiency of the cell. In cardiomyocytes, two types of MyHC proteins are expressed: α-MyHC and β-MyHC. Table 1.1 represents the distinguishing features of the cells that express either α-MyHC or β-MyHC:

***Table 1.1*:** Characterization of cardiac myosin heavy chains in rodents. Taken from Sieck, G. et al. (2001) (9).

	Located in	**ATP source**	**ATPase activity**	**Contraction velocity**	**Rate of fatigue**
α-MyHC	Adult hearts	Glycolysis	Fast	Fast	Fast
β-MyHC	Fetal hearts	Oxidative phosphorylation	Slow	Slow	Slow

Similar to skeletal muscles, cardiomyocytes are categorized into two distinct classes, based on the type of MyHC that is predominantly expressed. The two categories are the glycolytic, less energy efficient cells and the oxidative, more energy efficient cells. Cardiomyocytes that mainly express α-MyHC are found in adult hearts, contract in a more energy inefficient manner and are quicker to fatigue. In contrast, cardiomyocytes that express more β-MyHC are present in fetal and developing hearts, have a more energy efficient contraction and are more resistant to fatigue. Although hearts expressing mainly α-MyHC are have a higher rate of contraction, those expressing mainly β-MyHC contract in a more energy efficient manner (10-12). The contractile velocity of the human heart is faster at birth than in adulthood, whereas the opposite is true for rodents. This is because

the primary MyHC isoform expressed in human hearts is β-MyHC (>95%), whereas in rodent hearts is α-MyHC (>90%) (10). Moreover, β-MyHC is reactivated in pathophysiological cardiac growth, associated with the majority of cardiovascular diseases, in which adult hearts hypertrophies to a pathological state, leading to contractile defects, heart failure and death (13).

Heart failure and pathological cardiac hypertrophy

Cardiovascular diseases are disorders that prevent the proper functioning of the heart and blood vessels, causing abnormalities of the cardiovascular system, which lead to defects in the brain, kidneys, lungs and other parts of the body (14). According to the World Health Organization, cardiovascular diseases accounted for 29% of global deaths in 2004, making it one of the leading causes of death in the world (15). Furthermore, with an aging population, the number of patients diagnosed with heart disease in America is expected to double within the next 30 years, from 5 million to 10 million (16). In Canada, this disease was responsible for 31% of total deaths in 2005 (17).

An abnormality associated with all forms of cardiovascular diseases is the pathological enlargement of the left ventricle of the heart, a characteristic associated with a disease known as cardiac hypertrophy. Cardiac hypertrophy is induced by the release of hormones, cytokines, chemokines and peptide growth factors, which act on cardiomyocytes in an endocrine, paracrine and autocrine manner (18). The release of

these factors occurs in response to increased cardiac workload, myocardial injury or defects in the contractility of cardiomyocytes (19).

The initial events resulting in cardiac hypertrophy are an increased size and cell volume of cardiomyocytes, which are required to sustain the increased cardiac workload demanded by the hypertrophied heart through a process known as compensatory hypertrophy. As the disease progresses, the hypertrophied heart can no longer uphold the increased strain required to meet the body's hemodynamic demands and is subjected to pathophysiological remodeling such as dilatation of the left ventricular inner chamber, thinning of the heart walls, and an overall decrease in heart contractility and function, resulting to heart failure, cardiac arrhythmias and sudden death (20).

The detrimental consequences on cardiomyocytes as a result of pathological cardiac hypertrophy are not present during physiological heart growth, which occurs during pregnancy, childhood development, and aerobic training (21). A characteristic of pathologically hypertrophied hearts is cellular disarray, which is a disorganization of the proper alignment of cardiomyocytes. Misaligned cardiomyocytes disrupt the conduction of action potentials across cells, leading to compromised intracellular Ca^{2+} kinetics and decreased shortening of the muscle sarcomere, which compromises the contractitility and functionality of the heart.

A common end stage following cardiac hypertrophy is heart failure, which is defined as defects in "cardiomyocyte structure, function, rhythm or conduction" that prevents the heart from providing the necessary cardiac output required by the body (22). Individuals living with heart failure suffer from severe coughing, shortness of breath,

peripheral edema, and chronic venous congestions, all causing decreased exercise tolerance, physical and mental health. The most common cause of heart failure is ventricular dysfunction, caused by myocardial infarction and hypertension or both. In addition, valve diseases, dilated cardiomyopathies and alcoholic cardiomyopathies are inducers of heart failure (22). As heart failure progresses, the heart and the left ventricle undergo remodeling, resulting in apoptosis or damage to existing cardiomyocytes. Molecular, structural and functional changes in the heart due to failure are responsible for disrupting action potential conduction, contractile defects, and are detrimental to the function of the lungs, blood vessels, kidneys, muscles, liver and other vital organs (22,23).

In the Western world, cases of heart failure are on the rise. They are the fastest spreading with highest mortality rate, and leading cause of hospitalization in the elderly over the past decade (18). According to epidemiological studies, between 1-2% of adults have heart failure, although it mainly affects the elderly, where 6–10% of individuals over the age of 65 years develop this disorder (22). Heart failure is as deadly as it is disabling. Studies report that approximately 30–40% of patients die within a year of diagnosis and 60–70% die within 5 years, most from deteriorating heart function or from sudden death (22,24-26). The molecular signaling pathways, responsible for pathological cardiac hypertrophy and heart failure, are being extensively studied with the hopes of developing therapies to treat and prevent these diseases.

The Calcineurin-NFAT signaling pathway

The availability of intracellular Ca^{2+} in mammalian cells is critical for their existence and proper function. In addition to its role in muscle cell electrophysiology and contraction, Ca^{2+} acts as a secondary messenger in many signal transduction pathways, involved in physiological processes such as fertilization, memory, apoptosis, membrane trafficking and cell division (27). Furthermore, at the molecular level, Ca^{2+} has been implicated in regulation of gene transcription, DNA replication, DNA repair and both protein synthesis and degradation (28).

A common question in muscle cell biology is with its numerous downstream targets, how does Ca^{2+} specify and activate a particular signaling pathway? It is generally understood that Ca^{2+} influxes into the cytoplasm through Ca^{2+} channels on the sarcolemma as waves of Ca^{2+}. In the 1990s, researchers identified that depending on the amplitude and frequency at which Ca^{2+} waves penetrate the cell, different Ca^{2+}-dependent signaling pathways are activated, which also affects gene expression and cell differentiation (29-31). However, the exact molecular mechanisms in which specific Ca^{2+}-dependent pathways in contracting cardiomyocytes are regulated remains disputed due to the highly specialized rhythmic cycling of Ca^{2+} involved in the heart's ECC. Houser et al. (32) have suggested the existence of Ca^{2+} microdomains in the cytoplasm, which are relatively independent of the Ca^{2+} involved in the ECC. Within these microdomains, Ca^{2+} is locally regulated and can activate protein signaling pathways in that particular region.

Many proteins that require Ca^{2+} to be active cannot readily bind Ca^{2+}, and thus use calmodulin (CaM), a high affinity Ca^{2+}-binding protein, as a Ca^{2+} sensor and signal transducer. Expressed in all eukaryotic cells, CaM is a 17 kDa protein composed of four EF-hand motifs, each capable of binding a single Ca^{2+} ion. The affinity by which Ca^{2+} binds CaM depends on changes in intracellular Ca^{2+} concentrations. When cytoplasmic Ca^{2+} levels are low, CaM exists in a closed conformation, where the EF-hand motifs are packed together, masking the Ca^{2+} binding sites. Alternatively, when intracellular Ca^{2+} levels are high, Ca^{2+} ions bind to the EF-hand motifs on CaM, causing a conformational change that allows Ca^{2+} to bind more readily to the other motifs, allowing CaM to attain an open configuration (33). Because CaM is a small, flexible molecule with numerous targets, such conformational changes are required to expose specific hydrophobic regions on each domain, which allows the Ca^{2+}/CaM complex to bind and activate specific proteins (34).

One of the most recognized signaling pathways that requires the Ca^{2+}/CaM complex to be activated is the Calcineurin - Nuclear Factor of Activated T-cells cascade. Calcineurin (Cn), also referred to as protein phosphatase 2B (PP2B), is a Ca^{2+}-dependent serine/threonine phosphatase that was first discovered in 1979 as a CaM binding protein in brain extracts (35). Further research by Schreiber's group (36) identified that Cn played a prominent role in the immune system, where the addition of immunosuppressive drugs, cyclosporine A (CsA) and FK506, decreased Cn's activity. Cn is ubiquitously expressed in all cells and the gene that encodes the Cn protein is conserved from yeast to mammals, suggesting a common mode of regulation (34,37).

Once active, Cn can de-phosphorylate a number of transcription factors such as myocyte enhancer factor 2 (MEF2), nuclear factor kappa-light-chain-enhancer of activated B cells (NFκB) and nuclear factor of activated T-cells (NFAT) (38-41). In addition to transcription factors, Cn has been identified as a direct regulator of the pro-apoptotic factor, Bcl-2 (42). The most characterized downstream targets of Cn is the family of NFAT transcription factors. In the heart, the role of the Cn-NFAT signaling pathway in mediating pathological cardiac hypertrophy *in vitro* and *in vivo* has been extensively studied (43-48). Once de-phosphorylated, NFAT transcription factors translocate to the nucleus and dimerize with other transcription factors to reactivate cardiac fetal genes, leading to hypertrophy of the adult heart [Figure 1.4].

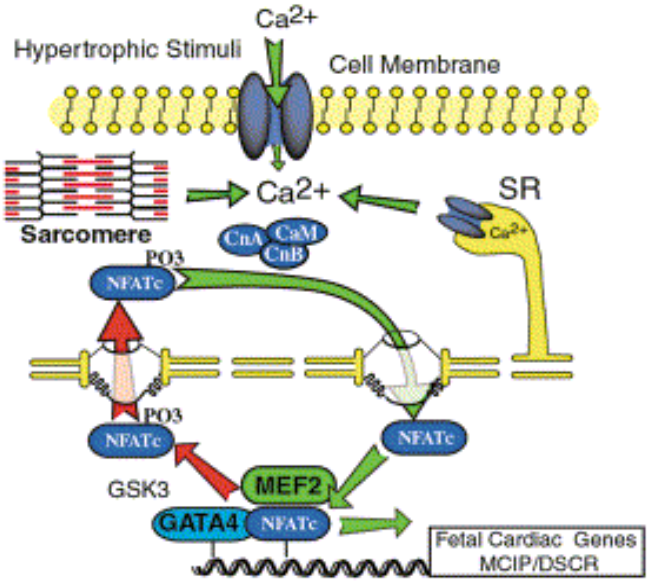

Figure 1.4: The Cn-NFAT signaling in pathological cardiac hypertrophy. Taken from Crabtree, G. et al. (2002) (49). Cytoplasmic Ca^{2+} interacts with Calmodulim (CaM) and the Ca^{2+}/CaM complex activates calcineurin (Cn). Once active, Cn de-phosphorylates nuclear factor of activated T-cell (NFAT) transcription factors, mediating their nuclear translocation in which NFAT can interact with other transcription factors, such as GATA-4 and MEF2, to induce the transcription of cardiac fetal genes. The regulatory kinase, Glycogen-Synthase Kinase 3 (GSK3), promotes NFAT nuclear export.

The crystal structure of calcineurin

The structure of human Cn was first solved in 1995, by Villafranca's group (50). Although sharing similar sequence with other serine/threonine protein phosphatases, the structure of Cn is unique due to its requirement of Ca^{2+} to be activated (51-53). From its structure, it was discovered that Cn exists as a heterodimer, consisting of two subunits: the 59 kDa catalytic subunit, calcineurin A (CnA), and the 19 kDa regulatory subunit, calcineurin B (CnB) (50).

The structure of CnA is comprised of two domains: a catalytic region, found on the N-terminus, and a regulatory domain, found on the C-terminal region (34). The catalytic domain is comprised of "two β-sheets flanked by a mixed α/β structure on one side and α-helices on another side" (54). The regulatory domain consists of three subdomains: a CnB binding domain, a CaM binding domain and an autoinhibitory

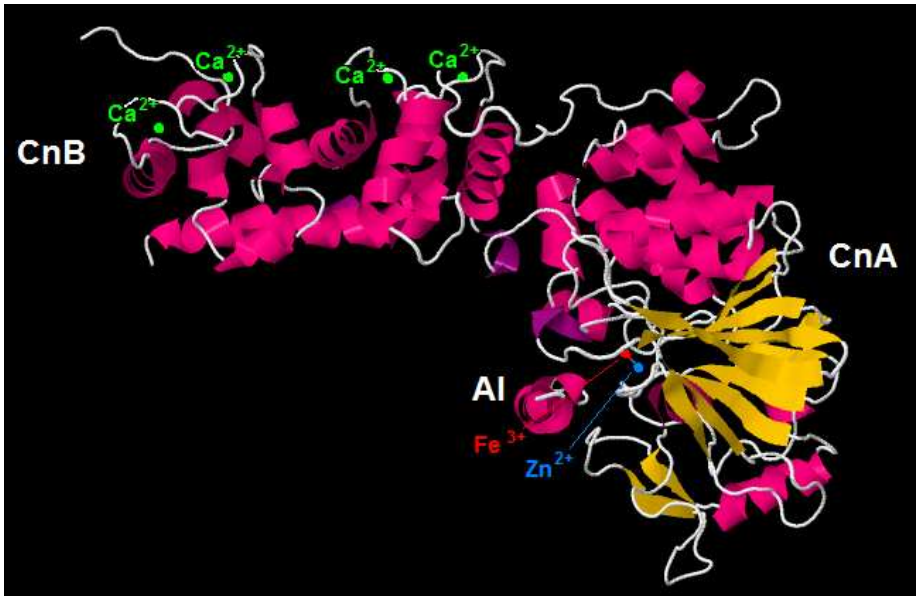

Figure 1.5: The crystal structure and domains of human Cn. Taken from the RCSB Protein Data Bank (55).

domain (AI) (54,56). Alternatively, the structure of CnB shares 35% sequence identity with CaM and contains four EF-hand motifs, allowing it to bind up to four Ca^{2+} ions in a similar mechanism as CaM (51,57). The structure of the human Cn heterodimer from the RCSB Protein Data Bank is shown [Figure 1.5].

In non-stimulated muscle cells, Cn is present in its inactive conformation in the cytoplasm, where the autoinhibitory domain sterically blocks CnA's catalytic domain, rendering the phosphatase inactive. Upon stimulation, cytoplasmic Ca^{2+} will bind CnB, causing a conformational change, which exposes the CaM binding domain on CnA. Once the Ca^{2+}/CaM complex docks onto its respective binding domain, another conformation change occurs which displaces the autoinhibitory domain from the catalytic domain, enabling the enzyme to be active.

The crystal structure of full length human Cn was solved with a resolution of 2.1Å. The globular structure of CnA consists of 521 residues, where residues 14-342 form the catalytic domain and residues 343-373 form an extended amphipathic α-helical region that interacts with hydrophobic residues within the CnB binding cleft (50). Residues 1-13, 374-468 and 487-521 are not visible in the crystal structure, as they are presumed to exist in random conformation (54). The AI domain is represented by a segment of residues 469-486, which lies over the substrate-binding cleft on the C-terminus of CnA. Residues 469-481 of the AI domain form two short α-helical regions, whereas residues 482-486 are in the extended conformation of the AI (54). The residues of the AI domain that interact with the substrate-binding cleft of CnA are conserved and those that have the strongest interactions are Glu481-Arg-Met-Pro484, where Glu481 hydrogen-bonds with water molecules bound to metal ions in Cn's active site (50).

The active site of Cn is composed of two layers of β-sheets and nine α-helices (54). Within the active site are two metal ions, Fe^{3+} and Zn^{2+}, which serve as Cn's dinuclear metal cofactors. Separated by 3.0 Å, these metal ions are responsible for interacting with residues and solvent molecules to maintain the stability of Cn's protein structure, as depicted [Figure 1.6].

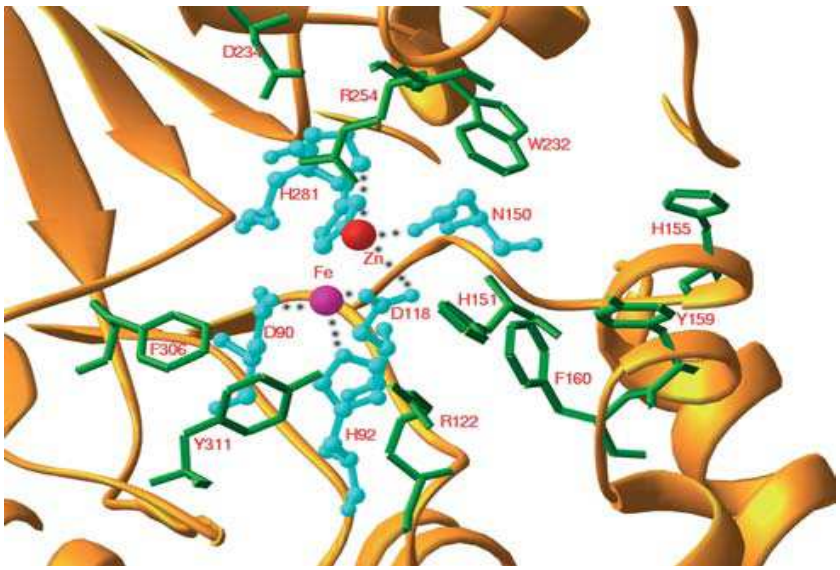

Figure 1.6: Interaction of Fe^{3+}/Zn^{2+} ions with residues in CnA's active site. Taken from Ke, H. et al. (2003) (54).

The Zn^{2+} metal ion interacts with the side chains of Asp118, Asn150, His199, His281, a water molecule and a phosphate oxygen. Alternatively, the Fe^{3+} ion interacts with the side chains of Asp90, His92, Asp118, a water molecule and a phosphate oxygen. These interactions stabilize the active site of CnA in an octahedral manner. Also found within or neighboring the active site are Arg112, His151, His155, Tyr159, Phe160, Trp232, Asp234, Arg254, Phe306 and Tyr311, which are involved in the binding of a Cn substrate (54).

The structure and regulation of NFAT proteins

NFAT transcription factors were first identified by the Crabtree group (58) where, similar to Cn, NFAT played an important role in the regulation of early T-cell activation genes. Since its discovery, researchers have provided evidence that the role of NFAT proteins was not restricted to T-cells, having been implicated in the "central nervous system, blood vessels, heart, kidney, bone, skeletal muscle and haematopoietic stem cells" (49,59-62).

NFAT proteins are part of the Rel-family of transcription factors. The molecular mass of NFAT ranges from 70-200 kDa, which is due to alternative splicing of genes resulting in varying protein sizes and differential phosphorylation states (63). The primary structure of NFAT consists of a moderately conserved N-homology region (NHR), a conserved Rel-homology region (RHR) and a non-conserved C-terminal domain (CTD) [Figure 1.7].

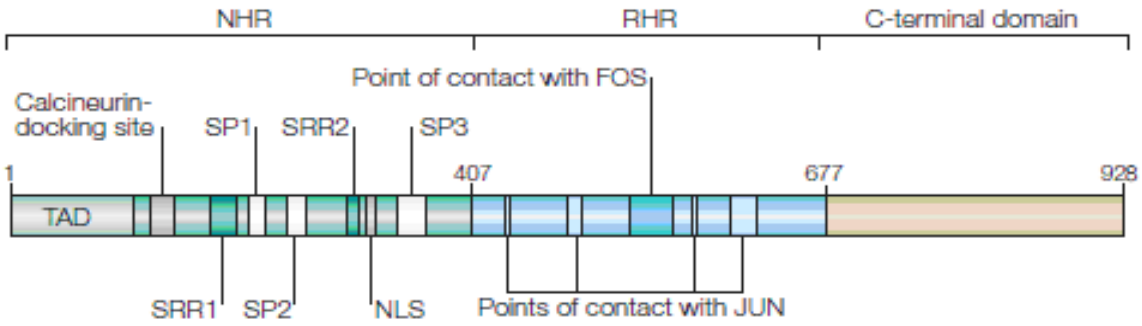

Figure 1.7: The primary structure of NFAT proteins. Taken from Macian, F. (2005) (59).

Firstly, the NHR (residues 1-407) contains a transactivation domain (TAD), a Cn docking site, a nuclear localization signal (NLS), serine-rich regions (SRR) and repeating

Ser-Pro-X-X motifs (SP), where X denotes any amino acid. The TAD is required for NFAT to bind the promoter region of genes to initiate transcriptional events. The Cn docking domain contains a SPRIEIT sequence, a variant of the PxIxIT motif found on Cn regulators, which allows Cn to bind to NFAT and de-phosphorylate serine residues, mediating the nuclear shuttling of NFAT. A nuclear export sequence (NES) was detected in NFATc1, however the exact location of the NES in the NFAT primary structure is unknown because its sequence is not conserved among NFAT family members (64,65).

Secondly, the RHR (residues 408-677), which is conserved among all Rel proteins, confers a shared DNA binding specificity (66). The C-terminus of the RHR contains a DNA binding motif, which permits Rel-proteins to bind the 5'-GGAAAAT-3' consensus sequence (58). The N-terminus of the RHR contains a domain that allows NFAT to interact with each other as monomers or dimers through the RHR and other transcription factors in the nucleus. Such molecular partners include the leucine zipper protein activator protein-1 (AP-1) Fos and Jun, the Zn^{2+}-finger protein GATA-4, the MCM1, Agamous, Deficiens, SRF (MADS) -box transcription factor myocytes enhancer factor-2 (MEF2) and many others (43,49,60,66).

Lastly, although the exact role of the CTD (residues 678-928) remains ill defined, due to the differences in the length of the CTD between NFAT isoforms, it is possible that the CTD is responsible for the different transcriptional activity of the NFAT isoforms, as shown by several groups (67,68).

NFAT transcription factors are ubiquitously expressed and consist of five isoforms: NFATc1 (a.k.a. NFATc, NFAT2), NFATc2 (a.k.a. NFATp, NFAT1), NFATc3

(a.k.a. NFATx, NFAT4), NFATc4 (a.k.a. NFAT3) and NFAT5 (a.k.a. tonicity-responsive enhancer-binding protein or TonEBP) (69). Of the five NFAT proteins, only NFATc1, NFATc2, NFATc3 and NFATc4 are regulated by Ca^{2+}-Cn signaling and have known roles in skeletal and cardiac muscles (63,68). NFAT5 cannot interact with Cn due to the absence of a SPRIEIT domain and is, therefore, insensitive to Ca^{2+}-Cn signaling (70). Rather, NFAT5 is regulated by osmotic stress and is known to control the expression of cytokines, such as tumor-necrosis factor (TNF) and lymphotoxin-β, in lymphocytes (59,71). Due to NFAT5's insensitivity to Cn and its unclear role in muscle cells, the remainder of this thesis will focus on the Ca^{2+}-Cn regulated NFAT isoforms: NFATc1, NFATc2, NFATc3 and NFATc4.

The regulation of NFAT proteins

The cellular localization of NFAT proteins depend on the phosphorylation state of approximately 14 serine residues on the NHR. Okamura et al. (72) showed that of these residues, 13 phosphoserines are targeted by Cn and are located in motifs SRR1, SP2 and SP3. Upon de-phosphorylation, the NLS sequence of NFAT is exposed and the NES is masked, prompting nuclear entry. NFAT kinases are regulators of NFAT transcription factors, which can interact with NFAT and reversibly phosphorylate the same serine residues that are targeted by Cn. Known NFAT kinases include Casein Kinase (CK), Glycogen-Synthase 3-β (GSK3-β), p38 and Janus-N-Terminal Kinase (JNK) (73-76).

Upon re-phosphorylation, the NES sequence is re-exposed whereas the NLS sequence is hidden, prompting nuclear export and cytoplasmic retention of NFAT (72). These kinases can either be classified as 1) maintenance kinases, which phosphorylate NFAT in the cytosol to prevent nuclear import or 2) export kinases, which target NFAT in the nucleus to promote nuclear export. Each kinase can phosphorylate serine residues on specific motifs. CK acts as both an export and maintenance kinase on SRR1 of NFATc2 (77). GSK3-β functions as an export kinase on both SP2 and SP3 of NFATc1 and SP2 on NFATc2 (59,78). The mitogen activated protein kinase (MAPK) family consists of p38, JNK and Extracellular-Regulated-Signal Kinases (ERK) and can

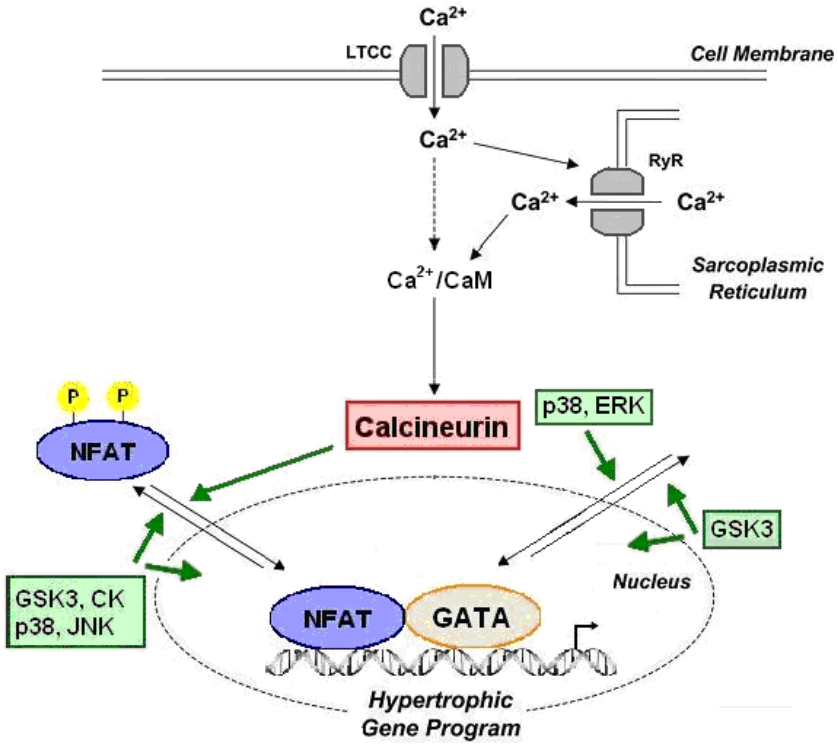

Figure 1.8: The regulation of Cn-NFAT signaling. Adapted from Fiedler, B. et al. (2004) (79). Regulatory kinases, located in the cytoplasm and nucleus, regulate the cellular distribution of NFAT and GATA transcription factors. Glycogen-Synthase Kinase 3 (GSK3), Casein Kinase (CK), p38 and JUN-N-terminal Kinase (JNK) promote NFAT nuclear export, where as GSK3 mediates GATA export. Alternatively, Extracellular-Regulated-Signal Kinase (ERK) and p38 increase GATA DNA binding affinity.

phosphorylate the first serine of SRR1 on different NFAT isoforms. JNK phosphorylates NFATc1, whereas p38 targets NFATc2 (75,76). CK-1 may be responsible for phosphorylating the remaining serines on SRR1 (59). Although a cell may have the potential to translate the different NFAT isoforms, depending on which NFAT kinase is expressed, only certain NFATs may be nuclear localized. An overview of the regulation of Cn-NFAT signaling by the regulatory kinases is shown [Figure 1.8].

Calcineurin-NFAT signaling in heart disease

Cn-NFAT signaling is described as a multifunctional regulator, where its function depends on the cell type in which this pathway is active. In the brain, Cn-NFAT signaling mediates numerous processes, which include memory, brain strokes, ischemic injury, Parkinson and Alzheimer's diseases and the regulation of the cAMP Response Element-Binding (CREB) transcription factor (80). In the lungs, Cn-NFAT signaling has been implicated in perinatal lung maturation and function, and in regulating genes involved in the homeostasis of pulmonary surfactant, which is required for proper breathing (81). In skeletal muscles, this pathway is required for functional-overload induced skeletal muscle hypertrophy and for mediating skeletal muscle-fiber type conversions from fast muscle fiber type to slow muscle fiber type (39,82). In the cardiovascular system, Cn is required for the early development of the heart, specifically the cardiac septum and valves (83,84). During heart disease, Cn-NFAT signaling promotes the reactivation of cardiac fetal genes, which are responsible for cardiac growth during development. The reactivation of

these genes in the adult heart is responsible for the pathological growth of the heart, and not normal physiological growth (85).

In 1998, Molkentin et al. (43) first reported the novel role that Cn-NFAT signaling played in mediating pathological cardiac hypertrophy. Among the major findings of their report was that Cn induces the de-phosphorylation of NFAT3 (NFATc4), prompting its nuclear entry and allow NFAT3 to interact with the GATA-4 transcription factor, leading to cardiac hypertrophy. In addition, cultured cardiomyocytes, treated with Cn inhibitors CsA and FK-506, blocked angiotensin II and phenylephrine-induced cardiac hypertrophy. To support their *in vitro* findings, transgenic mice that expressed a cardiac-specific constitutively active form of CnA (CnA*), in which the C-terminal autoinhibitory domain was cleaved, were generated (86). The hearts of CnA* overexpressing transgenic mice, compared to the hearts of wild-type counterparts, display a 2-to-3 fold increase in heart weight-to-body weight ratio, a thickening of the left ventricular wall and interventricular septum, a 2-fold increase in cross-sectional area of cardiomyocytes and extensive fibrosis. Furthermore, CnA* overexpressing mice have increased susceptibility to sudden death, mimicking the effects of heart failure in humans. Upon treatment with the Cn inhibitor, CsA, the hearts of CnA* transgenic mice were of normal size (43).

Many genes and proteins that are reactivated in response to heart disease have prominent functions in embryonic and fetal heart development. For example, cardiac fetal genes are active during the physiological growth in developing hearts. This family of genes consists of atrial natriuretic peptide (ANP), brain natriuretic peptide (BNP), α-skeletal actin, β-myosin heavy chain (β-MyHC), and many others (87). When the heart

has fully matured into an adult heart, the expression of these genes becomes dormant. During heart disease, hypertrophic stimuli reactivate the expression of these genes in the adult heart, which enables the heart to grow to a pathological state (88).

One of the most studied families of transcription factors that interact with NFAT to initiate cardiac hypertrophy are GATA proteins. GATA transcription factors consist of two conserved zinc fingers that are required to bind to the consensus DNA sequence 5'-(A/T)GATA(A/G)-3', as well as domains that allow GATA to interact with transcriptional cofactors (87,89,90). Of the six members of the GATA family (GATA-1 to GATA-6), GATA-4, GATA-5 and GATA-6 are expressed in the heart (91). Among the GATA proteins expressed in the heart, GATA-4 is associated with embryonic cardiogenesis, such as heart tube formation, and pathological growth of the adult heart (92,93). In addition, GATA-4 is a known regulator of the expression of cardiac structural genes during development (94-96).

GATA-4 gene targeted mice are embryonic lethal at E7-9.5 due to structural and functional defects of the heart (92). Alternatively, cultured cardiomyocyte overexpression of GATA-4 causes a 2-fold increase in cell surface area, whereas GATA-4 overexpressing transgenic mice have increased heart-weight-to-body weight ratio, cardiomyopathy features of the cells and upregulation in the expression of cardiac fetal genes (97).

The regulation of GATA-4 occurs post-translationally, where such modifications affect its DNA binding ability, transcriptional activity and cellular localization (93). A number of chemical stimuli that induce cardiac hypertrophy have been associated with

the phosphorylation of GATA-4, which increases both its DNA binding and transcriptional activity (87,93). Molkentin's group (98,99) identified that phosphorylation of Ser105 on GATA-4 by the ERK1/2 and p38 MAPK was responsible for GATA-4 increased DNA binding affinity and transactivation during heart failure. Another kinase that targets GATA-4 is GSK3-β, a known negative regulator of cardiac hypertrophy (100). GSK3-β-mediated phosphorylation of GATA-4 prompts its export from the nucleus, rescuing Cn-mediated cardiac hypertrophy (101).

A second family of transcription factors that is reactivated during heart disease is the myocyte enhancer factor 2 (MEF2). There are four members of the MEF2 family expressed in vertebrates: MEF2A, MEF2B, MEF2C and MEF2D. MEF2 proteins can either homodimerize or heterodimerize with other transcription factors such as NFAT and GATA, which can then bind to the DNA sequence 5'-CTA(A/T)$_4$TAG-3' to carry out transcriptional events (40,87,102,103). Although the MEF2 proteins are expressed in most cell types, their transcriptional activity is restricted to the immune system, neurons and striated muscle cells (104).

In the heart, MEF2 have critical roles in cardiac differentiation. MEF2C null mice are embryonic lethal, due to cardiac looping defects, an absence of the right ventricle and a downregulation of cardiac structural genes (87,105,106). The majority of MEF2A null mice died 2-10 days after birth because of defects in conduction and architecture of the heart. Surviving MEF2A null mice display reduced mitochondrial content and a less efficient conductive system. (107). In addition, transgenic mice that express a dominant negative MEF2 die shortly after birth because of cardiomyocyte hypoplasia, thinning of the ventricular walls and heart chamber dilation (87,108).

A greater workload imposed on the heart, a phenotype of cardiac hypertrophy, has been associated with increased MEF2 DNA binding (109,110). In cultured cardiomyocytes, adenoviral-mediated overexpression of MEF2A or MEF2C causes sarcomeric degeneration and cell elongation, both of which indicate cardiac dilatation. The hearts of transgenic mice overexpressing MEF2A or MEF2C are subject to contractile defects, ventricular dilation and are more readily hypertrophied when pressure overload stimulation is induced. However, when cells of the transgenic hearts are isolated, rather than having a greater cross-sectional area, the cardiomyocytes are more elliptical in shape, suggesting that MEF2 does not directly drive cardiac hypertrophy (87,111).

Another transcription factor known to mediate cardiac hypertrophy is cAMP-response-element binding protein (CREB), which is a 43 kDa leucine zipper that binds to the DNA sequence 5'- TGANNTCA-'3 as either a homodimer or a heterodimer with AP-1 transcription factors (87,112). CREB is predominantly expressed in excitable tissues, such as the brain, skeletal muscle and heart, where its function varies depending on the cell type. It is most well characterized in the brain, having roles in the development of long-term memory and drug addiction (113,114). In skeletal muscles, preliminary work from our lab suggests that CREB mediates the fast muscle fiber type program, causing the conversion of slower, more energy efficient muscle fibers to faster, less energy efficient muscle fibers. In the heart, CREB was identified as an important transcriptional regulator of cardiac hypertrophy (115).

The cellular localization and transcriptional activity of CREB depends on the phosphorylation state of serine residues. In its unphosphorylated state, CREB can readily

bind DNA, but cannot initiate transcription (116). CREB phosphorylation of Ser133 activates CREB and promotes its interaction with CREB-binding protein (CBP), which triggers transcriptional events (117,118). Kinases known to phosphorylate CREB at Ser133 include protein kinase A (PKA) and Ca^{2+}/CaM-dependent protein kinase, isoforms II and IV (CaMKII and CaMKIV) (119-121). Alternatively, a second site on CREB targeted by CaMKII is Ser142, where phosphorylation of this residue negatively regulates CREB by preventing PKA mediated phosphorylation and activation (121).

In the heart, Fentzke et al. (115) developed transgenic mice that overexpress a cardiac specific dominant negative form of CREB, where a Ser133Ala point mutation was made. These mice display significant dilated cardiomyopathy, decrease ventricular function, reduce contractile response and reactivation of cardiac fetal genes (115). In addition, this dominant negative overexpressing CREB transgenic mouse model did not improve survival or rescue dilated cardiomyopathy in response to long-term exercise (122). These findings suggest that CREB may participate in a signaling pathway responsible for regulating cardiomyocyte structure and function. Furthermore, numerous hypertrophic stimuli cause an increase in expression of a negative regulator of CREB transactivation, inducible cAMP early repressor (ICER), which leads to decreased cardiac hypertrophy and increased cardiomyocyte apoptosis (123,124). Taken together, although the exact molecular mechanism implicating CREB in cardiac hypertrophy remains unclear, these reports suggest that CREB plays an important transcriptional role in regulating the pathophysiological states of the adult heart.

IGF-1-AKT signaling in cardiac hypertrophy

Another major signaling pathway known to mediate heart growth is the IGF-1-AKT/PKB pathway. Insulin-like growth factor-1 (IGF-1) is among the best characterized muscle-promoting growth factors. IGF-1, primarily secreted by the liver, binds to the receptor tyrosine kinase IGF-1 receptor (IGF-R) in an autocrine and paracrine mechanism. This binding causes the activation of phosphoinositide 3-kinase (PI3K), which in turn phosphorylates the 3'carbon of phosphotidylinositols on the cell plasma membrane. Upon recognizing the PI3K phosphorylated lipids, inactive AKT (a protein kinase B) translocates from the cytoplasm towards the inner surface of the plasma membrane, which causes a

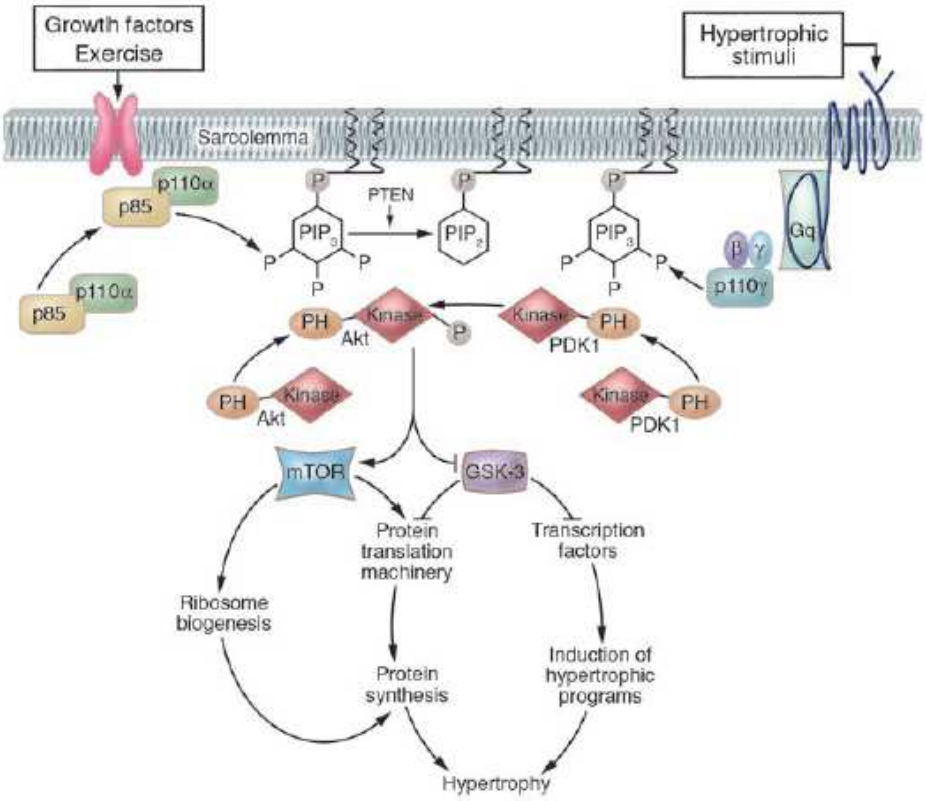

Figure 1.9: IGF-1/AKT signaling in normal and pathological cardiac hypertrophy. Taken from Dorn, G. et al. (2005) (125).

conformation change and allows AKT to be readily phosphorylated at Ser473 and Thr308 by pyruvate dehydrogenase kinase-1 (PDK1), rendering AKT active (126).

Two important protein synthesis pathways downstream of AKT are the mammalian target of rapamycin (mTOR) pathway, which is activated by AKT, and the GSK3-β pathway, which is inhibited by AKT (127). AKT activates the mTOR kinase by phosphorylating and inhibiting tuberous sclerosis 2 (TSC2), which when complexed with TSC1, inhibits RHEB, a small G protein required for mTOR activation. Active mTOR binds to co-activators GβL and raptor to form mTOR complex (mTORC1), which activates ribosomal protein S6 kinase ($p70^{S6K}$) leading to translational initiation (127). Alternatively, GSK3-β is a suppressor of translational initiators by promoting the nuclear export of NFAT and GATA transcription factors. The inhibition of GSK3-β by AKT, along with the mTORC1 pathway, will promote both gene transcription and protein translation, causing muscle hypertrophy and growth (127). The IGF-1/AKT signaling pathway in normal and pathological cardiac hypertrophy is depicted [Figure 1.9].

Of the three AKT genes expressed in the body (AKT1, AKT2 and AKT3), only AKT1 and AKT2 are present in the heart. AKT1 gene targeted mice display a decrease in body and heart mass, whereas AKT2 gene targeted mice do not show this phenotype (128,129). Furthermore, AKT1 -/- mice do not undergo physiological cardiac hypertrophy in response to long-term exercise, compared to wild-type counterparts. These results demonstrate the importance of AKT in the physiological growth of the heart. The short-term activation of the IGF-1/AKT pathway induced compensatory cardiac hypertrophy, where heart function remained unchanged. However, transgenic mice overexpressing constitutively activated AKT display severe cardiac dysfunction and heart failure,

suggesting that the long-term overexpression of AKT was sufficient to cause pathological cardiac hypertrophy (18,130).

To summarize, the understanding of such biochemical growth-associated signaling pathways responsible for mediating pathological cardiac hypertrophy and heart failure is critical for advancing our comprehension of these diseases at the molecular level. In addition, further research into these signaling pathways increases the opportunities to develop pharmacological drugs to counteract congenital heart diseases and heart failure.

Chapter 2: Altered growth-mediated signaling in the hearts of NFATc2 null mice

Patrick Sin-Chan and Robin N. Michel

Chemistry & Biochemistry and Exercise Science, Concordia University, Montreal, QC, Canada.

Keywords: calcineurin, NFAT, GATA-4, heart failure

Robin N. Michel, PhD

Concordia University

Department of Exercise Science

7141, Sherbrooke Street West

Montréal, Qc, H4B 1R6

Phone 514-848-2424 ext. 5749

Fax 514-848-8681

Email : rmichel@alcor.concordia.ca

Introduction

As cardiovascular disease is one of the leading causes of death in the modern world, research in this area has been thriving over the past decade. A common abnormality associated with the majority of cardiovascular diseases is pathological cardiac hypertrophy, in which hearts are subjected to an increased workload and decreased contractile efficiency. Pathological cardiac hypertrophy develops as an adaptive response of the heart to hypertension, myocardial infarctions, defects in contractile proteins, increased mechanical load and genetic mutations (18,43,131). Individuals living with this disease have a greater susceptibility to cardiac arrhythmias, organ failure and sudden death (132). A consequence of prolonged cardiac hypertrophy leads to heart failure, which the heart can no longer sustain the increased workload required to meet the body's hemodynamic demands, causing left ventricular dilatation, thinning of the myocardial walls, and overall decrease in heart contraction and function, resulting in eventual death (133).

The best characterized intracellular modulator of pathological cardiac hypertrophy is the Ca^{2+}/calmodulin (CaM)-dependent phosphatase, calcineurin (Cn) and its downstream transcriptional effector, nuclear factor of activated T-cells (NFAT) (85,134-136). Of the five known NFAT isoforms, four (NFATc1, NFATc2, NFATc3, NFATc4) are regulated by Cn signaling and their presence has been detected in the heart (63,137). In unstimulated cells, Cn exists in its inactive heterodimeric form and NFAT proteins reside in the cytoplasm in their phosphorylated state (138). Upon stimulation that promotes Ca^{2+} influx into the cytoplasm, Ca^{2+} ions will bind to CaM, and this complex will physically interact and induce a conformational change in Cn structure, exposing

Cn's catalytic domain (80,139). Once active, Cn can de-phosphorylate NFAT proteins, enabling NFAT to translocate to the nucleus, where it can interact with other cardiac factors to activate the transcription of cardiac fetal genes, which include β-myosin heavy chain (β-MyHC), atrial natriuretic peptide (ANP) and brain natriuretic peptide (BNP), thereby initiating the hypertrophic gene program (87). *In vivo* and *in vitro* studies have previously demonstrated the effectiveness of Cn-NFAT signaling in the mediation of cardiac hypertrophy and heart failure (43-48,63,85,140-142). Another well characterized inducer of cardiac hypertrophy is the GATA-4 transcription factor, in which transgenic mice overexpressing GATA-4 display increased heart sizes, cardiomyopathy and reactivation of the cardiac fetal genes (97). In addition, GATA-4 has been shown to cooperate with NFAT3 to synergistically activate the BNP promoter to induce cardiac hypertrophy (43).

Recently, loss-of-function studies have identified that of the NFAT proteins expressed in the heart, NFATc2 was the major NFAT isoform responsible for Cn-induced pathological cardiac hypertrophy, in that 1-2 month old young NFATc2-/- mice displayed a complete inhibition of forced hypertrophy, decreased cardiac fetal gene expression, reduced fibrosis and had restored contractile functions (143). However, the authors of this report failed to monitor changes in the biochemical signaling in the hearts of NFATc2-/- mice. We observe that 6-9 month old NFATc2-/- mice are physically frailer in appearance, are more susceptible to sudden death and have larger hearts upon autopsy. These empirical observations lead us to hypothesize that in younger NFATc2-/- mice, other transcription factors may be compensating for the absence of functional NFATc2.

Overtime, these compensatory transcription factors cannot fully restore normal cardiomyocyte growth and function, predisposing these mice to heart failure.

We provide evidence that although adult NFATc2-/- mice shared a similar heart weight-to-body weight ratio as wild-type mice, NFATc2-/- mice displayed left ventricular inner chamber dilatation and thinning of the right ventricle wall, indicative of heart failure. We demonstrate that NFATc2-/- mice have increased GATA-4 expression and both NFATc1 and GATA-4 nuclear translocation, which may be compensating for the loss of NFATc2 in a failed attempt to rescue cardiomyocyte growth. Correlated to increased GATA-4 and NFATc1 nuclear presence, we show that the NFAT/GATA-4 export kinase Glycogen Synthase 3-β (GSK3-β) is downregulated in NFATc2-/- mice. Moreover, when inducing cardiac hypertrophy using angiotensin II (Ang II), we observe that the overall heart morphology of Ang II-infused NFATc2-/- mice was more dilated with thinning of the right ventricular walls, suggesting that an increased workload on the hearts of these mice may subject NFATc2-/- mice to a more severe pathological heart state. We also show that the expression of β-MyHC was increased in Ang II-stimulated NFATc2-/- mice, indicating an alteration in contractile protein expression. Furthermore, the expression GATA-4 and activated AKT had a tendency to be downregulated whereas eukaryotic initiation of factor 2α (eIF2α) was unchanged in Ang II-infused NFATc2-/- mice, compared to wild-type counterparts, suggesting an inactivation of transcriptional and translational mechanisms in these mice. Our results suggest that the NFATc2 transcription factor may have an uncharacterized and essential role for normal heart function and growth-mediated biochemical signaling in adult mice, proposing that normal Cn-NFAT signaling is required for proper heart function.

Material and Methods

Mouse model, breeding and maintenance

Transgenic NFATc2 null (NFATc2-/-) mice were generously provided by Drs. Grace Pavlath (Emory University) and Laurie Glimcher (Harvard University). These mice harbored a disruption in the NFATc2 gene causing a loss of function mutation, as previously described (144). Breeding of heterozygous (NFATc2+/-) or homozygous (NFATc2-/-) mice yielded second generation NFATc2-/- mice. For the experimental design, NFATc2-/- mice were age and sex matched with wild-type (NFATc2+/+) counterparts, which were purchased from Charles River Laboratories, QC or generated from breeding. All mice were housed under standard environmental conditions (20-22ºC, 14:10 hour light:dark cycle) and provided with standard rodent food and tap water ad libitum. Mice between 6 and 9 months of age were used for all subsequent analyses. All animals were treated in accordance with the institutional guidelines of Concordia University Animal Research Ethics Committee (UAREC), set by the Canada Council of Animal Care (CCAC).

Mouse genotyping

DNA from mouse tails was amplified by adding 2 µl of cDNA to 1X Taq buffer with KCl (Fermentas, ON), 2 mM $MgCl_2$ (Fermentas, ON), 0.2 mM dNTP (Invitrogen, CA), 0.5 mM primers (Sigma Aldrich, MO) and 20 U Taq DNA polymerase (Fermentas, ON), yielding a final volume of 20 µl. The following primers were used 5'-gcaagcctcagtgacaaagtatccacttca-3', 5'-ccacgagctgcccatggtggagagacaaga-3' and 5'-agcgttggctacccgtgatattgctgaaga-3'. Cycling conditions were as follows: 1) initial denaturation at 95ºC for five minute, 2) denaturation at 94ºC for one minute, 3) primer

annealing at 60 ºC for one minute, extension at 72ºC for one minute, 4) cycle to step 2 for 36 cycles, 5) final extension at 72ºC for ten minutes. PCR products were loaded in a 1.5% agarose gel stained with ethidium bromide and resolved, after electrophoresis, under UV irradiation using the Alpha Innotec Fluorchem system (Cell Biosciences, CA).

Muscle extraction and preservation

Prior to muscle extraction, mice were anesthetized by an intramuscular injection of 1.6:1 volume ratio mixture of 100 mg/ml ketamine hydrochloride (Bimeda-MTC Animal Health Inc., ON) and 20 mg/ml xylazine (Bayer HealthCare, ON). A dosage of 0.12 ml/100 g of body weight was administered to each mouse. Hearts for biochemistry studies were extracted and frozen directly in liquid nitrogen. For histology, mice were euthanized by CO_2 asphyxiation and the hearts were infused with an equal volume of 5% gelatin (Sigma-Aldrich, MO) in each ventricle, embedded with Tissue-Tek *Optimum Cutting Temperature* compound (Fisher Scientific, ON) and frozen in a pool of melting isopentene cooled in liquid nitrogen. All samples were stored at -86ºC until used.

RNA extraction and semi-quantitative RT-PCR

RNA of mouse hearts was extracted following the procedure as previously described (145). Briefly, samples were homogenized in a 1 ml/100 mg of buffer consisting of 4 M guanidinium thiocyanate (Sigma-Aldrich, MO), 25 mM sodium citrate, 0.5% (v/v) N-laurylsarcosine (Sigma-Aldrich, MO) and 0.1 M 2-mercaptoethanol (Bioshop, ON). A one-tenth volume of 0.2 M sodium acetate (pH 4.0) was added and vortexed, followed by the addition of one volume of phenol (Sigma-Aldrich, MO) with vortexing. A one-fifth volume of a 24:1 volume ratio of chloroform:isoamyl alcohol was

added and vortexed until a white emulsion appeared. Samples were cooled in ice for fifteen minutes, and then centrifuged at 10000×g for ten minutes at 4ºC. The aqueous layer was collected, followed by the addition of two volumes of 99% ethanol and the solution was vortexed. Samples were centrifuged at 10000×g for ten minutes at 4ºC. The 99% ethanol was decanted and the RNA was resuspended in 200 µl of 70% ethanol, followed by a centrifugation at 10000×g for ten minutes at 4ºC. The 70% ethanol was decanted and the RNA pellet was air dried and resuspended in 15 µl of RNAse free H_2O (Bioshop, ON) per 10 mg of tissue. The RNA pellet was dissolved using intermittent vortexing and heating at 70ºC.

RNA concentration and purity was determined using an Eppendorf Biophotometer (Eppendorf, ON) at A_{260nm}. To validate RNA integrity, 2 µg of RNA was mixed with 12.5 µl of 2:1 formamide:ethidium bromide, 4 µl of formaldehyde (Sigma-Aldrich, MO), 2.5 µl of 10X MOPS (pH 7.0) and 1 µl of bromophenol blue, heated at 65ºC for ten minutes and loaded in a 1.5% agarose gel containing 1X MOPS and 1.91% (v/v) formaldehyde. The gel image was captured with irradiation using an Alpha Innotec Fluorchem system (Cell Biosciences, CA), where visualization of the 5S, 18S and 28S rRNA bands indicated intact RNA.

RT-PCR was performed by combining 2 µg of RNA, ultrapure water, for a final volume of 10 µl. The final volume of the RT mixture was 40 µl, which consisted of 0.625 µM random primer hexamers (Invitrogen, CA), 1X RT-buffer (Ambion, ON), 0.5 µM dNTP (Invitrogen, CA), 40 U of RNase Inhibitor (Ambion, ON) and 100 U of MMLV-RT (Ambion, ON). The RT-PCR program (Fifteen minutes at 20ºC, one hour at 37ºC, and ten minutes at 65 º C) was performed using a MJ Research PTC-100 thermalcycler.

As a negative control, RT samples were duplicated in the absence of MMLV-RT. The cDNA was stored at -20ºC until used.

The cDNA was amplified by adding 2.5 µl of cDNA to 1X Taq buffer with KCl (Fermentas, ON), 1.5 mM $MgCl_2$ (Fermentas, ON), 0.1 mM dNTP (Invitrogen, CA), 0.2 mM primers (Sigma Aldrich, MO) and 0.05 U/µl Taq DNA polymerase (Fermentas, ON), yielding a final volume of 50 µl. Primer sequences used are shown in Appendix II. Cycling conditions were as follows: 1) initial denaturation at 94ºC for one minute, 2) denaturation at 94ºC for one minute, 3) primer annealing at Tm for one minute, 4) extension at 72ºC for one minute, 5) cycle to step 2 for X number of cycles, 6) final extension at 72ºC for ten minutes, using a MJ Research PTC-100 thermalcycler. PCR products were loaded in a 1.5% agarose gel stained with ethidium bromide and resolved after electrophoresis under UV irradiation using the Alpha Innotec Fluorchem system (Cell Biosciences, CA).

Protein extraction and Western blotting

Whole hearts were homogenized using a hand-held Tissue Tearor homogenizer (Biospec Products Inc, OK) in 1X RIPA buffer solution (6 µl/mg of tissue) consisting of 1X PBS, 1% Igepal, 0.5% Sodium Deoxycholate, 0.1% Sodium Dodecyl Sulfate (SDS), 0.001 M Sodium Orthovanadate, 0.01 M Sodium Fluoride, 0.01 mg/ml Aprotinin, 0.01 mg/ml Leupeptin and 1 mM Phenylmethanesulfonyl fluoride (Sigma-Aldrich, MO). Homogenates were cooled, followed by a centrifugation at 15000×g for twenty minutes at 4ºC. Supernatant was collected and re-centrifuged. The whole cell protein was stored at -86ºC until used. Fractionated into cytoplasmic and nuclear protein was performed using

the NE-PER® Nuclear and Cytoplasmic Extraction Kit (Pierce Biotechnology, IL), according to the manufacturer's protocol.

Between 100 μg -150 μg of protein was loaded in an SDS polyacrylamide gel consisting of a 5% w/v stacking gel composed of 3.9% acrylamide (Sigma-Aldrich, MO), 0.125 M Tris (pH 6.8), 0.1% SDS, 0.06% ammonium persulfate and 0.14% Tetramethylethylenediamine (TEMED) (Bioshop, ON) and a 10% w/v separating gel composed of 9.9% acrylamide, 0.375 M Tris (pH 8.8), 0.1% SDS, 0.06% ammonium persulfate and 0.25% TEMED. Samples were electrophoresed at 120V until the protein sizes of interested were visibly separated on using the Amersham Full-Range Rainbow Molecular Weight Markers (GE Healthcare Bio-Sciences Corp, NJ).

Proteins were transferred onto a PVDF membrane (Millipore, MA) at 100V for one hour, followed by blocking in 5% non-fat milk or bovine serum albumin in 0.1% Tween-Tris Buffered Saline (T-TBS) for one hour. Antibodies to GATA-4 (sc-25310; 1°Ab. 1:1000, 2°Ab. 1:2000), JNK-2 (sc-827; 1°Ab. 1:1000, 2°Ab. 1:2000), NFATc2 (sc-7296; 1°Ab. 1:200, 2°Ab. 1:2000) (Santa Cruz Biotech, CA) Histone H3 (9715; 1°Ab. 1:1000, 2°Ab. 1:2000), GSK3-β (9315; 1°Ab. 1:1000, 2°Ab. 1:2000), p38-α (9218; 1°Ab. 1:1000, 2°Ab. 1:2000), ERK1/2 (4695; 1°Ab. 1:1000, 2°Ab. 1:2000), α-tubulin (2125; 1°Ab. 1:2000, 2°Ab. 1:2000), phospho-AKT (Ser473) (9271; 1°Ab. 1:1000, 2°Ab. 1:2000), phospho-eIF2α (Ser51) (9721; 1°Ab. 1:1000, 2°Ab. 1:2000), total eIF2α (9722; 1°Ab. 1:1000, 2°Ab. 1:2000) (Cell Signaling, MA), total AKT (610861; 1°Ab. 1:1000, 2°Ab. 1:2000) (BD Biosciences, ON) or GAPDH (ab9484; 1°Ab. 1:2000, 2°Ab. 1:2000) (Abcam, MA) were added to membranes based on the manufacturer's recommendation and incubated on a shaker at 4ºC overnight. The following day, membranes are washed

three times with 0.1% T-TBS and incubated with secondary antibody (Sigma-Aldrich, MO and Cell Signaling, MA) coupled to horseradish peroxidase for one hour. Membranes were washed three times with 0.1% T-TBS and developed with enhanced chemi-luminescence reagents (Millipore, MA) using the Alpha Innotec Fluorchem system (Cell Biosciences, CA).

Co-immunoprecipitation

Protein G Sepharose 4 Fast Flow beads (GE Healthcare Bio-Sciences Corp, NJ) were pre-washed three times with sterile water (Bioshop, ON) and two times with 1X RIPA buffer by shaking for five minutes, followed by a centrifugation at 1000×g for five minutes. The beads were suspended in 1X RIPA buffer to yield a 50% bead concentration. For separation, 1X RIPA buffer was added to 50 µg of whole cell heart protein to yield a final volume of 850 µl, followed by adding 50 µl of beads. The mixture was shaken for one hour, followed by adding 1% goat serum (Sigma-Aldrich, MO) with shaking for an additional hour. After a centrifugation at 1000×g for five minutes, 50 µl of supernatant was kept as depleted extract and a 1:10 NFATc2 dilution (Santa Cruz Biotech, CA) was added to the remaining supernatant with shaking overnight. The following day, 50 µl of beads were added to each sample with shaking for two hours, followed by three washes with 1X PBS and two times with sterile water with shaking for five minutes, followed by centrifugation at 1000×g for five minutes. The supernatant was discarded and the pellet kept at -86ºC until used. All work was performed at 4ºC.

Angiotensin II infusion

Alzet 2002 micro-osmotic pumps (Alzet, CA) were placed through a small dorsal incision in the skin between the scapulae in six month old female mice anesthetized as described above. Pumps were filled with angiotensin II (Sigma-Aldrich, MO), administered in a dosage of 432 $\mu g \cdot kg^{-1} \cdot day^{-1}$ in 150 mM NaCl-001N acetic acid. Angiotensin II was continuously infused into mice for a period of 14 days.

Histology, Staining and Microscopy

Hearts embedded in *Optimum Cutting Temperature* were transversally sectioned in 10 μm cuts using a Leica CM3060S cryostat (Leica Microsystems Inc., ON) and collected on Superfrost Plus microslides (VWR, PA). Samples were incubated in 0.5% Harris haematoxylin (Sigma-Aldrich, MO) for five minutes, rinsed with water, quickly immersed in 1% HCl/70% EtOH solution, rinsed with water, incubated in 1% eosin (Fisher Scientific, ON) for three minutes and rinsed with water. Slides were subsequently incubated in 70%, 80% and 90% EtOH solution for two minutes each and immersed in xylene (Fisher Scientific, ON) for thirty seconds. Slides were air dried and mounted in Permount (Fisher Scientific, ON). Images were captured on a Nikon SMZ1500 stereomicroscope.

For immunofluorescence, samples were fixed in 2% paraformaldehyde and washed with 1X PBS three times for five minutes. Tissues were blocked and permeabilized with 2% goat serum (Sigma-Aldrich, MO) and 0.2% Triton X-100 (Sigma-Aldrich, MO) for one hour. Samples were incubated overnight at 4ºC with primary antibody 1:50 NFATc1, 1:25 NFATc2, 1:25 NFATc3 and 1:50 NFATc4 (Santa Cruz

Biotech., CA) in 1X PBS containing 1% goat serum and 0.05% Triton X-100. The following day, samples were washed three times with 1X PBS and incubated with 1:50 or 1:100 anti-rabbit Alexa 488 (Molecular Probes, ON) in 1X PBS containing 1% goat serum and 0.05% Triton X-100 for one hour at room temperature. Slides are washed five times with 1X PBS, dried and mounted with Vectashield with DAPI (Vector Laboratories Inc., CA). Images were captures at 40x magnification using a Zeiss Axioplan fluorescence microscope.

Quantification and Statistics

The level of DNA and protein expression was quantified by measuring the density of the band of interest with respect to the control using the Alpha Innotec Fluorchem (Cell Biosciences, CA) system. Differences between experimental groups were evaluated for statistical significance using a Student's *t* test for assuming equal variance. All *p* values < 0.05 were considered to be statistically significant.

Results

Characterization of heart phenotype in NFATc2-/- mice

NFATc2-/- mice were generated by substituting the NFATc2 N-terminal DNA binding domain of the NFAT Rel Homology Domain with a neomycin cassette using

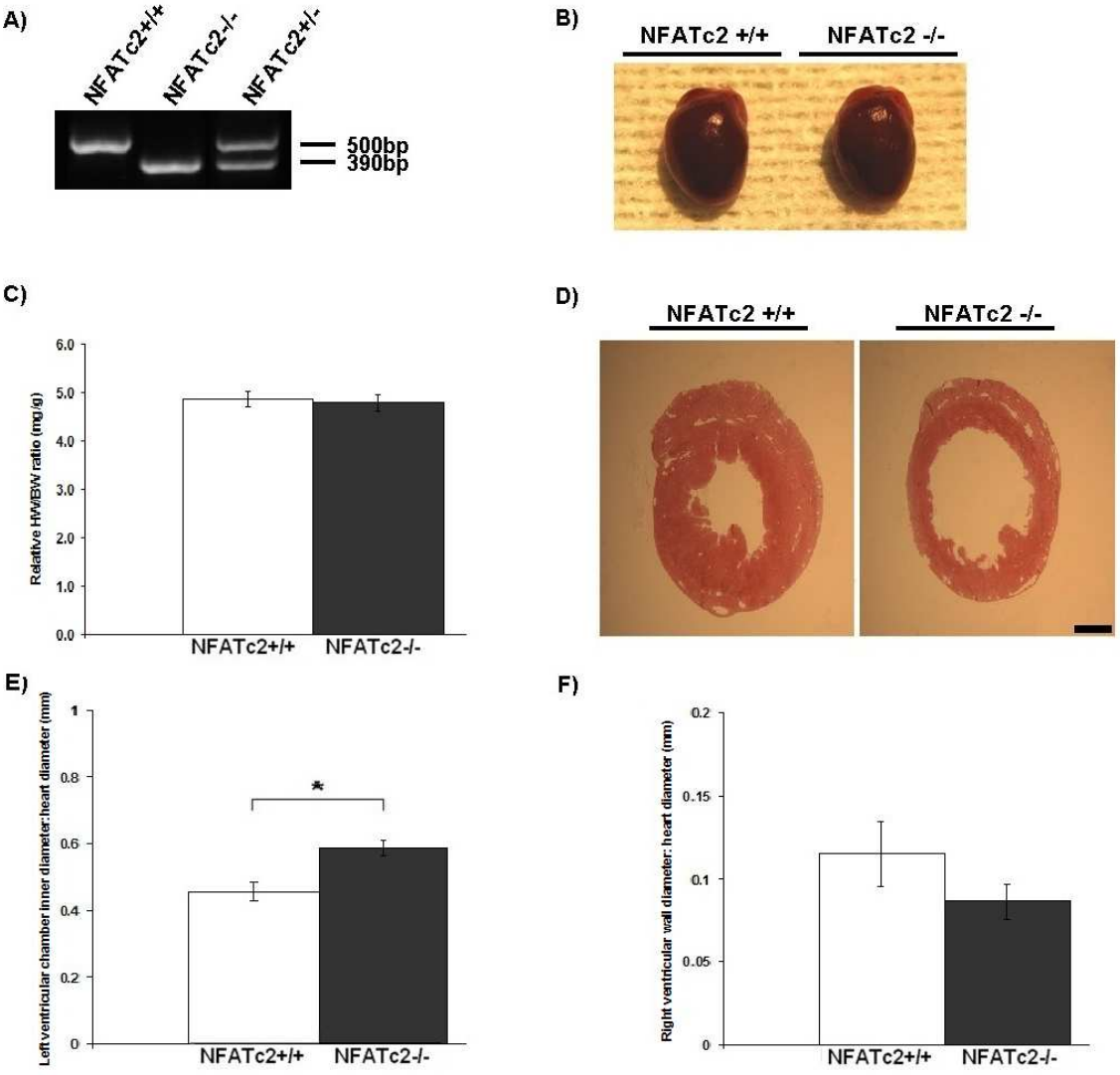

Figure 1. **Comparing the hearts of wild-type and NFATc2-/- mice**. A) Agarose gel image of PCR products from genomic DNA depicting the wild-type, NFATc2 knockout and heterozygous genotypes. B-C) Freshly extracted mice hearts and quantification of the relative heart weight-to-body weight ratio for wild-type (n=14) and NFATc2-/- (n=15) mice. D) Haematoxylin and eosin-stained heart sections and quantification of the E) left ventricle chamber inner wall diameter and F) right ventricle wall diameter normalized to total heart diameter (n=3 per group). *indicates statistical significance ($p<0.05$) compared to wild-type counterpart. Scale bar represents 1mm.

homologous recombination (144). The genotypes of experimental mice were validated by amplifying DNA isolated from the tail by PCR and resolved on an ethidium bromide-stained agarose gel (Fig. 1A). Wild-type and NFATc2-/- mice were anesthetized and the hearts were surgically extracted. Normotensive hearts of NFATc2-/- mice displayed a comparable overall gross morphology (Fig. 1B) and a similar relative heart weight-to-body weight (HW/BW) ratio (Fig. 1C), compared to wild-type mice. To examine heart morphology, we monitored changes in the sizes of heart ventricles and myocardial wall thickness because these are well-characterized markers of heart disease and failure. To determine whether the hearts of NFATc2-/- mice were more susceptible to failure, gelatin-infused hearts were transversally sectioned by histology and stained with haematoxylin and eosin (Fig. 1D). The ratio of the left ventricular chamber inner diameter to total heart diameter showed that the left ventricular chamber of NFATc2 -/- mice was approximately 28% more dilated than wild-type hearts (Fig. 1E). In addition, the thickness of the right ventricular wall was approximately 25% thinner than wild-type hearts (Fig. 1F). The collective findings showed that although hearts of adult NFATc2-/- mice shared similar overall shape and morphology as wild-type hearts, changes in both ventricular dilatation and thickness of the myocardial wall suggested that adult NFATc2-/- mice were more susceptible to heart disease and failure.

The transcript expression of NFATc1-c4 is unchanged, whereas the nuclear localization of NFATc1 is increased in the hearts of NFATc2-/- mice

The presence of all four Cn-regulated NFAT isoforms (NFATc1, NFATc2, NFATc3 and NFATc4) in the heart has been previously demonstrated (63). To monitor the ability of NFATc1, NFATc3 and NFATc4 to compensate for the absence of functional NFATc2 at the mRNA level, semi-quantitative PCR was conducted on cDNA that was reverse transcribed from RNA isolated from experimental hearts. Results showed no significant change in the expression of other NFAT isoforms in normotensive hearts of wild-type and NFATc2-/- mice (Fig. 2A, B). Note that the NFATc2 transcript remains expressed in NFATc2-/- mice because the NFATc2-/- mouse model used in these experiments is a loss-of-function mutation, where a mutant protein is synthesized. As transcription factors, NFAT proteins exert their transcriptional activities when localized in the nucleus in their unphosphorylated state. We therefore performed immunofluorescene to monitor the cellular distribution of NFATc1, NFATc3 and

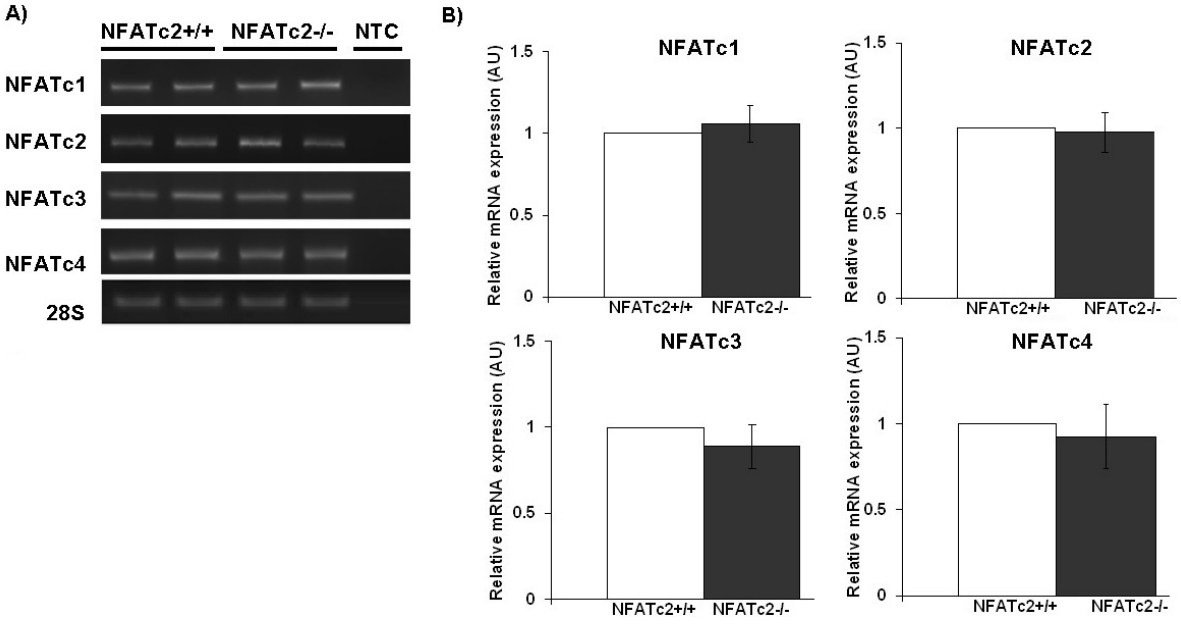

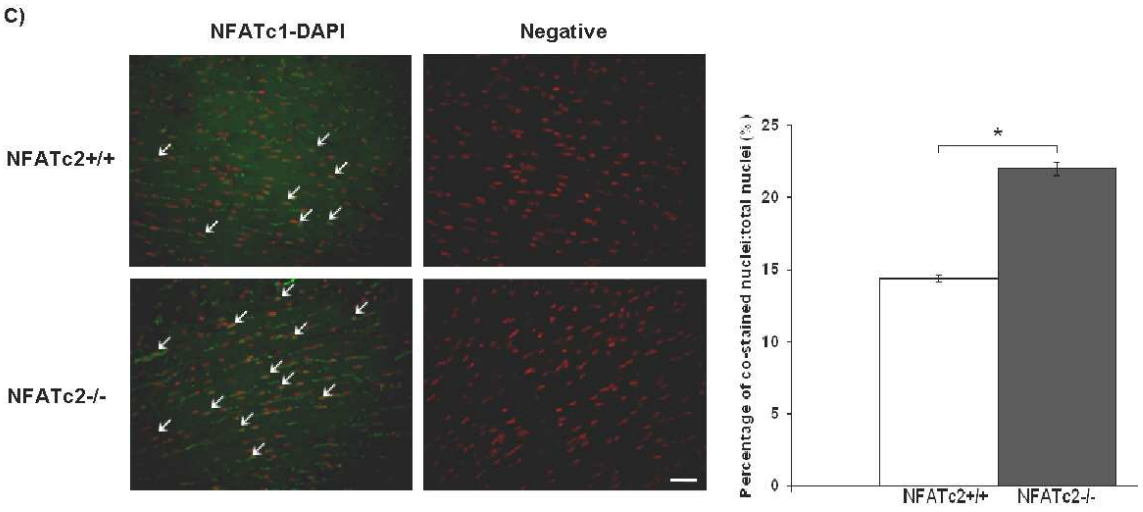
C)
NFATc1-DAPI
Negative
NFATc2+/+
NFATc2-/-
Percentage of co-stained nuclei:total nuclei (%)
25
20
15
10
5
0
*
NFATc2+/+
NFATc2-/-

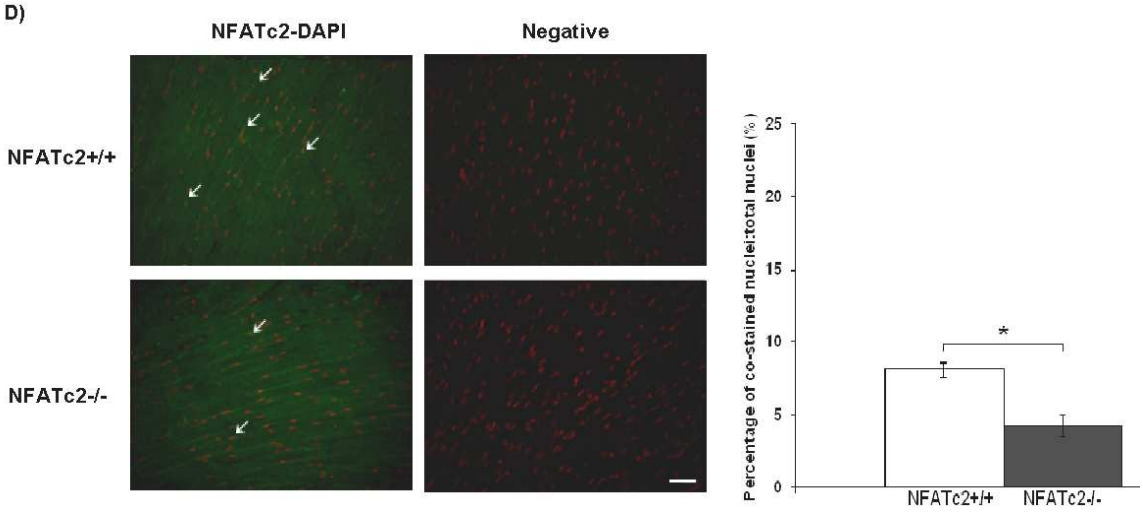
D)
NFATc2-DAPI
Negative
NFATc2+/+
NFATc2-/-
Percentage of co-stained nuclei:total nuclei (%)
25
20
15
10
5
0
*
NFATc2+/+
NFATc2-/-

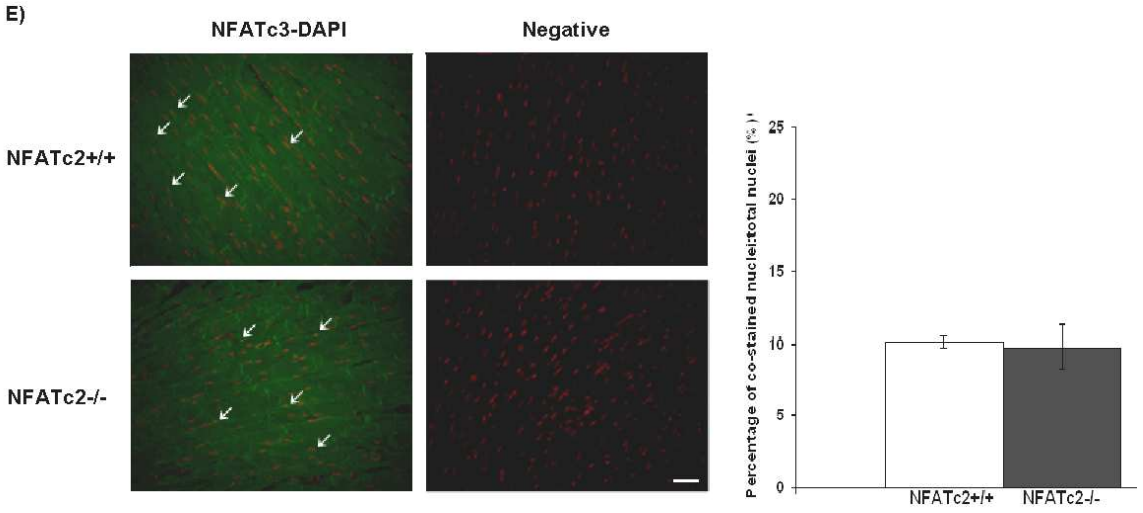
E)
NFATc3-DAPI
Negative
NFATc2+/+
NFATc2-/-
Percentage of co-stained nuclei:total nuclei (%)
25
20
15
10
5
0
NFATc2+/+
NFATc2-/-

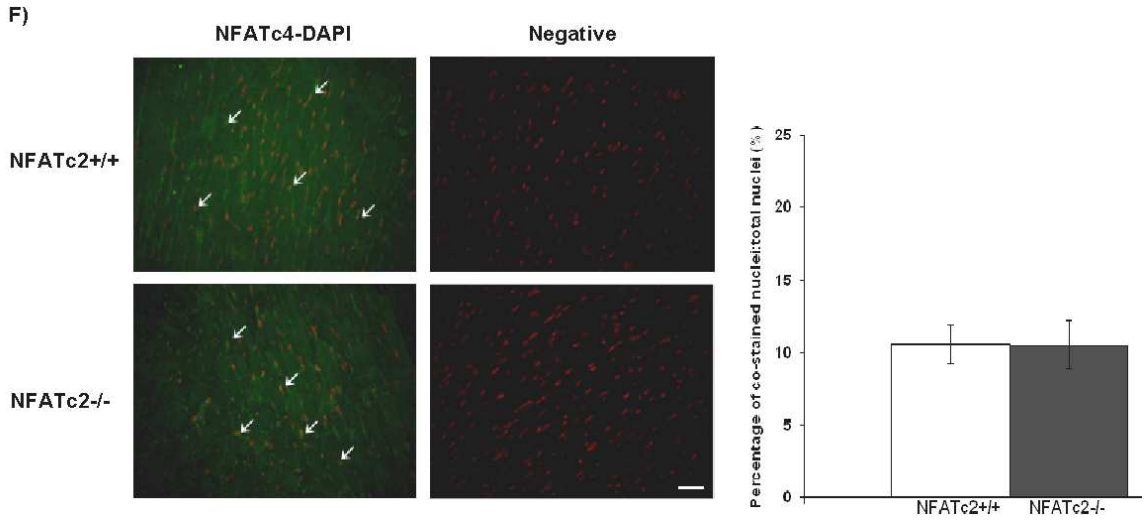

Figure 2. **NFATc1 is more nuclear localized in the hearts of NFATc2-/- mice**. A-B) Agarose gel image of PCR products for NFATc1-c4 and their quantifications normalized to ribosomal 28S gene expression (n=3 per group). No template control (NTC) is the addition of water instead of cDNA. C-F) Immunofluorescene images and quantifications of positively stained nuclei to total nuclei per field of view depicting the localization of NFAT isoforms (n=3 per group). The nuclei are visualized with DAPI, which was changed to red. To control for unspecific secondary antibody staining, the negative images have only the secondary antibody conjugated to the fluorophor Alexa 488 added, without a primary antibody. Note that DAPI does not require antibodies to be visualized, and is detected in the negative control panels. *indicates statistical significance ($p<0.05$) compared to wild-type counterpart. Scale bar represents 20μm.

NFATc4 in the absence of functional NFATc2. Our results showed that of the NFAT isoforms, only NFATc1 had a significantly higher nuclear presence in the hearts of NFATc2-/- mice (Fig. 2C). The nuclear translocation of NFATc3 and NFATc4 were unchanged between wild-type and NFATc2-/- mice (Fig. 2E, F). In addition, NFATc2 had a decreased nuclear presence in NFATc2-/- mice, which is likely a characteristic of the loss-of-function mutation (Fig. 2D). These results showed that, although no change was detected in transcript expression of NFAT members, NFATc1 was the only isoform which had a higher nuclear transit when functional NFATc2 protein was absent and therefore potentially compensates for the absence of non-functional NFATc2.

The GATA-4 transcription factor has a higher protein expression and nuclear transit in the hearts of NFATc2-/- mice

One of the most well characterized proteins required for cardiac morphogenesis and a marker of adult cardiac failure is the GATA-4 transcription factor (93). Amongst its numerous molecular partners, GATA-4 can interact with NFATc4 to synergistically activate the transcription of peptides leading to cardiac growth and eventually heart failure (43). Because the Cn-regulated NFAT isoforms share a conserved REL homology domain, we wanted to determine whether GATA-4 and NFATc2 could interact and if so, whether GATA-4 expression is altered in response to the absence of functional NFATc2. Using co-immunoprecipitation, we showed that GATA-4 and NFATc2 interacted and that the extent of this interaction was similar in the hearts of wild-type and NFATc2-/- mice, which suggests that the mutant NFATc2 protein also binds to GATA-4 (Fig. 3A). To control for the NFATc2 immunoprecipitation antibody specificity, we substituted this antibody with pre-immune goat serum. Neither GATA-4 nor NFATc2 bands were visible in the serum lanes, confirming the effectiveness of the immunoprecipitation assay. Furthermore, to test the purity of the immunoprecipitation, non-precipitated supernatant was loaded alongside the immunoprecipitated samples. We detected that α-tubulin, a globular protein found in the extracellular matrix and does not interact with NFAT, was expressed only in the supernatant extract, and not the immunoprecipitated samples. This eliminates the possibility that non-NFATc2 interacting proteins were present in our immunoprecipitated samples. Although GATA-4 was not upregulated in the hearts of adult NFATc2-/- mice at the transcript level (Fig. 3B, C), it was significantly upregulated at the protein level (Fig. 3D, E), suggesting that the expression of GATA-4 was increased

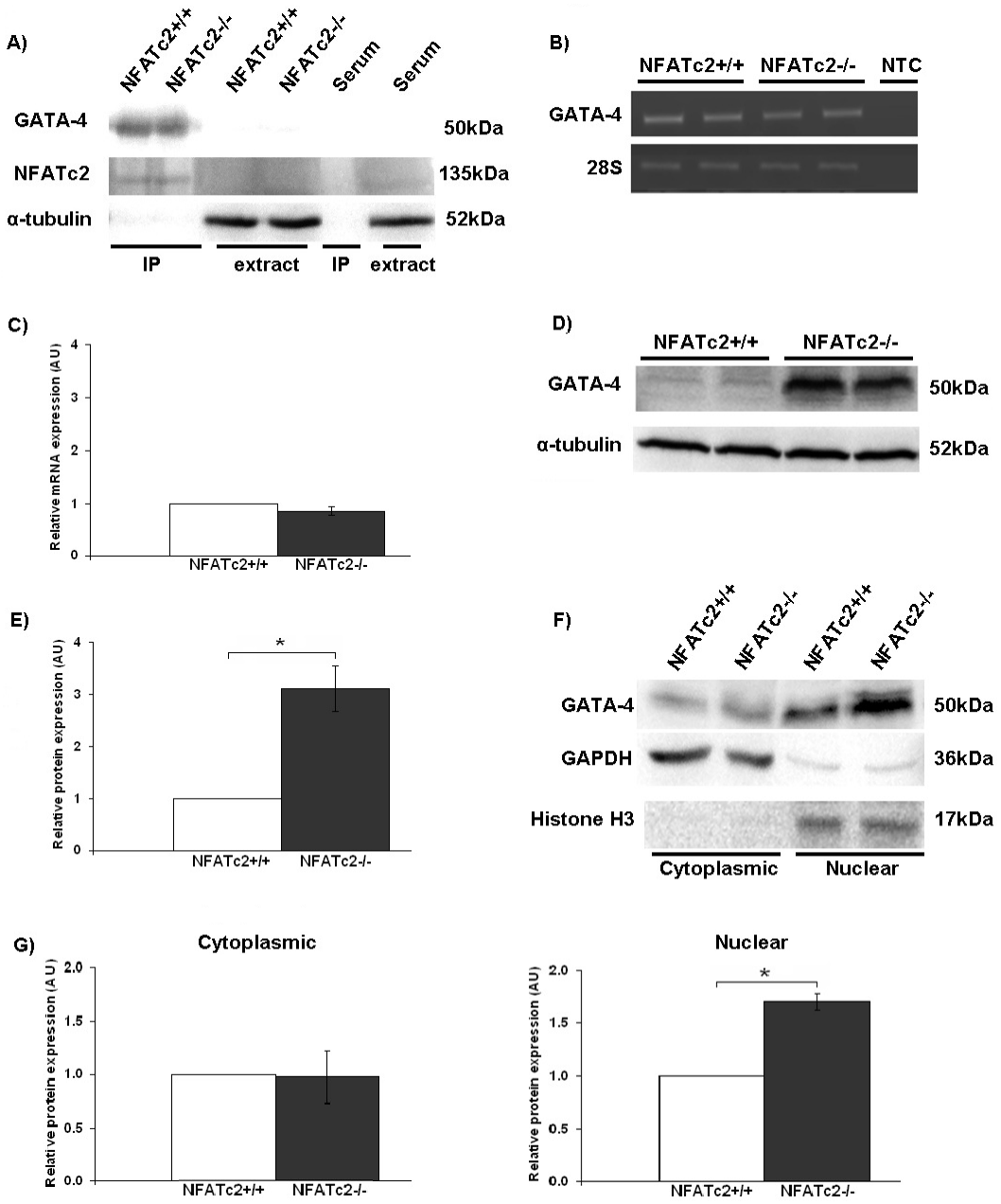

Figure 3. **GATA-4 is increased and has higher nuclear transit in NFATc2-/- mice**. A) Western blot representing GATA-4 and NFATc2 co-immunoprecipitation (n=3 per group). As a control, immunoprecipitated (IP) samples, supernatant extract and goat serum treated samples were loaded together. B-C) Agarose gel image of PCR products for GATA-4 and its quantification normalized to ribosomal 28S gene expression (n=3 per group). D-E) Western blot of GATA-4 expression in whole heart protein homogenate and its quantification normalized to α-tubulin expression (n=3 per group). F-G) Western blot and respective quantifications of hearts fractionated in cytoplasmic and nuclear protein extracts (n=3 per group). A double band is visualized in the nuclear fraction possibly due to additional phosphorylated sites on GATA-4. *indicates statistical significance ($p<0.05$) compared to wild-type counterpart.

to compensate for the loss of a functional DNA binding mutation in the NFATc2 protein. To determine whether there was also an increased nuclear transit of GATA-4 in the hearts of adult NFATc2-/- mice, we fractionated the hearts into cytoplasmic and nuclear protein extracts using glyceraldehyde-3-phosphate dehydrogenase (GAPDH) and Histone H3 as protein controls to verify the purity of the fractionation. Results showed that GATA-4 expression was comparable in the cytoplasmic fraction of wild-type and NFATc2-/- mice cardiomyocytes, whereas GATA-4 was significantly upregulated in the nuclear fraction of these cells in NFATc2-/- mice, compared to the wild-type counterparts (Fig 3F, G). Note that two bands are visible in the GATA-4 nuclear fraction because GATA-4 may be phosphorylated at other serine residues (146). These results indicated that as a molecular partner of NFATc2, GATA-4 was both upregulated and had an increased nuclear transit when functional NFATc2 was not available, suggesting that GATA-4 compensated for the mutated NFATc2 in a failed attempt to rescue cardiac growth and overt cardiac failure.

The expression of GSK-3β is lowered in the hearts of NFATc2-/- mice, whereas MAPK and CK-1α expression remain unchanged

Several kinases, such as GSK3-β, CK and the family of mitogen activated protein kinases (MAPK): JNK, p38 and ERK, are known to regulate the cellular locations of NFAT and GATA-4 transcription factors through their phosphorylation status. GSK3- β is a known NFAT/GATA export kinase, CK-1α and JNK-2 are NFAT export kinases, whereas p38-1α and ERK1/2 are also NFAT exporters, but increase GATA-4 DNA

binding under hypertrophic stimulations (93). Because the nuclear presence of NFATc1 and GATA-4 was increased in NFATc2-/- mice, we monitored the expression of these kinases to determine whether changes in their expression were representative of the

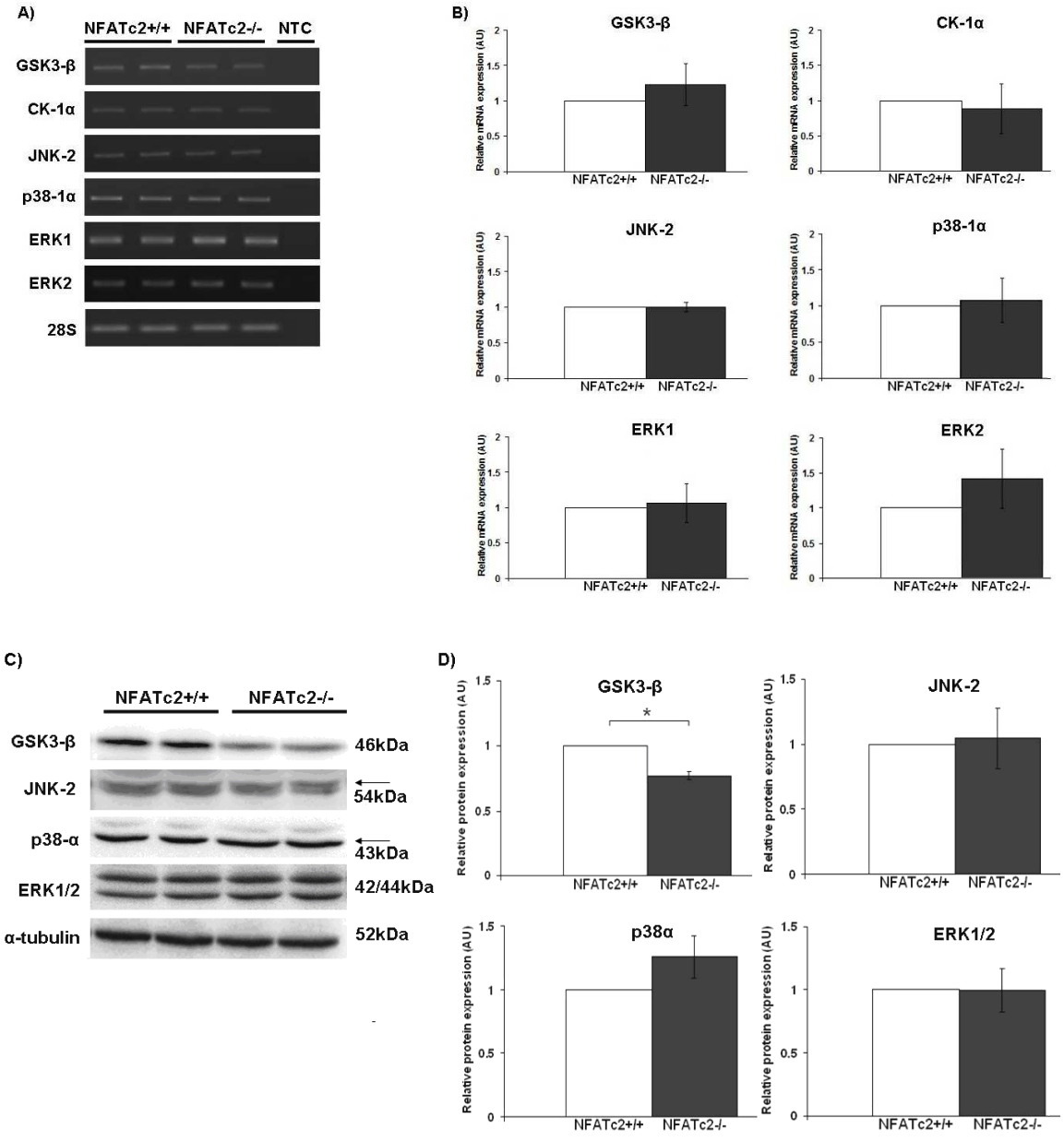

Figure 4. **GSK3-β expression is downregulated in the hearts of NFATc2-/-mice**. A-B) Agarose gel image of PCR products for GSK3-β, CK-1α, JNK-2, p38-1α and ERK1/2 and their quantifications normalized to ribosomal 28S gene expression (n=3 per group). C-D) Western blots of total kinase expression and their quantifications normalized to α-tubulin expression (n=3 per group). *indicates statistical significance ($p<0.05$) compared to wild-type counterpart.

increased nuclear localization of these factors. At the transcript level, the expression of these kinases were not different between the wild-type and NFATc2-/- hearts (Fig. 4A, B). At the protein level, only GSK3-β was found to be significantly downregulated in the absence of functional NFATc2, whereas the expressions of members of the MAPK family were unchanged (Fig. 4C, D). As a major regulator of pathological cardiac hypertrophy and heart failure, the collective results suggested that this change in the expression of GSK3-β correlates with the increased nuclear presence of NFATc1 and GATA-4 in normotensive hearts of adult NFATc2-/- mice.

Angiotensin II-mediated cardiac hypertrophy suggests NFATc2-/- mice have exacerbated morphological and anatomical markers of heart failure

Because normotensive adult NFATc2-/- mice displayed both physiological and biochemical alterations indicative of heart failure, we induced acute cardiac hypertrophy in these mice using angiotensin II (Ang II) administration. Ang II is a peptide from the renin-angiotensin system known to promote vasoconstriction, increases in blood pressure and rapid cardiac hypertrophy (147). We hypothesized that by imposing further strain on NFATc2-/- mice by using a functional overload, the hearts of these mice would display a more severe pathological state. Ang II-mediated cardiac hypertrophy was validated by a 15% increased HW/BW ratio (Fig. 5A) and elevated expression of the cardiac fetal genes, β-MyHC, ANP and BNP, in wild-type mice (Fig. 5E-H). We observed that Ang II-infused adult NFATc2-/- mice had a similar HW/BW ratio as non-infused NFATc2-/- mice (Fig. 5A), suggesting that the hearts of normotensive NFATc2-/- mice are already in

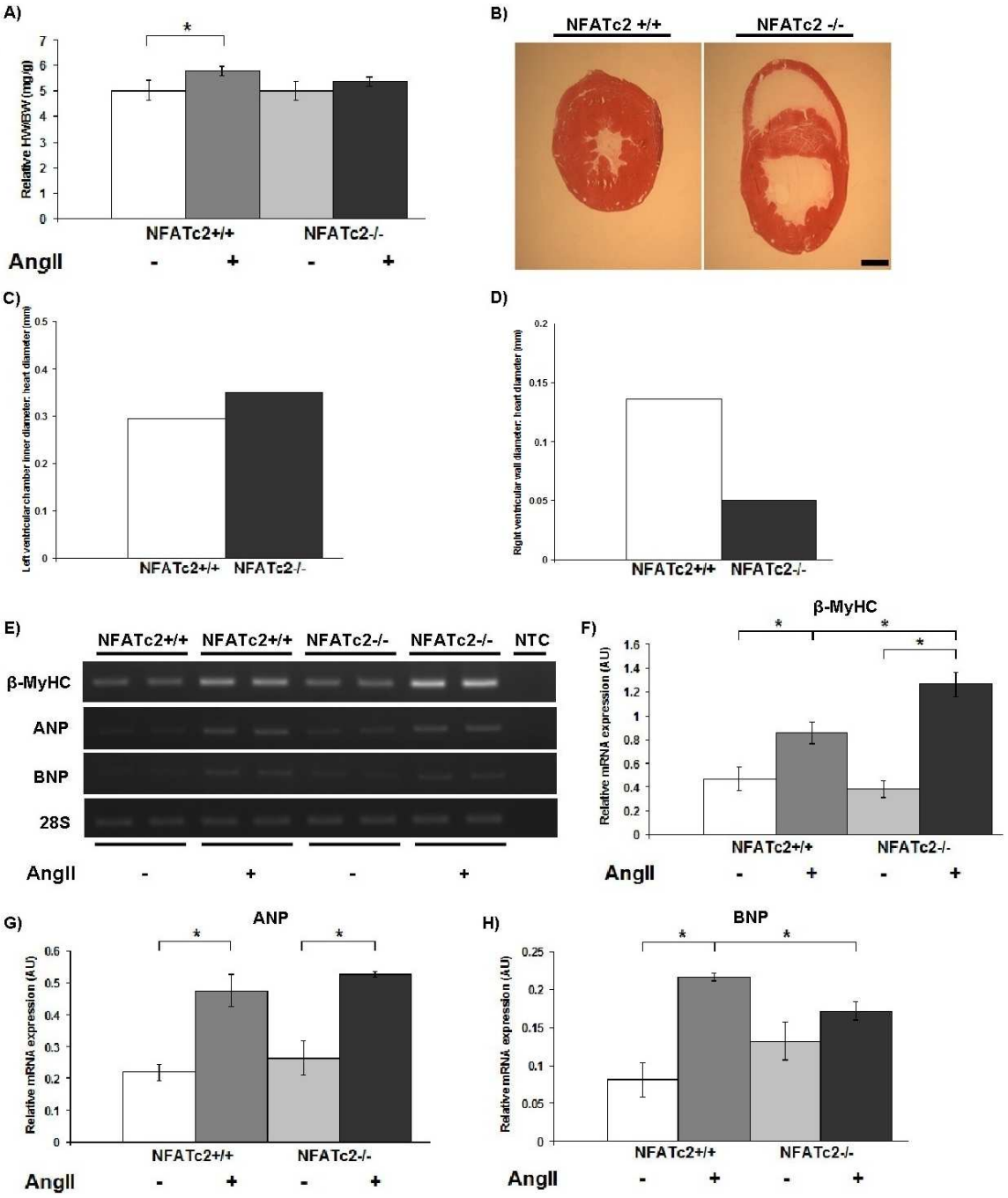

Figure 5. **Ang II-infused NFATc2-/- mice display a more severe heart pathology**. A) HW/BW ratio of non-stimulated and Ang II-infused adult wild-type and NFATc2-/- mice (n=3 per group). B) Haematoxylin and eosin-stained heart sections of Ang II-infused hearts and its quantification of the C) left ventricle chamber inner wall diameter and D) right ventricle wall diameter normalized to total heart diameter (n=1 per group). E-H) Agarose gel image of PCR products for β-MyHC, ANP and BNP and their quantifications normalized to ribosomal 28S gene expression (n=3 per group). *indicates statistical significance ($p<0.05$). Scale bar represents 1mm.

an advanced pathological state. When comparing the left ventricular inner chamber diameter and thickness of the right ventricular wall in Ang II-infused wild-type and NFATc2-/- mice, we observed that NFATc2-/- mice had a more drastic left ventricular heart chamber dilatation and thinning of the ventricle walls, implying that imposed acute pharmacological stress on these mice causes these hearts to undergo morphological changes towards a more advanced state of failure (Fig. 5B-D). Also, these data present the idea that hearts of NFATc2-/- mice are in a diseased state not because of the usual markers of cardiac hypertrophy (ie: HW/BW ratio), but moreso as a result of more accurate morphological markers of heart chamber dilatation and thinner ventricular walls. The reactivation and increased expression of cardiac fetal genes are another hallmark feature of hearts undergoing a pathophysiological hypertrophy and damage. We showed that of all fetal genes tested, only the β-MyHC gene was increased in expression, whereas both ANP and BNP genes were either unchanged or downregulated in expression, when comparing Ang II-induced NFATc2-/- mice to wild-type counterparts (Fig. 5E-H). These results suggest that not only is Ang II-stimulation causing the hearts of NFATc2-/- mice to exhibit more severe morphological signs of failure, but that changes in the expression of cardiac fetal genes may be regulated by separate mechanisms.

GATA-4 and phospho-AKT tends to be downregulated, whereas phospho-eIF2 is unchanged in hearts of angiotensin II-infused NFATc2-/- mice,

Because we hypothesized the hearts of Ang II-stimulated NFATc2-/- mice were more likely to fail due to an acutely increased workload on an already failing heart, we were interested in determining whether GATA-4 would be produced at a higher level in the hearts of Ang II-infused NFATc2-/- mice. Our preliminary data (n=2) suggested that GATA-4 expression tended to increase in the hearts of Ang II-infused wild-type but decreased in Ang II-infused NFATc2-/- mice, compared to non-stimulated hearts (Fig. 6A, B). This suggests that in the normotensive hearts of NFATc2-/- mice, NFATc1 and GATA-4 are compensating for the mutated NFATc2 protein, in an effort to promote increased gene transcription and heart growth. However, because functional NFATc2 is absent in these mice, these hearts cannot readily hypertrophy, causing increased imposed cardiac workload in NFATc2-/- mice. When cardiac hypertrophy was induced, GATA-4 protein expression in Ang II-infused NFATc2-/- mice was not different from the hearts of unstimulated wild-type mice, which implies that the additional cardiac workload in NFATc2-/- mice caused an inactivation of transcription-mediated growth in these mice.

We then investigated whether pathways regulating protein translation were also inactivated in Ang II-infused NFATc2-/- mice. The IGF-1/AKT signaling pathway is one of the most studied growth pathways involved in promoting both gene transcription and protein translation, as well as inhibiting the activation of pathways resulting in protein degradation. In addition, phospho-AKT (Ser473), the active form of AKT, negatively regulates GSK3-β activity, which in turn promotes the nuclear export of NFAT and GATA-4 transcription factors. Based on our findings that GATA-4-mediated gene

transcription was shut down in Ang II-induced cardiac hypertrophy of NFATc2-/- mice, we speculated that the expression of activated AKT would also be downregulated in Ang II-infused NFATc2-/- mice. Preliminary data (n=2) suggested that phospho-AKT expression was upregulated in the hearts of Ang-II wild-type mice but downregulated in

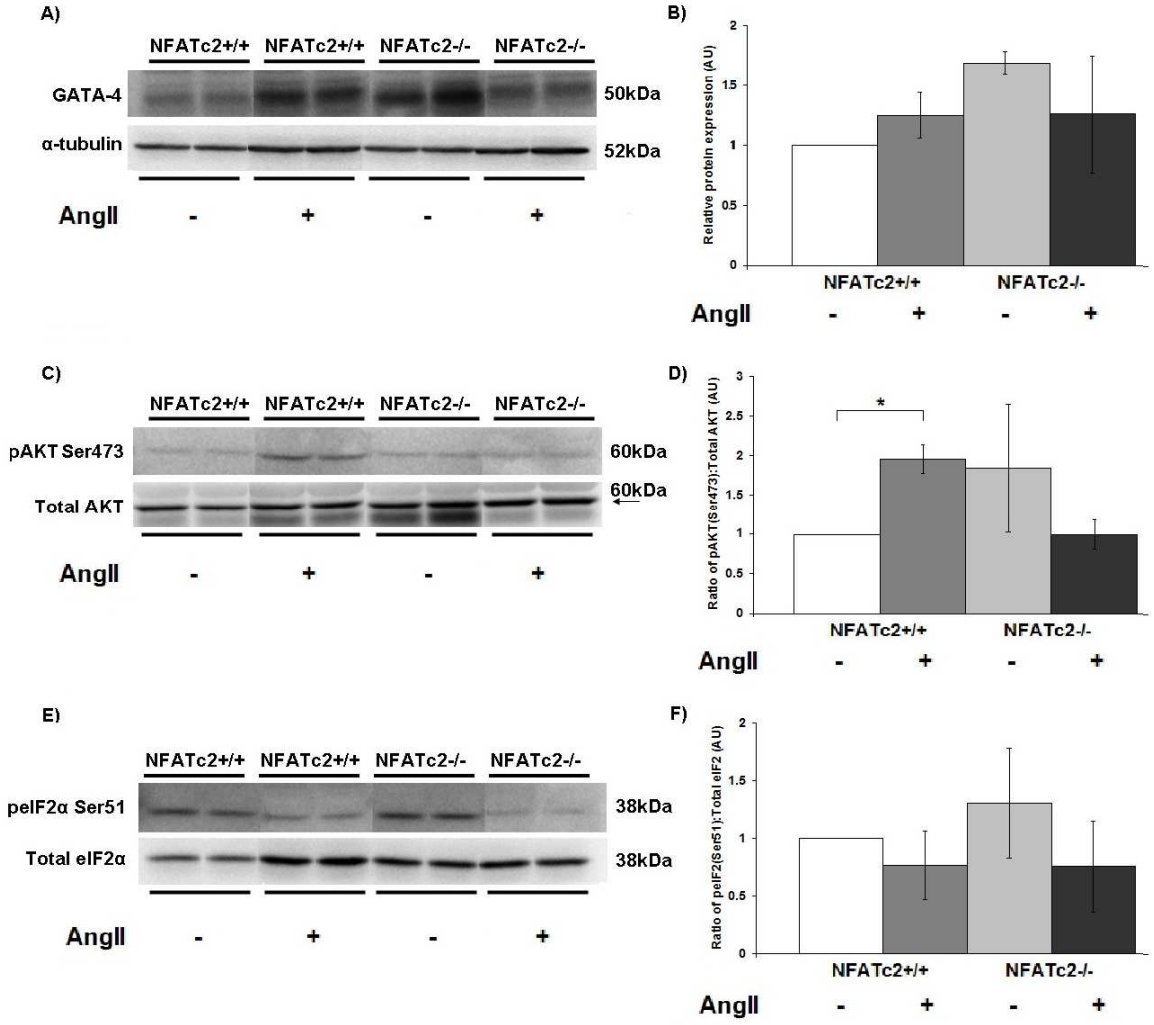

Figure 6. **GATA-4 and AKT are decreased in Ang II-infused NFATc2-/- mice**. A-B) Western blot of GATA-4 expression in non-stimulated and AngII-infused wild-type and NFATc2-/- mice and its quantification normalized to α-tubulin expression (n=2 per group). C-D) Western blot of phospho-AKT (Ser473) expression in non-stimulated and AngII-infused wild-type and NFATc2-/- mice and its quantification normalized to total AKT expression (n=2 per group). E-F) Western blot of phospho-eIF2α (Ser51) expression in non-stimulated and AngII-infused wild-type and NFATc2-/- and its quantification normalized to total eIF2α expression (n=2 per group). *indicates statistical significance ($p<0.05$) compared to wild-type counterpart.

Ang II-infused NFATc2-/- mice, compared to non-stimulated hearts (Fig. 6C, D). Although two bands are visible when probing for total AKT, the lower band was deemed unspecific in mice using alkaline phosphatase treatment and western blots on rat muscles (data not shown).

As a marker to measure translational control in NFATc2-/- mice, we monitored the expression of eukaryotic initiation factor 2 (eIF2), a protein required for transferring the $tRNA^{met}$ to the 40S ribosome in a GTP-dependent manner to initiate protein translation. Furthermore, eIF2 promotes protein translation by exchanging GDP to GTP, which is catalyzed by the guanine nucleotide exchange factor, eukaryotic initiation factor 2B (eIF2B). When eIF2 is phosphorylated at Ser51 on its α-subunit by serine kinases, phosphorylated eIF2 has an increased affinity to bind eIF2B, which decreases eIF2 activity by inhibiting the GDP to GTP exchange, therefore blocking successive rounds of protein translation (148). Our results showed that the expression of phospho-eIF2α (Ser51) was unchanged between Ang II-mediated cardiac hypertrophy of wild-type and NFATc2-/- mice, which correlated with a downregulated activated AKT expression, suggesting that translation in the hearts of Ang II-infused NFATc2-/- mice was switched off. These results suggest the increased strain that Ang II infusions have on the hearts of NFATc2-/- mice causes a shutdown of both transcriptional and translational mechanisms, which prevents the heart from attempting to hypertrophy, possibly to avert cell damage and eventual heart failure.

Discussion

Recently published work proposed that young 1-2 month old NFATc2-/- mice are more resistant to Cn-mediated cardiac hypertrophy and have restored heart function (143). This finding suggested that the NFATc2 transcription factor was the major NFAT isoform involved in promoting pathological cardiac hypertrophy and heart failure; however the authors failed to study the molecular mechanisms implicated in this response. We thus set out to explore the changes in growth-mediated signaling pathways in the hearts of NFATc2-/- mice.

During the initial phase of our study, we observed that adult 6-9 month old NFATc2-/- mice were more susceptible to sudden death and had enlarged hearts when autopsied. Our results demonstrate that adult NFATc2-/- mice displayed left ventricular inner chamber dilatation and thinner ventricular walls, characteristic of heart failure. In addition, modulations in the Cn-NFAT signaling, as well as other growth-mediated pathways parallel to Cn-NFAT, are indicative that other transcription factors compensate for the genetic loss of NFATc2, in a failed attempt to promote cardiac growth. By administering Ang II to impose an increased cardiac workload on NFATc2-/- mice, we also observed an inactivation of transcriptional and translational mechanisms, suggesting that increased strain on these mice inhibits pro-survival and growth-mediated signaling. Thus, our findings appear to be in contrast to previous work done in younger mice, which proposes that a loss-of-function mutation in NFATc2 may appear beneficial in young mice based solely on improved physiological appearance and heart function, although these young NFATc2-/- mice could display changes in biochemical signaling. Overtime,

changes in growth-mediated signaling may predispose these mice to eventual heart deterioration and overt heart failure, which is seen in adult NFATc2-/- mice.

Functional NFATc2 is required for proper heart function in adult mice

One finding which we did not anticipate in this study was that, although the hearts of 6-9 month old NFATc2-/- mice shared an overall similar gross morphology and HW/BW ratio as age and sex-matched wild-type mice, NFATc2-/- mice displayed a more dilated left ventricular chamber inner diameter and a thinner right ventricle wall, both of which are characteristic of compromised cardiac contractility and eventual heart failure. Previously published work (143) has demonstrated that hearts of 1-2 month old NFATc2-/- mice displayed no significant change in left ventricular internal diameter and contractility of the left ventricle compared to wild-type mice, which diverges from our findings in adult mice. The idea that adult 6-9 month old NFATc2-/- mice exhibited heart failure-like symptoms correlated with our empirical observations that these mice appeared frailer, more susceptible to sudden death and displayed cardiac dilatation upon autopsy. Our findings support the idea that the absence of functional NFATc2 (ie: with DNA binding ability) appears to be beneficial in the early stages of physiological development as a mean to resist stress-induced cardiac hypertrophy and failure, but may be detrimental towards overall heart function at later stages of life. Because NFATc2 was shown to be the major isoform responsible for cardiac hypertrophy, a scenario which may explain the idea that NFATc2-/- mice are more susceptible to long-term heart failure is that in younger mice, other transcription factors may be compensating for the absence of

NFATc2, which allows these mice to overcome heart failure. However, in adulthood, these transcription factors no longer compensate for NFATc2, which may also shutdown pro-growth signaling pathways, thereby disposing adult NFATc2-/- mice to physiological and biochemical characteristics of heart failure.

NFAT isoforms are differentially localized in the hearts of NFATc2-/- mice

In the heart, the four Cn-regulated NFATs are expressed and exist in multiple splice variants, which are encoded by four independent genes. Because no compensation by NFATc1, NFATc3 and NFATc4 for the absence of functional NFATc2 was detected at the transcript level, we opted to monitor NFAT cellular localization. As transcription factors, NFAT proteins effectuate their transcriptional activities upon being de-phosphorylated by Cn, enabling nuclear translocation which leads to transactivation of cardiac fetal genes during heart disease. Our immunofluorescene results indicated that the nuclear translocation of NFATc1 was significantly higher, whereas nuclear NFATc3 and NFATc4 levels were unchanged in the normotensive hearts of NFATc2-/- mice. In addition, a decreased nuclear presence of NFATc2 in NFATc2-/- mice is likely attributed to the inability of mutant NFATc2 to bind to DNA, resulting in NFATc2 being more readily exported from the nucleus by export kinases.

Because NFATc1 has higher nuclear transit in the hearts of NFATc2-/- mice, it may be compensating for NFATc2 in an attempt to increase growth-mediated transcription. Dunn et al. (149) have identified that Cn-mediated de-phosphorylation of NFATc1 was correlated with increased muscle usage, in which normal weightbearing

soleus and functional overload-induced plantaris muscles expressed more de-phosphorylated NFATc1. In addition, Shen et al. (150) have demonstrated that NFATc1 has a higher cytoplasmic to nuclear shuttling in resting skeletal muscle cells, compared to other NFAT proteins, which suggests that the Cn-NFATc1 has a higher basal activity than other NFAT isoforms. In addition, the role of the NFATc1 transcription factor in heart function remains the least understood of all the isoforms because although NFATc1 is important in the formation of the heart valves and cardiogenesis, NFATc1-/- mice are embryonic lethal and die at E14.5, whereas other NFAT knockout models remain viable (83). This suggests that NFATc1 is likely an important factor for physiological heart growth, which may explain why NFATc1, but not NFATc3 or NFATc4, is the NFAT isoform which compensates for the genetic loss of NFATc2 function in the heart. However, although NFATc1 has an increased nuclear translocation in response to the absence of NFATc2, NFATc1 might not be able to fully restore proper cardiomyocyte growth, function and size because NFATc2-/- mice display changes in the ventricles which are characteristic of heart failure.

The loss of functional NFATc2 alters the signaling of other cardiac growth-mediated pathways

NFAT transcription factors are known to interact with molecular partners in the nucleus to reactivate cardiac fetal genes in response to hypertrophic stimuli leading to heart failure (43,49,60,66). Our results demonstrate that GATA-4 and NFATc2 can co-precipitate, suggesting they interact to modulate cardiac gene expression, which is in

correlation to findings form other groups (43,151,152). Previous work has shown that NFATc4 and GATA-4 binding sites exist upstream and proximal to the BNP promoter, a known cardiac fetal gene, and that the dimerization of both transcription factors is required to activate BNP transcription, inducing the cardiac hypertrophic response (43,94). As in all Rel proteins, NFATc2 shares the conserved C-terminal DNA binding domain of the RHR, enabling NFATc2 to bind to NFAT binding sites near the BNP promoter. In addition to BNP, GATA-4 has been shown to directly bind to the promoters of the ANP, α-MyHC and β-MyHC genes, regulating their expression in the heart (91). NFAT proteins can regulate certain T-cell genes by binding to a common DNA sequence with AP-1 factors. Although the exact mechanism of how NFAT and GATA proteins interact remains ill-defined, due to the binding sites of both these factors not being immediately adjacent to one another, it could suggest that they cooperate either by intermediate players or by looping of the DNA (43,153). To address this point, immunoprecipitation, EMSA and ChIP could be used to identify other interacting proteins in the NFAT-GATA complex bound, their DNA binding ability and sequence, as well as *in vitro* luciferase assays to monitor transcriptional activities of possible intermediate factors.

In addition, we show that the overall expression and nuclear translocation of GATA-4 protein is significantly elevated in both whole homogenate and fractionated hearts of NFATc2-/- mice. As a well characterized marker of cardiac hypertrophy, such an increased level of GATA-4 protein is a strong indicator of a heart that is diseased, overly stressed and more likely to fail. Both *in vitro* and *in vivo* overexpression of GATA-4 is necessary and sufficient to induce morphological, functional, molecular and

structural changes resulting in cardiomyocyte remodeling and failure (97,154,155). Liang et al. (97) used adenoviral-mediated gene transfer to overexpress GATA-4 in neonatal cardiomyocytes, which resulted in a 2-fold increase in cardiomyocyte area and increased protein translation. In addition, transgenic mice overexpressing GATA-4 in the heart displayed increased cardiac hypertrophy, fibrosis, reactivation of cardiac fetal genes and reduced function (97). Despite GATA-4 -/- mice being embryonic lethal, Oka et al. (156) successfully generated a cardiac-specific GATA-4 deletion in mice using a Cre-loxP method of recombination. In addition to these mice failing to undergo pressure overload and exercise-induced cardiac hypertrophy, they also displayed a compromised contractility, induced dilatation, enhanced myocyte apoptosis, increased β-MyHC gene expression and decreased lifespan following pressure overload, all of which implies that controlled levels of GATA-4 are required for normal maintenance and function of the heart. In response to forced swimming, the hearts of GATA-4 deleted hypertrophied to a lesser extent compared to wild-type mice, suggesting that GATA-4 may have a role in physiological cardiac growth (156).

The significant increase in GATA-4 protein expression and nuclear import in NFATc2-/- mice suggests that GATA-4 is compensating for the absence of functional NFATc2. Similar to NFATc1, GATA-4 may be attempting to promote transcriptional growth in the hearts of NFATc2-/- mice, but cannot completely compensate for the lack of NFATc2, causing these hearts to fail in adulthood. Another possibility is that GATA-4 is increased in overall expression is that because mutant NFATc2 cannot bind to DNA, as its transcriptional partner, GATA-4 may also have an impaired ability to bind DNA. This

may promote more GATA-4 cytoplasmic to nuclear shuttling, while the cell continues to produce more GATA-4 in response to the absence of NFATc2.

GATA-6, another GATA protein expressed in the heart, has been identified as a regulator of pathological cardiac hypertrophy, where it was found to be necessary and sufficient to regulate the cardiac hypertrophic response, either independently or in coordination with GATA-4 (157). GATA-6 deleted mice are resistant to pressure overload and Ang II-induced cardiac hypertrophy, but developed heart failure whereas mice with a deletion of both GATA-4 and GATA-6 resulted in severe dilated cardiomyopathy. Both models showed cardiac dilatation, thinned myocardial walls, decreased functionality, severe heart failure, and the GATA-4/GATA-6 deleted mice died by 4 months of age (157). Because GATA-6 deleted mice remain viable, whereas GATA-4/GATA-6 deleted mice are not, this suggests that GATA-4 may be compensating for GATA-6, in a failed attempt to restore normal cardiac growth, which is similar to our findings that NFATc1 and GATA-4 are striving to compensate for a mutant NFATc2.

In parallel with our finding that both NFATc1 and GATA-4 have higher nuclear levels in the absence of functional NFATc2, we observed that GSK3-β was significantly downregulated, whereas the expression of p38, ERK1/2 and JNK were unchanged in the hearts of NFATc2-/- mice. GSK3 kinase has been previously described as the master regulator of growth and death in cardiac myocytes because of its ability to counter and reverse stress-induced cardiac hypertrophy and failure (158). Haq et al. (100) identified that GSK3-β was phosphorylated on Ser9, thereby inhibiting GSK3-β activity, in response to endothelin-1 (ET-1) in cultured cardiomyocytes. In addition, a mutation of GSK3-β Ser9Ala was sufficient to prevent phenylephrine (PE) and ET-1-induced

cardiomyocyte hypertrophy and sarcomere rearrangement (100). In addition, Antos et al. (140) showed that transgenic mice overexpressing GSK3-β in the heart were resistant to isoproterenol, pressure overload and CnA*-induced cardiac hypertrophy. Furthermore, stimulation of cardiomyocytes with β-adrenergic receptor agonists promoted GSK3-β-mediated nuclear export of GATA-4, suggesting that GATA-4 was a key downstream target of GSK3-β (101). The lowered protein expression of GSK3-β found in the hearts of NFATc2-/- mice is in agreement to the increased nuclear presence of both GATA-4 and NFATc1, which further suggests that signaling which promotes cardiac hypertrophy and failure are activated in NFATc2-/- mice.

Based to the observed increased GATA-4 nuclear presence, we speculated the expression of p38 and ERK protein kinases would be increased in NFATc2-/- mice, because of their role in mediating the phosphorylation of Ser105 of GATA-4, which promotes increased DNA binding activity in response to cardiac hypertrophy stimulation (98,99,159). ERK is proposed to be a regulator of basal GATA-4 activity; whereas both p38 and ERK activate GATA-4 when stimulated with endothelin-1 (93). Although we did not observe any changes in expression of total ERK or p38 protein expression, there exists additional, unknown mechanisms, other than ERK and p38, that could potentially regulate GATA-4 Ser105 phosphorylation (93). Arceci et al. (146) have identified that GATA-4 contains at least six other serine residues which could be targets of the MAPK or other regulatory mechanisms to control the cellular localization and DNA binding activity of GATA-4. In addition to total ERK and p38 expression, future experiments consist of monitoring the expression of activated phospho-ERK1/2 (Thr202/Tyr 204, Thr185/Tyr187) and phospho-p38 (Thr180/Tyr182). It is noteworthy to also monitor

upstream regulators of the MAPK, with specific emphasis on MAPK kinase kinases (MEKK and Raf) and MAPK kinases (MEK1/2, MKK3/6 and MKK4/7), which in turn phosphorylate and activate the MAPK (135).

Stress-induced cardiac growth of NFATc2-/- mice leads to alterations in fetal gene expression and growth mediated-signaling

Because some changes in signaling are minimal or absent in normotensive hearts, we stimulated cardiac hypertrophy in mice using Ang II. As observed in normotensive hearts, the HW/BW ratio of adult 6 month old Ang II-infused NFATc2-/- mice was similar that of Ang II-infused wild-type mice, which differs from previous work showing that younger 1-2 month old Ang II-infused NFATc2-/- mice displayed a HW/BW ratio that was significantly lower than wild-type counterparts (143). The Ang II-infused adult NFATc2-/- mice also displayed a much thinner right ventricular wall and increased left ventricular inner chamber diameter, compared to the hearts of normotensive adult NFATc2-/- mice, which suggests that by imposing increased cardiac workload, adult NFATc2-/- mice are more likely be subjected to severe heart failure.

We expected that the transcript expression of β-MyHC, ANP and BNP would be increased in Ang II-stimulated adult NFATc2-/- mice, which would suggest of that these mice are more vulnerable to cardiac disease. Our results were unexpected because although we observed increased β-MyHC expression, ANP expression was unchanged and BNP expression was lowered in Ang II-infused NFATc2-/- mice. The regulatory mechanisms that control the expression of cardiac fetal genes is complex and remains poorly understood. Yokota et al. (160) first proposed that hypertension-induced cardiac

hypertrophy, α and β-MyHC isoform conversion and the production and secretion of natriuretic peptides were differentially regulated based on the location of the heart and stage of heart failure. One report has shown that aldosterone-stimulated cardiac hypertrophy did not induce an α-to-β-MyHC conversion in rat hearts (161). Furthermore, ANP and BNP are differentially regulated, in which ANP plasma levels are increased in both compensatory cardiac hypertrophy and overt heart failure, which is indicative of atrial hemodynamic overload (162). Alternatively, BNP plasma levels are increased only in overt heart failure, which is reflective of ventricular hypertrophy and heart failure. As a major structural protein in the myocardial sarcomeric contractile unit, β-MyHC is thought to be a more representative indirect marker of pathological cardiac hypertrophy and failure (163). Abraham et al. (163) found that β-MyHC transcript expression incrementally declined when treating patients with idiopathic dilated cardiomyopathy with β-blockers, whereas ANP expression decreased in both placebo and β-blocker treated groups. This indicates that ANP responds non-specifically to the method of treatment and that the regulation of other cardiac fetal genes is controlled by a separate mechanism from the cardiac MyHC isoforms.

Because we found that β-MyHC was the only cardiac fetal gene tested to be upregulated in Ang II-infused NFATc2-/- mice, it suggests that NFATc2-/- mice may have defective contractile proteins, which would compromise its ability to properly contract. Because we aren't seeing this change in normotensive hearts, it supports our hypothesis that GATA-4 and NFATc1 are attempting to accommodate for the absence of functional NFATc2. However, once the hearts of NFATc2-/- mice are hypertrophied with

Ang II, we see changed in contractile protein expression, which suggest that these hearts are more likely to fail.

Our preliminary data suggested that GATA-4 protein expression had a tendency to be upregulated in the Ang II-infused wild-type mice, but decreased in Ang II-infused NFATc2-/- mice, with respect to unstimulated hearts. This observation suggests that GATA-4 can compensate in normotensive hearts for a mutant NFATc2 by attempting to promote cardiomyocyte growth. Upon imposing a greater cardiac workload on these mice, GATA-4 transcriptional activity is shut down, causing increased likelihood of heart failure and cell death in NFATc2-/- mice. Furthermore, we observed that activated AKT tended to be increased in the hearts of Ang II-infused wild-type mice but decreased in the hearts of Ang II-infused NFATc2-/- mice, which suggests an inactivation of translational-mediated cardiac growth in NFATc2-/- mice. Interestingly, we observed no change in phospho-eIF2α protein expression in Ang II-infused NFATc2-/- mice, which reinforces our findings that growth-mediated mechanisms are shut down in the heart once NFATc2-/- mice are subjected to increased cardiac workload, which disposes these mice to heart failure and death. Biswas et al. (164) have recently shown that Cn could mediate the de-phosphorylation of eIF6, another eukaryotic initiation factor, promoting its nuclear shuttling which leads to the biogenesis of the 60S ribosome. It would be interesting to monitor changes in eIF6 expression, where we hypothesize that its expression would also be decreased in Ang II-infused NFATc2-/- mice, supporting our hypothesis of translational silencing in these mice.

Because AKT has multi-functional roles in numerous biological processes, this decrease in activated AKT expression in the hearts of Ang II-infused NFATc2-/- could be

affecting other branches of IGF-1/AKT pathway (165). Apart from proliferation, protein synthesis, transcription and cell survival, AKT is a known regulator of protein degradation, where activated AKT mediates the phosphorylation of the Forkhead family of transcription factors (FOXO). In its unphosphorylated state, FOXO induced the transcription of ubiquitin ligases Murf-1 and atrogin-1, leading to muscle degeneration. Upon phosphorylation by AKT, FOXO transcription factors are exported from the nucleus, thereby inhibiting protein degradation and muscle breakdown (166). This could suggest that decreased phospho-AKT expression in Ang II-infused NFATc2-/- mice could also contribute to increased muscle atrophy in the hearts of adult NFATc2 hearts, causing increased fibrosis, cell damage and eventually cell death.

The data presented in this study suggest an uncharacterized yet necessary role for the NFATc2 transcription factor for normal heart contractile function and cardiac biochemical signaling required for non-pathophysiological changes. Both normotensive and Ang II-stimulated NFATc2-/- mice were subjected to increased left ventricular inner chamber dilation and thinning of the right ventricular wall, a characteristic we believe is associated with the inability of NFATc1 and GATA-4 to fully compensate for the absence of functional NFATc2 in the heart, leading to eventual heart failure. Although our results provide further evidence towards clarifying our understanding of the Cn-NFATc2 pathway in the mediation of heart failure in adult mice, there is still much to be explored about this branch of Cn-mediated cardiac hypertrophy. Bourajjaj et al. (143) proposed that because the hearts of young 1-2 month old NFATc2-/- or NFATc3-/- mice are either totally or partially impaired in their ability to grow in response to Cn-mediated hypertrophy, a combined NFATc2c3-/- mouse would display an even more complete

inhibition to hypertrophy. Unpublished results from our lab show that the HW/BW of NFATc3-/- mice is the same as wild-type mice (4.711±0.336 vs 5.513±0.131) whereas adult NFATc2c3-/- mice display a significantly higher HW/BW ratio compared to wild-type animals (7.200±0.961 vs 5.153±0.131). This suggests that other transcription factors do not adequately compensate for a combinatorial deletion of NFATc2 and NFATc3, which would cause severe heart failure in these mice.

There are many signaling effectors that can regulate both physiological and pathophysiological cardiac growth and it is difficult to identify which other pathways could be activated or inactivated in the NFATc2-/- mouse model. An interesting pathway to investigate in NFATc2-/- mice would be the Ca^{2+}/CaM dependent kinases (CaMK) because it is likely that a disruption of Cn-NFATc2 signaling may be compensated by a parallel branch of the Ca^{2+}/CaM pathway. Transgenic mice overexpressing CaMKII in the heart are subjected to cardiac hypertrophy, which is likely caused by increased dissociation and nuclear export of class II histone deacetylases (HDAC) from the DNA, allowing MEF-2 and other transcription factors to bind DNA more readily to compensate for the absence of NFATc2 (93,167-169). Another interesting transcription factor to study is CREB, which is a known regulator of cardiac hypertrophy (115). Upon phosphorylation of Ser133 by PKA, CREB can initiate its transactivation activities in the nucleus. It is hypothesized, from unpublished work in our lab, that CREB is responsible for activating the switch to a less energy efficient muscle program, in which we would expect higher phospho-CREB (Ser133) nuclear presence in NFATc2-/- mice, based on the idea that these mice are more likely to undergo heart failure.

Our work provides evidence that normal Cn-NFAT signaling has a crucial role in the normal function of the adult heart, which is contrary to the general understanding that Cn signaling is responsible cardiac disorders, heart failure and sudden death. Physiological and biochemical signaling alterations in the hearts of NFATc2-/- mice indicate that these mice are susceptible to disease, which provides us with further insights towards understanding the importance of the Cn-NFATc2 pathway in the adult heart.

Chapter 3: Conclusion

As one of the best characterized mediators of pathological cardiac hypertrophy and heart failure, research to better understand how alterations in the Cn-NFAT pathway affect the heart is the focus of many labs across the globe. We provide evidence that NFATc1 and GATA-4 compensate for the absence of functional NFATc2 in adult mice, however these transcription factors cannot fully restore normal cardiomyocyte growth, predisposing these mice to heart failure. This is evidenced by NFATc2-/- mice models displayed left ventricular inner chamber dilatation and a thinner right ventricular wall. In addition, Ang II-infused NFATc2-/- mice displayed an inactivation of transcriptional and translational mechanisms, and changes in β-MyHC gene expression, indicative of contractility defects, severe heart failure and increased cell damage. Based on these findings, we propose that normal Cn-NFAT signaling may have a beneficial role in maintaining normal heart physiology and biochemical signaling in adult mice, which is contrary to the idea that the Cn-NFAT pathway induces only heart disease, pathological cardiac hypertrophy, and overt heart failure in adulthood.

By identifying that NFATc2 plays a major role in the heart, it is interesting to pursue further work in NFATc2-/- mice to gain further of understanding of cross talk between growth signaling pathways, such as IGF-1/AKT, myostatin, and CaMK/CREB in the heart. This would advance our understanding of the roles that these proteins have in the progression of heart disease and failure at the molecular level. In addition, further work in these pathways would provide increased opportunities to develop biochemical and pharmacological treatments to prevent or completely reverse pathologically hypertrophied hearts, which may restore normal heart function and quality of life.

Bibliography

1. Martini, F., and Nath, J. (2009) The Tissue Level of Organization. in *Fundamentals of Anatomy & Physiology*, 8th Ed., Pearson Education, Inc. pp 326-328
2. Widmaier, E., Raff, H., and Strang, K. (2006) Muscle. in *Vander's Human Physiology*, 12th Ed., McGraw Hill. pp 281
3. Marieb, E., and Hoehn, K. (2007) *Human Anatomy and Physiology*, 7 ed., Peason Benjamin Cummings
4. Sherwood, L. (2006) Cardiac Physiology. in *Fundamentals of Physiology: A Human Perspective*, 3rd Ed., Brooks Cole. pp 246-255
5. Bers, D. (2002) *Nature* **415**, 198-205
6. Berridge, M. J. (2006) *Cell Calcium* **40**, 405-412
7. Endo, M., Tanaka, M., and Ebashi, S. (1968) *Proc. Intern. Congr. Physiol. Sci.* **7**, 126
8. Ford, L., and Podolsky, R. (1968) *Federation Proc.* **27**, 375
9. Sieck, G. C., and Regnier, M. (2001) *J Appl Physiol* **90**, 1158-1164
10. Nakao, K., Minobe, W., Roden, R., Bristow, M. R., and Leinwand, L. A. (1997) *J Clin Invest* **100**, 2362-2370
11. Alpert, N. R., and Mulieri, L. A. (1982) *Circ Res* **50**, 491-500
12. Holubarsch, C., Goulette, R. P., Litten, R. Z., Martin, B. J., Mulieri, L. A., and Alpert, N. R. (1985) *Circ Res* **56**, 78-86
13. Izumo, S., Lompre, A. M., Matsuoka, R., Koren, G., Schwartz, K., Nadal-Ginard, B., and Mahdavi, V. (1987) *J Clin Invest* **79**, 970-977
14. Public Health Agency of Canada. (2009) Cardiovascular Diseases. (Canada, P. H. A. o. ed.
15. World Health Organization. (2009) Cardiovascular diseases. (No.317, F. S. ed.
16. Hobbs, R. (2004) *Am J Ther* **11**, 467-472
17. Statistics Canada. (2009) Statistics Canada: Mortality, Summary List of Causes 2005.
18. Heineke, J., and Molkentin, J. (2006) *Nat Rev Mol Cell Biol* **7**, 589-600
19. Molkentin, J. (2000) *Circ Res* **87**, 731-738
20. Berenji, K., Drazner, M., Rothermel, B., and Hill, J. (2005) *Am J Physiol Heart Circ Physiol* **289**, H8-H16
21. Oakley, D. (2001) *Heart* **86**, 722-726
22. McMurray, J. J., and Pfeffer, M. A. (2005) *Lancet* **365**, 1877-1889
23. Francis, G. S. (2001) *Am J Med* **110 Suppl 7A**, 37S-46S
24. Bleumink, G. S., Knetsch, A. M., Sturkenboom, M. C., Straus, S. M., Hofman, A., Deckers, J. W., Witteman, J. C., and Stricker, B. H. (2004) *Eur Heart J* **25**, 1614-1619
25. Roger, V. L., Weston, S. A., Redfield, M. M., Hellermann-Homan, J. P., Killian, J., Yawn, B. P., and Jacobsen, S. J. (2004) *JAMA* **292**, 344-350
26. Cowie, M. R., Wood, D. A., Coats, A. J., Thompson, S. G., Suresh, V., Poole-Wilson, P. A., and Sutton, G. C. (2000) *Heart* **83**, 505-510
27. Bers, D. M. (2008) *Annu Rev Physiol* **70**, 23-49
28. Kahl, C. R., and Means, A. R. (2003) *Endocr Rev* **24**, 719-736
29. Dolmetsch, R. E., Lewis, R. S., Goodnow, C. C., and Healy, J. I. (1997) *Nature* **386**, 855-858
30. Berridge, M. J. (1997) *Nature* **386**, 759-760
31. Dolmetsch, R. E., Xu, K., and Lewis, R. S. (1998) *Nature* **392**, 933-936
32. Houser, S. R., and Molkentin, J. D. (2008) *Sci Signal* **1**, pe31
33. Chin, D., and Means, A. R. (2000) *Trends Cell Biol* **10**, 322-328

34. Al-Shanti, N., and Stewart, C. E. (2009) *Biol Rev Camb Philos Soc* **84**, 637-652
35. Klee, C. B., Crouch, T. H., and Krinks, M. H. (1979) *Proc Natl Acad Sci U S A* **76**, 6270-6273
36. Liu, J., Farmer, J. D., Jr., Lane, W. S., Friedman, J., Weissman, I., and Schreiber, S. L. (1991) *Cell* **66**, 807-815
37. Rusnak, F., and Mertz, P. (2000) *Physiol Rev* **80**, 1483-1521
38. Alzuherri, H., and Chang, K. C. (2003) *Cell Signal* **15**, 471-478
39. Michel, R. N., Dunn, S. E., and Chin, E. R. (2004) *Proc Nutr Soc* **63**, 341-349
40. Blaeser, F., Ho, N., Prywes, R., and Chatila, T. A. (2000) *J Biol Chem* **275**, 197-209
41. Jain, J., McCaffrey, P. G., Miner, Z. K., T.K., Lambert, J. N., Verdine, G. L., Curran, T., and Rao, A. (1993) *Nature* **365**, 352-355
42. Wang, H. G., Pathan, N., Ethell, I. M., Krajewski, S., Yamaguchi, Y., Shibasaki, F., McKeon, F., Bobo, T., Franke, T. F., and Reed, J. C. (1999) *Science* **284**, 339-343
43. Molkentin, J. D., Lu, J. R., Antos, C. L., Markham, B., Richardson, J., Robbins, J., Grant, S. R., and Olson, E. N. (1998) *Cell* **93**, 215-228
44. Sussman, M. A., Lim, H. W., Gude, N., Taigen, T., Olson, E. N., Robbins, J., Colbert, M. C., Gualberto, A., Wieczorek, D. F., and Molkentin, J. D. (1998) *Science* **281**, 1690-1693
45. Bueno, O. F., Wilkins, B. J., Tymitz, K. M., Glascock, B. J., Kimball, T. F., Lorenz, J. N., and Molkentin, J. D. (2002) *Proc Natl Acad Sci U S A* **99**, 4586-4591
46. De Windt, L. J., Lim, H. W., Bueno, O. F., Liang, Q., Delling, U., Braz, J. C., Glascock, B. J., Kimball, T. F., del Monte, F., Hajjar, R. J., and Molkentin, J. D. (2001) *Proc Natl Acad Sci U S A* **98**, 3322-3327
47. Hill, J. A., Rothermel, B., Yoo, K. D., Cabuay, B., Demetroulis, E., Weiss, R. M., Kutschke, W., Bassel-Duby, R., and Williams, R. S. (2002) *J Biol Chem* **277**, 10251-10255
48. Zou, Y., Hiroi, Y., Uozumi, H., Takimoto, E., Toko, H., Zhu, W., Kudoh, S., Mizukami, M., Shimoyama, M., Shibasaki, F., Nagai, R., Yazaki, Y., and Komuro, I. (2001) *Circulation* **104**, 97-101
49. Crabtree, G. R., and Olson, E. N. (2002) *Cell* **109 Suppl**, S67-79
50. Kissinger, C. R., Parge, H. E., Knighton, D. R., Lewis, C. T., Pelletier, L. A., Tempczyk, A., Kalish, V. J., Tucker, K. D., Showalter, R. E., Moomaw, E. W., and et al. (1995) *Nature* **378**, 641-644
51. Klee, C. B., Draetta, G. F., and Hubbard, M. J. (1988) *Adv Enzymol Relat Areas Mol Biol* **61**, 149-200
52. Kincaid, R. L., Nightingale, M. S., and Martin, B. M. (1988) *Proc Natl Acad Sci U S A* **85**, 8983-8987
53. Griffith, J. P., Kim, J. L., Kim, E. E., Sintchak, M. D., Thomson, J. A., Fitzgibbon, M. J., Fleming, M. A., Caron, P. R., Hsiao, K., and Navia, M. A. (1995) *Cell* **82**, 507-522
54. Ke, H., and Huai, Q. (2003) *Biochem Biophys Res Commun* **311**, 1095-1102
55. ProteinDataBank, R. (2010) Human Calcineurin Heterodimer.
56. Klee, C. B., Ren, H., and Wang, X. (1998) *J Biol Chem* **273**, 13367-13370
57. Kretsinger, R. H., and Nockolds, C. E. (1973) *J Biol Chem* **248**, 3313-3326
58. Shaw, J. P., Utz, P. J., Durand, D. B., Toole, J. J., Emmel, E. A., and Crabtree, G. R. (1988) *Science* **241**, 202-205
59. Macian, F. (2005) *Nat Rev Immunol* **5**, 472-484
60. Hogan, P. G., Chen, L., Nardone, J., and Rao, A. (2003) *Genes Dev* **17**, 2205-2232
61. Graef, I. A., Chen, F., and Crabtree, G. R. (2001) *Curr Opin Genet Dev* **11**, 505-512
62. Kiani, A., Habermann, I., Haase, M., Feldmann, S., Boxberger, S., Sanchez-Fernandez, M. A., Thiede, C., Bornhauser, M., and Ehninger, G. (2004) *J Leukoc Biol* **76**, 1057-1065

63. van Rooij, E., Doevendans, P. A., de Theije, C. C., Babiker, F. A., Molkentin, J. D., and de Windt, L. J. (2002) *J Biol Chem* **277**, 48617-48626
64. Klemm, J. D., Beals, C. R., and Crabtree, G. R. (1997) *Curr Biol* **7**, 638-644
65. Macian, F., Lopez-Rodriguez, C., and Rao, A. (2001) *Oncogene* **20**, 2476-2489
66. Chen, L., Glover, J. N., Hogan, P. G., Rao, A., and Harrison, S. C. (1998) *Nature* **392**, 42-48
67. Rinne, A., Kapur, N., Molkentin, J. D., Pogwizd, S. M., Bers, D. M., Banach, K., and Blatter, L. A. (2010) *Am J Physiol Heart Circ Physiol*
68. Calabria, E., Ciciliot, S., Moretti, I., Garcia, M., Picard, A., Dyar, K. A., Pallafacchina, G., Tothova, J., Schiaffino, S., and Murgia, M. (2009) *Proc Natl Acad Sci U S A* **106**, 13335-13340
69. Feske, S., Okamura, H., Hogan, P. G., and Rao, A. (2003) *Biochem Biophys Res Commun* **311**, 1117-1132
70. Lopez-Rodriguez, C., Aramburu, J., Rakeman, A. S., and Rao, A. (1999) *Proc Natl Acad Sci U S A* **96**, 7214-7219
71. Lopez-Rodriguez, C., Aramburu, J., Jin, L., Rakeman, A. S., Michino, M., and Rao, A. (2001) *Immunity* **15**, 47-58
72. Okamura, H., Aramburu, J., Garcia-Rodriguez, C., Viola, J. P., Raghavan, A., Tahiliani, M., Zhang, X., Qin, J., Hogan, P. G., and Rao, A. (2000) *Mol Cell* **6**, 539-550
73. Zhu, J., Shibasaki, F., Price, R., Guillemot, J. C., Yano, T., Dotsch, V., Wagner, G., Ferrara, P., and McKeon, F. (1998) *Cell* **93**, 851-861
74. Beals, C. R., Sheridan, C. M., Turck, C. W., Gardner, P., and Crabtree, G. R. (1997) *Science* **275**, 1930-1934
75. Chow, C. W., Rincon, M., Cavanagh, J., Dickens, M., and Davis, R. J. (1997) *Science* **278**, 1638-1641
76. Gomez del Arco, P., Martinez-Martinez, S., Maldonado, J. L., Ortega-Perez, I., and Redondo, J. M. (2000) *J Biol Chem* **275**, 13872-13878
77. Okamura, H., Garcia-Rodriguez, C., Martinson, H., Qin, J., Virshup, D. M., and Rao, A. (2004) *Mol Cell Biol* **24**, 4184-4195
78. Beals, C. R., Clipstone, N. A., Ho, S. N., and Crabtree, G. R. (1997) *Genes Dev* **11**, 824-834
79. Fiedler, B., and Wollert, K. C. (2004) *Cardiovasc Res* **63**, 450-457
80. Shibasaki, F., Hallin, U., and Uchino, H. (2002) *J Biochem* **131**, 1-15
81. Dave, V., Childs, T., Xu, Y., Ikegami, M., Besnard, V., Maeda, Y., Wert, S. E., Neilson, J. R., Crabtree, G. R., and Whitsett, J. A. (2006) *J Clin Invest* **116**, 2597-2609
82. Dunn, S. E., Burns, J. L., and Michel, R. N. (1999) *J Biol Chem* **274**, 21908-21912
83. de la Pompa, J. L., Timmerman, L. A., Takimoto, H., Yoshida, H., Elia, A. J., Samper, E., Potter, J., Wakeham, A., Marengere, L., Langille, B. L., Crabtree, G. R., and Mak, T. W. (1998) *Nature* **392**, 182-186
84. Ranger, A. M., Grusby, M. J., Hodge, M. R., Gravallese, E. M., de la Brousse, F. C., Hoey, T., Mickanin, C., Baldwin, H. S., and Glimcher, L. H. (1998) *Nature* **392**, 186-190
85. Wilkins, B. J., Dai, Y. S., Bueno, O. F., Parsons, S. A., Xu, J., Plank, D. M., Jones, F., Kimball, T. R., and Molkentin, J. D. (2004) *Circ Res* **94**, 110-118
86. O'Keefe, S. J., Tamura, J., Kincaid, R. L., Tocci, M. J., and O'Neill, E. A. (1992) *Nature* **357**, 692-694
87. Oka, T., Xu, J., and Molkentin, J. D. (2007) *Semin Cell Dev Biol* **18**, 117-131
88. Komuro, I., and Yazaki, Y. (1993) *Annu Rev Physiol* **55**, 55-75
89. Merika, M., and Orkin, S. H. (1993) *Mol Cell Biol* **13**, 3999-4010
90. Ko, L. J., and Engel, J. D. (1993) *Mol Cell Biol* **13**, 4011-4022
91. Molkentin, J. D. (2000) *J Biol Chem* **275**, 38949-38952

92. Molkentin, J. D., Lin, Q., Duncan, S. A., and Olson, E. N. (1997) *Genes Dev* **11**, 1061-1072
93. Pikkarainen, S., Tokola, H., Kerkela, R., and Ruskoaho, H. (2004) *Cardiovasc Res* **63**, 196-207
94. Grepin, C., Dagnino, L., Robitaille, L., Haberstroh, L., Antakly, T., and Nemer, M. (1994) *Mol Cell Biol* **14**, 3115-3129
95. Molkentin, J. D., Kalvakolanu, D. V., and Markham, B. E. (1994) *Mol Cell Biol* **14**, 4947-4957
96. Thuerauf, D. J., Hanford, D. S., and Glembotski, C. C. (1994) *J Biol Chem* **269**, 17772-17775
97. Liang, Q., De Windt, L. J., Witt, S. A., Kimball, T. R., Markham, B. E., and Molkentin, J. D. (2001) *J Biol Chem* **276**, 30245-30253
98. Liang, Q., Wiese, R. J., Bueno, O. F., Dai, Y. S., Markham, B. E., and Molkentin, J. D. (2001) *Mol Cell Biol* **21**, 7460-7469
99. Charron, F., Tsimiklis, G., Arcand, M., Robitaille, L., Liang, Q., Molkentin, J. D., Meloche, S., and Nemer, M. (2001) *Genes Dev* **15**, 2702-2719
100. Haq, S., Choukroun, G., Kang, Z. B., Ranu, H., Matsui, T., Rosenzweig, A., Molkentin, J. D., Alessandrini, A., Woodgett, J., Hajjar, R., Michael, A., and Force, T. (2000) *J Cell Biol* **151**, 117-130
101. Morisco, C., Seta, K., Hardt, S. E., Lee, Y., Vatner, S. F., and Sadoshima, J. (2001) *J Biol Chem* **276**, 28586-28597
102. McKinsey, T. A., Zhang, C. L., and Olson, E. N. (2002) *Trends Biochem Sci* **27**, 40-47
103. Morin, S., Charron, F., Robitaille, L., and Nemer, M. (2000) *EMBO J* **19**, 2046-2055
104. Akazawa, H., and Komuro, I. (2003) *Circ Res* **92**, 1079-1088
105. Lin, Q., Schwarz, J., Bucana, C., and Olson, E. N. (1997) *Science* **276**, 1404-1407
106. Bi, W., Drake, C. J., and Schwarz, J. J. (1999) *Dev Biol* **211**, 255-267
107. Naya, F. J., Black, B. L., Wu, H., Bassel-Duby, R., Richardson, J. A., Hill, J. A., and Olson, E. N. (2002) *Nat Med* **8**, 1303-1309
108. Kolodziejczyk, S. M., Wang, L., Balazsi, K., DeRepentigny, Y., Kothary, R., and Megeney, L. A. (1999) *Curr Biol* **9**, 1203-1206
109. Nadruz, W., Jr., Kobarg, C. B., Constancio, S. S., Corat, P. D., and Franchini, K. G. (2003) *Circ Res* **92**, 243-251
110. Molkentin, J. D., and Markham, B. E. (1993) *J Biol Chem* **268**, 19512-19520
111. Xu, J., Gong, N. L., Bodi, I., Aronow, B. J., Backx, P. H., and Molkentin, J. D. (2006) *J Biol Chem* **281**, 9152-9162
112. Hoeffler, J. P., Meyer, T. E., Yun, Y., Jameson, J. L., and Habener, J. F. (1988) *Science* **242**, 1430-1433
113. Yin, J. C., Wallach, J. S., Del Vecchio, M., Wilder, E. L., Zhou, H., Quinn, W. G., and Tully, T. (1994) *Cell* **79**, 49-58
114. Yin, J. C., Del Vecchio, M., Zhou, H., and Tully, T. (1995) *Cell* **81**, 107-115
115. Fentzke, R. C., Korcarz, C. E., Lang, R. M., Lin, H., and Leiden, J. M. (1998) *J Clin Invest* **101**, 2415-2426
116. Yamamoto, K. K., Gonzalez, G. A., Biggs, W. H., 3rd, and Montminy, M. R. (1988) *Nature* **334**, 494-498
117. Gonzalez, G. A., and Montminy, M. R. (1989) *Cell* **59**, 675-680
118. Chrivia, J. C., Kwok, R. P., Lamb, N., Hagiwara, M., Montminy, M. R., and Goodman, R. H. (1993) *Nature* **365**, 855-859
119. Dash, P. K., Karl, K. A., Colicos, M. A., Prywes, R., and Kandel, E. R. (1991) *Proc Natl Acad Sci U S A* **88**, 5061-5065

120. Chen, A. E., Ginty, D. D., and Fan, C. M. (2005) *Nature* **433**, 317-322
121. Sun, P., Enslen, H., Myung, P. S., and Maurer, R. A. (1994) *Genes Dev* **8**, 2527-2539
122. Spencer, K. T., Collins, K., Korcarz, C., Fentzke, R., Lang, R. M., and Leiden, J. M. (2000) *Am J Physiol Heart Circ Physiol* **279**, H210-215
123. Watson, P. A., Reusch, J. E., McCune, S. A., Leinwand, L. A., Luckey, S. W., Konhilas, J. P., Brown, D. A., Chicco, A. J., Sparagna, G. C., Long, C. S., and Moore, R. L. (2007) *Am J Physiol Heart Circ Physiol* **293**, H246-259
124. Tomita, H., Nazmy, M., Kajimoto, K., Yehia, G., Molina, C. A., and Sadoshima, J. (2003) *Circ Res* **93**, 12-22
125. Dorn, G. W., 2nd, and Force, T. (2005) *J Clin Invest* **115**, 527-537
126. Datta, S. R., Brunet, A., and Greenberg, M. E. (1999) *Genes Dev* **13**, 2905-2927
127. Sandri, M. (2008) *Physiology (Bethesda)* **23**, 160-170
128. Chen, W. S., Xu, P. Z., Gottlob, K., Chen, M. L., Sokol, K., Shiyanova, T., Roninson, I., Weng, W., Suzuki, R., Tobe, K., Kadowaki, T., and Hay, N. (2001) *Genes Dev* **15**, 2203-2208
129. Cho, H., Mu, J., Kim, J. K., Thorvaldsen, J. L., Chu, Q., Crenshaw, E. B., 3rd, Kaestner, K. H., Bartolomei, M. S., Shulman, G. I., and Birnbaum, M. J. (2001) *Science* **292**, 1728-1731
130. Matsui, T., Li, L., Wu, J. C., Cook, S. A., Nagoshi, T., Picard, M. H., Liao, R., and Rosenzweig, A. (2002) *J Biol Chem* **277**, 22896-22901
131. Oliveira, R. S., Ferreira, J. C., Gomes, E. R., Paixao, N. A., Rolim, N. P., Medeiros, A., Guatimosim, S., and Brum, P. C. (2009) *J Physiol* **587**, 3899-3910
132. Lorell, B. H., and Carabello, B. A. (2000) *Circulation* **102**, 470-479
133. Firth, B. G., and Dunnmon, P. M. (1990) *Cardiovasc Drugs Ther* **4**, 1363-1374
134. Wilkins, B. J., and Molkentin, J. D. (2004) *Biochem Biophys Res Commun* **322**, 1178-1191
135. Molkentin, J. D. (2004) *Cardiovasc Res* **63**, 467-475
136. Bueno, O. F., van Rooij, E., Molkentin, J. D., Doevendans, P. A., and De Windt, L. J. (2002) *Cardiovasc Res* **53**, 806-821
137. Wilkins, B. J., De Windt, L. J., Bueno, O. F., Braz, J. C., Glascock, B. J., Kimball, T. F., and Molkentin, J. D. (2002) *Mol Cell Biol* **22**, 7603-7613
138. Park, J., Yaseen, N. R., Hogan, P. G., Rao, A., and Sharma, S. (1995) *J Biol Chem* **270**, 20653-20659
139. Yang, S. A., and Klee, C. B. (2000) *Biochemistry* **39**, 16147-16154
140. Antos, C. L., McKinsey, T. A., Frey, N., Kutschke, W., McAnally, J., Shelton, J. M., Richardson, J. A., Hill, J. A., and Olson, E. N. (2002) *Proc Natl Acad Sci U S A* **99**, 907-912
141. Rothermel, B. A., McKinsey, T. A., Vega, R. B., Nicol, R. L., Mammen, P., Yang, J., Antos, C. L., Shelton, J. M., Bassel-Duby, R., Olson, E. N., and Williams, R. S. (2001) *Proc Natl Acad Sci U S A* **98**, 3328-3333
142. Diedrichs, H., Chi, M., Boelck, B., Mehlhorn, U., and Schwinger, R. H. (2004) *Eur J Heart Fail* **6**, 3-9
143. Bourajjaj, M., Armand, A. S., da Costa Martins, P. A., Weijts, B., van der Nagel, R., Heeneman, S., Wehrens, X. H., and De Windt, L. J. (2008) *J Biol Chem* **283**, 22295-22303
144. Hodge, M. R., Ranger, A. M., Charles de la Brousse, F., Hoey, T., Grusby, M. J., and Glimcher, L. H. (1996) *Immunity* **4**, 397-405
145. Gauthier, E. R., Madison, S. D., and Michel, R. N. (1997) *Pflugers Arch* **433**, 664-668
146. Arceci, R. J., King, A. A., Simon, M. C., Orkin, S. H., and Wilson, D. B. (1993) *Mol Cell Biol* **13**, 2235-2246

147. Izzo, J., Sica, D., and Black, H. (2008) *Hypertension Primer: The Essentials of High Blood Pressure: Basic Science, Population Science, and Clinical Management*, 4 ed., Williams and Wilkins
148. Welsh, G. I., Miyamoto, S., Price, N. T., Safer, B., and Proud, C. G. (1996) *J Biol Chem* **271**, 11410-11413
149. Dunn, S. E., Simard, A. R., Bassel-Duby, R., Williams, R. S., and Michel, R. N. (2001) *J Biol Chem* **276**, 45243-45254
150. Shen, T., Liu, Y., Cseresnyes, Z., Hawkins, A., Randall, W. R., and Schneider, M. F. (2006) *Mol Biol Cell* **17**, 1570-1582
151. Musaro, A., McCullagh, K. J., Naya, F. J., Olson, E. N., and Rosenthal, N. (1999) *Nature* **400**, 581-585
152. Zhang, D. H., Yang, L., Cohn, L., Parkyn, L., Homer, R., Ray, P., and Ray, A. (1999) *Immunity* **11**, 473-482
153. Wolfe, S. A., Zhou, P., Dotsch, V., Chen, L., You, A., Ho, S. N., Crabtree, G. R., Wagner, G., and Verdine, G. L. (1997) *Nature* **385**, 172-176
154. Hasegawa, K., Lee, S. J., Jobe, S. M., Markham, B. E., and Kitsis, R. N. (1997) *Circulation* **96**, 3943-3953
155. Herzig, T. C., Jobe, S. M., Aoki, H., Molkentin, J. D., Cowley, A. W., Jr., Izumo, S., and Markham, B. E. (1997) *Proc Natl Acad Sci U S A* **94**, 7543-7548
156. Oka, T., Maillet, M., Watt, A. J., Schwartz, R. J., Aronow, B. J., Duncan, S. A., and Molkentin, J. D. (2006) *Circ Res* **98**, 837-845
157. van Berlo, J. H., Elrod, J. W., van den Hoogenhof, M. M., York, A. J., Aronow, B. J., Duncan, S. A., and Molkentin, J. D. *Circ Res*
158. Matsuda, T., Zhai, P., Maejima, Y., Hong, C., Gao, S., Tian, B., Goto, K., Takagi, H., Tamamori-Adachi, M., Kitajima, S., and Sadoshima, J. (2008) *Proc Natl Acad Sci U S A* **105**, 20900-20905
159. Suzuki, Y. J. (2003) *Free Radic Biol Med* **34**, 1589-1598
160. Yokota, N., Bruneau, B. G., Fernandez, B. E., de Bold, M. L., Piazza, L. A., Eid, H., and de Bold, A. J. (1995) *Am J Hypertens* **8**, 301-310
161. Martin, A. F., Paul, R. J., and McMahon, E. G. (1986) *Hypertension* **8**, 128-132
162. Langenickel, T., Pagel, I., Hohnel, K., Dietz, R., and Willenbrock, R. (2000) *Am J Physiol Heart Circ Physiol* **278**, H1500-1506
163. Abraham, W. T., Gilbert, E. M., Lowes, B. D., Minobe, W. A., Larrabee, P., Roden, R. L., Dutcher, D., Sederberg, J., Lindenfeld, J. A., Wolfel, E. E., Shakar, S. F., Ferguson, D., Volkman, K., Linseman, J. V., Quaife, R. A., Robertson, A. D., and Bristow, M. R. (2002) *Mol Med* **8**, 750-760
164. Biswas, A., Mukherjee, S., Das, S., Shields, D., Chow, C. W., and Maitra, U. *J Biol Chem*
165. Shiojima, I., and Walsh, K. (2006) *Genes Dev* **20**, 3347-3365
166. Tremblay, M. L., and Giguere, V. (2008) *Cell Metab* **7**, 101-103
167. Frey, N., McKinsey, T. A., and Olson, E. N. (2000) *Nat Med* **6**, 1221-1227
168. Chien, K. R. (2000) *J Clin Invest* **105**, 1339-1342
169. McKinsey, T. A., Zhang, C. L., and Olson, E. N. (2000) *Proc Natl Acad Sci U S A* **97**, 14400-14405

Appendix I: Experimental Animals

Animal	Genotype	D.O.B	Extracted	HW (mg)	BW (g)	Experiment
X6-1	WT	25/05/2009	12/04/2010	231.0	35.2	WC
N112-2	KO	19/05/2009	12/04/2010	233.5	34.2	WC
BalbC	WT	20/06/2008	23/06/2009	111.7	N/A	WC
N99-1	KO	06/08/2008	23/06/2009	134.4	28.0	WC
X15-5	WT	03/03/2010	04/10/2010	142.0	31.4	WC
N123-2	KO	10/02/2010	04/10/2010	130.4	30.0	WC
BalbC-1	WT	R.B	14/04/2009	135.1	25.5	WC
N95-2	KO	18/02/2008	27/03/2009	154.4	32.5	WC
BalbC-2	WT	R.B	14/04/2009	129.7	25.0	WC
N95-3	KO	19/02/2008	27/02/2008	157.4	33.0	WC
BalbC-2	WT	18/02/2010	24/09/2010	136.4	24.0	WC AngII
N121-1	KO	09/02/2010	24/09/2010	122.8	24.0	WC AngII
BalbC-4	WT	18/02/2010	24/09/2010	117.3	21.0	WC AngII
N120-1	KO	04/01/2010	24/09/2010	176.2	30.0	WC AngII
BalbC-1	WT	03/03/2010	24/09/2010	128.2	25.0	WC AngII
N120-2	KO	04/01/2010	24/09/2010	162.1	30.0	WC AngII
BalbC-55	WT	11/08/2009	18/12/2009	136.9	30.0	C/N
N113-1	KO	31/08/2009	10/12/2009	120.8	28.0	C/N
BalbC-52	WT	11/08/2009	18/12/2009	135.2	31.0	C/N
N113-2	KO	31/08/2008	10/12/2009	131.4	28.0	C/N
BalbC-3	WT	R.B	14/04/2009	147.3	29.6	C/N
NN20-1	KO/WT	07/04/2008	27/03/2009	136.4	28.0	C/N
BalbC.1	WT	12/08/2009	26/05/2010	129.5	27.2	IP
N111-1	KO	19/05/2009	26/05/2010	139.0	27.5	IP
BalbC.2	WT	12/08/2009	26/05/2010	116.5	26.2	IP
N111-3	KO	19/05/2009	26/05/2010	110.6	25.5	IP
BalbC.3	WT	12/08/2009	26/05/2010	120.3	24.1	IP
N111-4	KO	19/05/2009	26/05/2010	110.8	26.8	IP
BalbC	WT	R.B	25/05/2009	116.5	26.0	RNA
N102-1	KO	28/12/2008	25/05/2009	133.3	28.0	RNA
K36-2	WT	02/09/2008	12/05/2009	185.2	37.0	RNA
N98-1	KO	06/08/2008	12/05/2009	176.1	38.0	RNA
X1-1	WT	12/08/2009	22/02/2010	141.0	31.2	RNA
N115-2	KO	19/10/2009	22/02/2010	127.3	27.0	RNA
BalbC	WT	15/07/2008	13/02/2009	158.9	35.0	RNA
N96-6	KO	01/06/2008	13/02/2009	129.1	27.8	RNA
BalbC-2	WT	03/03/2010	24/09/2010	140.0	22.5	AngII RNA
N122-1	KO	16/02/2010	04/11/2010	133.5	23.5	AngII RNA
BalbC-3	WT	10/02/2010	09/08/2010	148.7	25.5	AngII RNA

N122-2	KO	16/02/2010	04/11/2010	126.7	27.5	AngII RNA
BalbC-4	WT	03/03/2010	24/09/2010	136.2	21.7	AngII RNA
N122-4	KO	16/02/2010	04/11/2010	147.1	26.0	AngII RNA
X7-1	WT	25/11/2009	03/08/2010	N/A	35.5	Histology
N119-1	KO	04/01/2010	04/08/2010	N/A	35.0	Histology
X8-1	WT	03/12/2009	03/08/2010	N/A	36.5	Histology
N117-2	KO	31/12/2009	04/08/2010	N/A	28.0	Histology
X8-2	WT	03/12/2009	03/08/2010	N/A	37.0	Histology
N117-3	KO	31/12/2009	04/08/2010	N/A	29.0	Histology

D.O.B: Date of Birth

HW: Heart Weight

BW: Body Weight

R.B: Retired Breeder

WC: Whole Cell Protein Extraction

C/N: Cytoplasmic/Nuclear Protein Extraction

IP: Immunoprecipitation

Appendix II: PCR Primer Sequences

Gene	Forward Primer	Reverse Primer	Size (bp)
NFATc1	5'-ttccagcaccttcggaagggtgc-3'	5'-agtgagccctgtggtgagac -3'	205
NFATc2	5'-tctgctgttctcatggatgccc-3'	5'-ggatgcagtcacagggatgct-3'	282
NFATc3	5'-cgatctgctcaagaactccc-3'	5'-ggcagatgtaactgctgggt-3'	246
NFATc4	5'-ctgaggatcgaggtacagcc-3'	5'-ttgttctctgggagcaaggt -3'	293
GATA-4	5'-gatgacttctcagaaggcag-3'	5'-catggagcttcatgtagagg-3'	283
GSK-3β	5'-tgtgattctggagaactggttgccat-3'	5'-ggacgtgtaatcagtggctccaaagatc-3'	483
CK-1α	5'-gtacagagacaacaggacaa-3'	5'-caacaggagtggacatcttc-3'	248
JNK-2	5'-ctctggagcccaaggaattgtttgt-3'	5'-agtcaaggatcttgagggtacagtctga-3'	410
p38-1α	5'-ccagagatcatgctgaattgg-3'	5'-tgatcctcttatctgagtcc -3'	322
ERK1	5'-gctttctgacggagtatgtg-3'	5'-atgcaattaaggtcctcctg-3'	220
ERK2	5'-ccattcagctaacgttctgc-3'	5'-atagcatctctgccaggatg-3'	248
β-MyHC	5'-gccaacaccaacctgtccaagttc-3'	5'-tgcaaaggctccaggtctgagggc-3'	205
ANP	5'-ttggcttccaggccataattg-3'	5'-aagagggcagatctatcgga-3'	282
BNP	5'-atggatctcctgaaggtgct-3'	5'-tcttgtgcccaaagcagctt-3'	505
28S	5'-ttgttgccatggtaatcctgctcagtacg-3'	5'-tctgacttagaggcgttcagtcataatccc-3'	132

Appendix III: PCR Quantification Data

	NFATc1:28S	
	Raw value	Normalized
Balbc	0.428	1
N102-1	0.402	0.939252336
K36-2	0.396	1
N98-1	0.378	0.954545455
Balbc	0.485	1
N115-2	0.623	1.284536082

t-Test: Two-Sample Assuming Equal Variances

	Variable 1	*Variable 2*
Mean	1	1.059444624
Variance	0	0.038058093
Observations	3	3
Pooled Variance	0.01902905	
Hypothesized Mean Difference	0	
Df	4	
t Stat	-0.5277761	
P(T<=t) one-tail	0.31278771	
t Critical one-tail	2.13184678	
P(T<=t) two-tail	0.62557543	
t Critical two-tail	2.77644511	

	NFATc2:28S	
	Raw data	Normalized
Balbc	1.924	1
N102-1	2.143	1.113825364
K36-2	1.91	1
N98-1	1.427	0.747120419
Balbc	0.408	1
N115-2	0.433	1.06127451

t-Test: Two-Sample Assuming Equal Variances

	Variable 1	*Variable 2*
Mean	1	0.974073431
Variance	0	0.03932115
Observations	3	3
Pooled Variance	0.01966058	

Hypothesized Mean Difference	0
df	4
t Stat	0.22646056
P(T<=t) one-tail	0.41597258
t Critical one-tail	2.13184678
P(T<=t) two-tail	0.83194515
t Critical two-tail	2.77644511

	NFATc3:28S	
	Raw data	Normalized
Balbc	2.12	1
N102-1	2.12	1
K36-2	2.34	1
N98-1	1.49	0.636752137
Balbc	1.62	1
N115-2	1.66	1.024691358

t-Test: Two-Sample Assuming Equal Variances

	Variable 1	*Variable 2*
Mean	1	0.887147832
Variance	0	0.047175919
Observations	3	3
Pooled Variance	0.023588	
Hypothesized Mean Difference	0	
df	4	
t Stat	0.8999334	
P(T<=t) one-tail	0.2095185	
t Critical one-tail	2.1318468	
P(T<=t) two-tail	0.419037	
t Critical two-tail	2.7764451	

	NFATc4:28S	
	Raw data	Normalized
Balbc	0.426	1
N102-1	0.329	0.772300469
K36-2	0.565	1
N98-1	0.732	1.295575221
Balbc	0.728	1
N115-2	0.514	0.706043956

t-Test: Two-Sample Assuming Equal Variances

	Variable 1	*Variable 2*
Mean	1	0.924639882
Variance	0	0.104292251
Observations	3	3
Pooled Variance	0.05214613	
Hypothesized Mean Difference	0	
df	4	
t Stat	0.40418126	
P(T<=t) one-tail	0.35337854	
t Critical one-tail	2.13184678	
P(T<=t) two-tail	0.70675707	
t Critical two-tail	2.77644511	

	GATA-4:28S	
	Raw value	Normalized
Balbc	2.11818182	1
N96-6	2.22101449	1.048547615
Balbc	1.98333333	1
N102-1	1.5	0.756302521
K36-2	2.61888112	1
N98-1	2.21328671	0.845126836

t-Test: Two-Sample Assuming Equal Variances

	Variable 1	*Variable 2*
Mean	1	0.883325657
Variance	0	0.022446161
Observations	3	3
Pooled Variance	0.01122308	
Hypothesized Mean Difference	0	
df	4	
t Stat	1.34885403	
P(T<=t) one-tail	0.12434371	
t Critical one-tail	2.13184678	
P(T<=t) two-tail	0.24868742	
t Critical two-tail	2.77644511	

	GSK3-β:28S	
	Raw data	Normalized
Balbc	0.40022422	1
N102-1	0.31550218	0.788313579
K36-2	0.32653061	1
N98-1	0.35623679	1.090975159
Balbc	0.20848375	1
N115-2	0.37399031	1.793858269

t-Test: Two-Sample Assuming Equal Variances

	Variable 1	*Variable 2*
Mean	1	1.224382335
Variance	0	0.266128137
Observations	3	3
Pooled Variance	0.13306407	
Hypothesized Mean Difference	0	
df	4	
t Stat	-0.7533623	
P(T<=t) one-tail	0.24657354	
t Critical one-tail	2.13184678	
P(T<=t) two-tail	0.49314708	
t Critical two-tail	2.77644511	

	CK-1α:28S	
	Raw data	Normalized
Balbc	0.4246862	1
N102-1	0.2227074	0.524404672
K36-2	1.2209302	1
N98-1	1.1	0.900952381
Balbc	0.4055375	1
N115-2	0.5	1.232931727

t-Test: Two-Sample Assuming Equal Variances

	Variable 1	*Variable 2*
Mean	1	1.658220073
Variance	0	2.450501678
Observations	3	3
Pooled Variance	1.2252508	
Hypothesized Mean Difference	0	
df	4	
t Stat	-0.7282898	

P(T<=t) one-tail	0.2533911
t Critical one-tail	2.1318465
P(T<=t) two-tail	0.5067822
t Critical two-tail	2.7764509

	JNK-2:28S	
	Raw data	Normalized
Balbc	0.326335878	1
N102-1	0.362416107	1.110561639
K36-2	0.3608	1
N98-1	0.3655	1.013026608
Balbc	0.4264	1
N115-2	0.3775	0.885318949

t-Test: Two-Sample Assuming Equal Variances

	Variable 1	*Variable 2*
Mean	1	1.002969065
Variance	0	0.012759433
Observations	3	3
Pooled Variance	0.006379716	
Hypothesized Mean Difference	0	
df	4	
t Stat	-0.045526545	
P(T<=t) one-tail	0.482934914	
t Critical one-tail	2.131846486	
P(T<=t) two-tail	0.965869828	
t Critical two-tail	2.776450856	

	p38-1α:28S	
	Raw data	Normalized
Balbc	0.111635	1
N102-1	0.181319	1.624206779
K36-2	0.602326	1
N98-1	0.623684	1.035460272
Balbc	0.191489	1
N115-2	0.109037	0.569417158

t-Test: Two-Sample Assuming Equal Variances

	Variable 1	*Variable 2*

Mean	1	1.076361403
Variance	0	0.279399963
Observations	3	3
Pooled Variance	0.1397	
Hypothesized Mean Difference	0	
df	4	
t Stat	-0.25022	
P(T<=t) one-tail	0.407372	
t Critical one-tail	2.131846	
P(T<=t) two-tail	0.814744	
t Critical two-tail	2.776451	

	ERK1:28S	
	Raw data	Normalized
Balbc	1.025641	1
N102-1	0.66	0.6435
K36-2	1.66875	1
N98-1	1.636612	0.980741
Balbc	0.55119	1
N115-2	0.860179	1.560584

t-Test: Two-Sample Assuming Equal Variances

	Variable 1	*Variable 2*
Mean	1	1.061608
Variance	0	0.215165
Observations	3	3
Pooled Variance	0.107583	
Hypothesized Mean Difference	0	
df	4	
t Stat	-0.23005	
P(T<=t) one-tail	0.414671	
t Critical one-tail	2.131846	
P(T<=t) two-tail	0.829342	
t Critical two-tail	2.776451	

	ERK2:28S	
	Raw data	Normalized
Balbc	1.257813	1
N102-1	1.325243	1.053609
K36-2	3.056	1
N98-1	2.837607	0.928536
Balbc	0.586134	1

N115-2	1.323529	2.258065

t-Test: Two-Sample Assuming Equal Variances

	Variable 1	*Variable 2*
Mean	1	1.413403
Variance	0	0.539
Observations	3	3
Pooled Variance	0.2695	
Hypothesized Mean Difference	0	
df	4	
t Stat	-0.9753	
P(T<=t) one-tail	0.192317	
t Critical one-tail	2.131847	
P(T<=t) two-tail	0.384635	
t Critical two-tail	2.776445	

ANP:28S			
Non-stimulated		**Angiotensin II**	
	Raw Data		Raw Data
Balbc	0.25	BalbC-2	0.376687
N102-1	0.33651551	N122-1.2	0.509662
K36-2	0.16359773	BalbC-3	0.546203
N98-1	0.15633245	N122-2.2	0.543316
Balbc	0.24224022	BalbC-4	0.503484
N115-2	0.3	N122-4.2	0.524876

Non-stimulated NFATc2:Non-stimulated WT

t-Test: Two-Sample Assuming Equal Variances

	Variable 1	*Variable 2*
Mean	0.25483788	0.264282656
Variance	0.00631222	0.00907328
Observations	3	3
Pooled Variance	0.00769275	
Hypothesized Mean Difference	0	
df	4	
t Stat	-0.1318853	
P(T<=t) one-tail	0.45072141	
t Critical one-tail	2.13184678	
P(T<=t) two-tail	0.90144282	
t Critical two-tail	2.77644511	

Angiotensin II WT:Non-stimulated WT
t-Test: Two-Sample Assuming Equal Variances

	Variable 1	*Variable 2*
Mean	0.21861265	0.475458
Variance	0.002285034	0.007773
Observations	3	3
Pooled Variance	0.005029005	
Hypothesized Mean Difference	0	
df	4	
t Stat	-4.435844281	
P(T<=t) one-tail	0.005685224	
t Critical one-tail	2.131846782	
P(T<=t) two-tail	0.011370448	
t Critical two-tail	2.776445105	

Angiotensin II NFATc2:Non-stimulated NFATc2
t-Test: Two-Sample Assuming Equal Variances

	Variable 1	*Variable 2*
Mean	0.264283	0.525951
Variance	0.009073	0.000284
Observations	3	3
Pooled Variance	0.004679	
Hypothesized Mean Difference	0	
df	4	
t Stat	-4.68529	
P(T<=t) one-tail	0.004705	
t Critical one-tail	2.131847	
P(T<=t) two-tail	0.009411	
t Critical two-tail	2.776445	

Angiotensin II NFATc2:Angiotensin II WT
t-Test: Two-Sample Assuming Equal Variances

	Variable 1	*Variable 2*
Mean	0.475458	0.525951
Variance	0.007773	0.000284
Observations	3	3
Pooled Variance	0.004028	
Hypothesized Mean Difference	0	
df	4	
t Stat	-0.97433	
P(T<=t) one-tail	0.192532	
t Critical one-tail	2.131847	
P(T<=t) two-tail	0.385064	
t Critical two-tail	2.776445	

β-MyHC:28S			
Non-stimulated		**Angiotensin II**	
	Raw Data		Raw Data
Balbc	0.40642077	BalbC-2	0.958282
N102-1	0.40811456	N122-1.2	1.211353
K36-2	0.65864023	BalbC-3	0.66962
N98-1	0.49208443	N122-2.2	1.125134
Balbc	0.33873144	BalbC-4	0.941928
N115-2	0.25647059	N122-4.2	1.464552

Non-stimulated NFATc2:Non-stimulated WT
t-Test: Two-Sample Assuming Equal Variances

	Variable 1	*Variable 2*
Mean	0.46793081	0.385556526
Variance	0.02842302	0.01426012
Observations	3	3
Pooled Variance	0.02134157	
Hypothesized Mean Difference	0	
df	4	
t Stat	0.69059607	
P(T<=t) one-tail	0.2639014	
t Critical one-tail	2.13184678	
P(T<=t) two-tail	0.5278028	
t Critical two-tail	2.77644511	

Angiotensin II WT:Non-stimulated WT
t-Test: Two-Sample Assuming Equal Variances

	Variable 1	*Variable 2*
Mean	0.467930812	0.85661
Variance	0.028423022	0.026291
Observations	3	3
Pooled Variance	0.027356902	
Hypothesized Mean Difference	0	
df	4	
t Stat	-2.878085098	
P(T<=t) one-tail	0.02254996	
t Critical one-tail	2.131846782	
P(T<=t) two-tail	0.04509992	
t Critical two-tail	2.776445105	

Angiotensin II NFATc2:Non-stimulated NFATc2
t-Test: Two-Sample Assuming Equal Variances

	Variable 1	*Variable 2*

Mean	0.385557	1.267013
Variance	0.01426	0.031125
Observations	3	3
Pooled Variance	0.022692	
Hypothesized Mean Difference	0	
df	4	
t Stat	-7.16648	
P(T<=t) one-tail	0.001004	
t Critical one-tail	2.131847	
P(T<=t) two-tail	0.002007	
t Critical two-tail	2.776445	

Angiotensin II NFATc2:Angiotensin II WT

t-Test: Two-Sample Assuming Equal Variances

	Variable 1	*Variable 2*
Mean	0.85661	1.267013
Variance	0.026291	0.031125
Observations	3	3
Pooled Variance	0.028708	
Hypothesized Mean Difference	0	
df	4	
t Stat	-2.96658	
P(T<=t) one-tail	0.020642	
t Critical one-tail	2.131847	
P(T<=t) two-tail	0.041284	
t Critical two-tail	2.776445	

BNP:28S			
Non-stimulated		**Angiotensin II**	
	Raw Data		Raw Data
Balbc	0.04166667	BalbC-2	0.206748
N102-1	0.18019093	N122-1.2	0.152174
K36-2	0.1203966	BalbC-3	0.225316
N98-1	0.09894459	N122-2.2	0.169519
Balbc	0.0802969	BalbC-4	0.216028
N115-2	0.11647059	N122-4.2	0.192786

Non-stimulated NFATc2:Non-stimulated WT

t-Test: Two-Sample Assuming Equal Variances

	Variable 1	*Variable 2*
Mean	0.08078672	0.131868703
Variance	0.00154978	0.001828068

Observations	3	3
Pooled Variance	0.00168892	
Hypothesized Mean Difference	0	
df	4	
t Stat	-1.5223281	
P(T<=t) one-tail	0.10129281	
t Critical one-tail	2.13184678	
P(T<=t) two-tail	0.20258561	
t Critical two-tail	2.77644511	

Angiotensin II WT:Non-stimulated WT

t-Test: Two-Sample Assuming Equal Variances

	Variable 1	*Variable 2*
Mean	0.080786721	0.216031
Variance	0.001549781	8.62E-05
Observations	3	3
Pooled Variance	0.000817987	
Hypothesized Mean Difference	0	
df	4	
t Stat	-5.791502237	
P(T<=t) one-tail	0.0022091	
t Critical one-tail	2.131846782	
P(T<=t) two-tail	0.004418201	
t Critical two-tail	2.776445105	

Angiotensin II NFATc2:Non-stimulated NFATc2

t-Test: Two-Sample Assuming Equal Variances

	Variable 1	*Variable 2*
Mean	0.131869	0.171493
Variance	0.001828	0.000415
Observations	3	3
Pooled Variance	0.001122	
Hypothesized Mean Difference	0	
df	4	
t Stat	-1.44902	
P(T<=t) one-tail	0.110459	
t Critical one-tail	2.131847	
P(T<=t) two-tail	0.220918	
t Critical two-tail	2.776445	

Angiotensin II NFATc2:Angiotensin II WT

t-Test: Two-Sample Assuming Equal Variances

	Variable 1	*Variable 2*

Mean	0.216031	0.171493
Variance	8.62E-05	0.000415
Observations	3	3
Pooled Variance	0.000251	
Hypothesized Mean Difference	0	
df	4	
t Stat	3.444901	
P(T<=t) one-tail	0.013088	
t Critical one-tail	2.131847	
P(T<=t) two-tail	0.026176	
t Critical two-tail	2.776445	

Appendix IV: Western Blot Quantification Data

	GATA-4:α-tubulin	
	Raw value	Normalized
Balbc	0.319205804	1
NN16-2	0.913907285	2.863066003
BalbC 1	0.196959459	1
N95-2	0.778585592	3.953024616
Balbc 2	0.293008413	1
N95-3	0.735336608	2.509609196

t-Test: Two-Sample Assuming Equal Variances

	Variable 1	*Variable 2*
Mean	1	3.108566605
Variance	0	0.566064928
Observations	3	3
Pooled Variance	0.283032464	
Hypothesized Mean Difference	0	
df	4	
t Stat	-4.854168274	
P(T<=t) one-tail	0.004157147	
t Critical one-tail	2.131846782	
P(T<=t) two-tail	0.008314293	
t Critical two-tail	2.776445105	

	GATA-4:GAPDH		GATA-4:Histone H3	
	Cytoplasmic		Nuclear	
	Raw Data	Normalized	Raw Data	Normalized
Balbc	0.37623	1	1.850746	1
NN20-1	0.543422	1.44438774	3.200535	1.729321582
BalbC 53	0.887	1	1.629	1
N95-2	0.729	0.82187148	2.952	1.812154696
Balbc 52	1.006	1	1.715	1
N95-3	0.66	0.65606362	2.659	1.550437318

Cytoplasmic Fraction
t-Test: Two-Sample Assuming Equal Variances

	Variable 1	*Variable 2*
Mean	1	0.97410761
Variance	0	0.17274561
Observations	3	3
Pooled Variance	0.086373	
Hypothesized Mean Difference	0	
df	4	
t Stat	0.107902	
P(T<=t) one-tail	0.459635	
t Critical one-tail	2.131846	
P(T<=t) two-tail	0.919269	
t Critical two-tail	2.776451	

Nuclear Fraction
t-Test: Two-Sample Assuming Equal Variances

	Variable 1	*Variable 2*
Mean	1	1.697304532
Variance	0	0.017892815
Observations	3	3
Pooled Variance	0.008946	
Hypothesized Mean Difference	0	
df	4	
t Stat	-9.02909	
P(T<=t) one-tail	0.000417	
t Critical one-tail	2.131846	
P(T<=t) two-tail	0.000833	
t Critical two-tail	2.776451	

	GSK3-β:α-tubulin	
	Raw value	Normalized
Balbc	1.082	1
N112-1	0.9054	0.836783734
BalbC 1	1.197	1
N95-2	0.8714	0.727986633
Balbc 2	1.327	1
N95-3	0.9843	0.741748304

t-Test: Two-Sample Assuming Equal Variances

	Variable 1	*Variable 2*
Mean	1	0.768839557
Variance	0	0.003509654
Observations	3	3
Pooled Variance	0.001754827	
Hypothesized Mean Difference	0	
df	4	
t Stat	6.758370206	
P(T<=t) one-tail	0.001249919	
t Critical one-tail	2.131846486	
P(T<=t) two-tail	0.002499838	
t Critical two-tail	2.776450856	

	JNK-2:α-tubulin	
	Raw value	Normalized
X6-1	0.21298	1
N112-2	0.254912	1.19688538
BalbC	0.215696	1
N99-1	0.291164	1.34987925
Balbc 2	0.208732	1
N95-3	0.121924	0.58411706

t-Test: Two-Sample Assuming Equal Variances

	Variable 1	*Variable 2*
Mean	1	1.04362723
Variance	0	0.16421398
Observations	3	3
Pooled Variance	0.082107	
Hypothesized Mean Difference	0	
df	4	
t Stat	-0.18647	
P(T<=t) one-tail	0.430575	
t Critical one-tail	2.131846	
P(T<=t) two-tail	0.86115	
t Critical two-tail	2.776451	

	ERK1/2:α-tubulin	
	Raw value	Normalized
X6-1	1.87717	1
N112-2	1.832464	0.97618479
BalbC	2.111832	1
N99-1	2.735373	1.295260691
Balbc 2	3.077399	1
N95-3	2.187417	0.710800422

t-Test: Two-Sample Assuming Equal Variances

	Variable 1	*Variable 2*
Mean	1	0.994081968
Variance	0	0.085638683
Observations	3	3
Pooled Variance	0.042819	
Hypothesized Mean Difference	0	
df	4	
t Stat	0.035027	
P(T<=t) one-tail	0.486868	
t Critical one-tail	2.131846	
P(T<=t) two-tail	0.973736	
t Critical two-tail	2.776451	

	p38-α:α-tubulin	
	Raw value	Normalized
X6-1	0.575434	1
N112-2	0.766076	1.331301
BalbC	1.178626	1
N99-1	1.780998	1.51108
Balbc 2	0.766254	1
N95-3	0.724368	0.945336

t-Test: Two-Sample Assuming Equal Variances

	Variable 1	*Variable 2*
Mean	1	1.262572
Variance	0	0.083559
Observations	3	3
Pooled Variance	0.04178	
Hypothesized Mean Difference	0	
df	4	
t Stat	-1.5733	
P(T<=t) one-tail	0.095379	

t Critical one-tail	2.131846
P(T<=t) two-tail	0.190758
t Critical two-tail	2.776451

GATA-4:α-tubulin					
Non-stimulated			Angiotensin II		
	Raw Data	Normalized		Raw Data	Normalized
Balbc	0.212496227	1	BalbC-4	0.305983	1.439947507
N99-1	0.378378378	1.780635749	N120-1	0.37082	1.745064735
Balbc	1.136585366	1	BalbC-2	1.200784	1.056484053
N112-2	1.807860262	1.590606668	N121-1	0.874057	0.769020385

Non-stimulated NFATc2:Non-stimulated WT

t-Test: Two-Sample Assuming Equal Variances

	Variable 1	*Variable 2*
Mean	1	1.09311932
Variance	0	1.021709228
Observations	2	2
Pooled Variance	0.510854614	
Hypothesized Mean Difference	0	
df	2	
t Stat	-0.130284016	
P(T<=t) one-tail	0.454131874	
t Critical one-tail	2.91998558	
P(T<=t) two-tail	0.908263748	
t Critical two-tail	4.30265273	

Angiotensin II WT:Non-stimulated WT

t-Test: Two-Sample Assuming Equal Variances

	Variable 1	*Variable 2*
Mean	1	1.24821578
Variance	0	0.07352211
Observations	2	2
Pooled Variance	0.036761	
Hypothesized Mean Difference	0	
df	2	
t Stat	-1.2946	
P(T<=t) one-tail	0.162388	
t Critical one-tail	2.919986	
P(T<=t) two-tail	0.324775	
t Critical two-tail	4.302653	

Angiotensin II NFATc2:Non-stimulated NFATc2
t-Test: Two-Sample Assuming Equal Variances

	Variable 1	*Variable 2*
Mean	1.685621	1.25704256
Variance	0.018056	0.476331287
Observations	2	2
Pooled Variance	0.247193	
Hypothesized Mean Difference	0	
df	2	
t Stat	0.86201	
P(T<=t) one-tail	0.239766	
t Critical one-tail	2.919986	
P(T<=t) two-tail	0.479532	
t Critical two-tail	4.302653	

Angiotensin II NFATc2:Angiotensin II WT
t-Test: Two-Sample Assuming Equal Variances

	Variable 1	*Variable 2*
Mean	1.248216	1.257043
Variance	0.073522	0.476331
Observations	2	2
Pooled Variance	0.274927	
Hypothesized Mean Difference	0	
df	2	
t Stat	-0.01683	
P(T<=t) one-tail	0.494049	
t Critical one-tail	2.919986	
P(T<=t) two-tail	0.988097	
t Critical two-tail	4.302653	

pAKT(Ser473):Total AKT					
Non-stimulated			**Angiotensin II**		
	Raw Data	Normalized		Raw Data	Normalized
Balbc	0.201530612	1	BalbC-4	0.430414	2.135725764
N99-1	0.53298153	2.644667847	N120-1	0.238964	1.185745897
Balbc	0.296714076	1	BalbC-2	0.524614	1.768078911
N112-2	0.308714919	1.040445817	N121-1	0.243146	0.819462531

Non-stimulated NFATc2:Non-stimulated WT
t-Test: Two-Sample Assuming Equal Variances

	Variable 1	*Variable 2*

Mean	1	1.842556832
Variance	0	1.28676416
Observations	2	2
Pooled Variance	0.64338208	
Hypothesized Mean Difference	0	
df	2	
t Stat	-1.050424214	
P(T<=t) one-tail	0.201862587	
t Critical one-tail	2.91998558	
P(T<=t) two-tail	0.403725174	
t Critical two-tail	4.30265273	

Angiotensin II WT:Non-stimulated WT

t-Test: Two-Sample Assuming Equal Variances

	Variable 1	*Variable 2*
Mean	1	1.95190234
Variance	0	0.0675821
Observations	2	2
Pooled Variance	0.033791	
Hypothesized Mean Difference	0	
df	2	
t Stat	-5.17835	
P(T<=t) one-tail	0.017664	
t Critical one-tail	2.919986	
P(T<=t) two-tail	0.035328	
t Critical two-tail	4.302653	

Angiotensin II NFATc2:Non-stimulated NFATc2

t-Test: Two-Sample Assuming Equal Variances

	Variable 1	*Variable 2*
Mean	1.842557	1.002604214
Variance	1.286764	0.067081752
Observations	2	2
Pooled Variance	0.676923	
Hypothesized Mean Difference	0	
df	2	
t Stat	1.020905	
P(T<=t) one-tail	0.207344	
t Critical one-tail	2.919986	
P(T<=t) two-tail	0.414687	
t Critical two-tail	4.302653	

Angiotensin II NFATc2:Angiotensin II WT
t-Test: Two-Sample Assuming Equal Variances

	Variable 1	*Variable 2*
Mean	1.951902	1.002604
Variance	0.067582	0.067082
Observations	2	2
Pooled Variance	0.067332	
Hypothesized Mean Difference	0	
df	2	
t Stat	3.658408	
P(T<=t) one-tail	0.033633	
t Critical one-tail	2.919986	
P(T<=t) two-tail	0.067265	
t Critical two-tail	4.302653	

peIF2α(Ser51):Total eIF2α					
Non-stimulated			**Angiotensin II**		
	Raw Data	Normalized		Raw Data	Normalized
Balbc	0.113463447	1	BalbC-4	0.120616	1.063041613
N99-1	0.202443857	1.784220935	N120-1	0.130468	1.149867722
Balbc	0.492985002	1	BalbC-2	0.23	0.466545633
N112-2	0.406464251	0.824496179	N121-1	0.17967	0.36445311

Non-stimulated NFATc2:Non-stimulated WT
t-Test: Two-Sample Assuming Equal Variances

	Variable 1	*Variable 2*
Mean	1	1.304358557
Variance	0	0.460535804
Observations	2	2
Pooled Variance	0.230267902	
Hypothesized Mean Difference	0	
df	2	
t Stat	-0.634262178	
P(T<=t) one-tail	0.295390292	
t Critical one-tail	2.91998558	
P(T<=t) two-tail	0.590780583	
t Critical two-tail	4.30265273	

Angiotensin II WT:Non-stimulated WT
t-Test: Two-Sample Assuming Equal Variances

	Variable 1	*Variable 2*

Mean	1	0.76479362
Variance	0	0.17790373
Observations	2	2
Pooled Variance	0.088952	
Hypothesized Mean Difference	0	
df	2	
t Stat	0.788627	
P(T<=t) one-tail	0.256482	
t Critical one-tail	2.919986	
P(T<=t) two-tail	0.512964	
t Critical two-tail	4.302653	

Angiotensin II NFATc2:Non-stimulated NFATc2

t-Test: Two-Sample Assuming Equal Variances

	Variable 1	*Variable 2*
Mean	1.304359	0.757160416
Variance	0.460536	0.308438056
Observations	2	2
Pooled Variance	0.384487	
Hypothesized Mean Difference	0	
df	2	
t Stat	0.882478	
P(T<=t) one-tail	0.235304	
t Critical one-tail	2.919986	
P(T<=t) two-tail	0.470608	
t Critical two-tail	4.302653	

Angiotensin II NFATc2:Angiotensin II WT

t-Test: Two-Sample Assuming Equal Variances

	Variable 1	*Variable 2*
Mean	0.764794	0.75716
Variance	0.177904	0.308438
Observations	2	2
Pooled Variance	0.243171	
Hypothesized Mean Difference	0	
df	2	
t Stat	0.015479	
P(T<=t) one-tail	0.494528	
t Critical one-tail	2.919986	
P(T<=t) two-tail	0.989055	
t Critical two-tail	4.302653	

Appendix V: Immunofluorescene Data

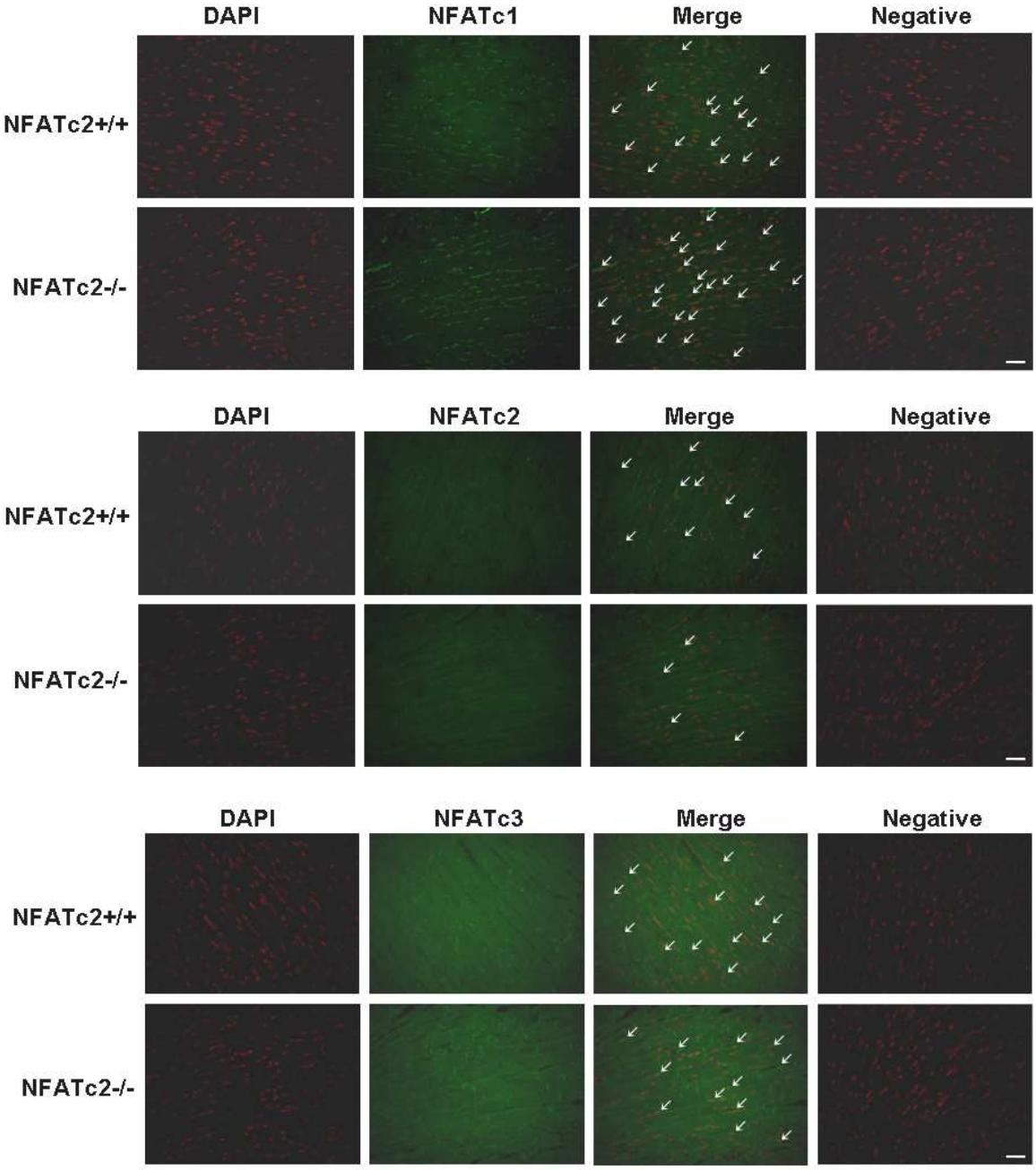

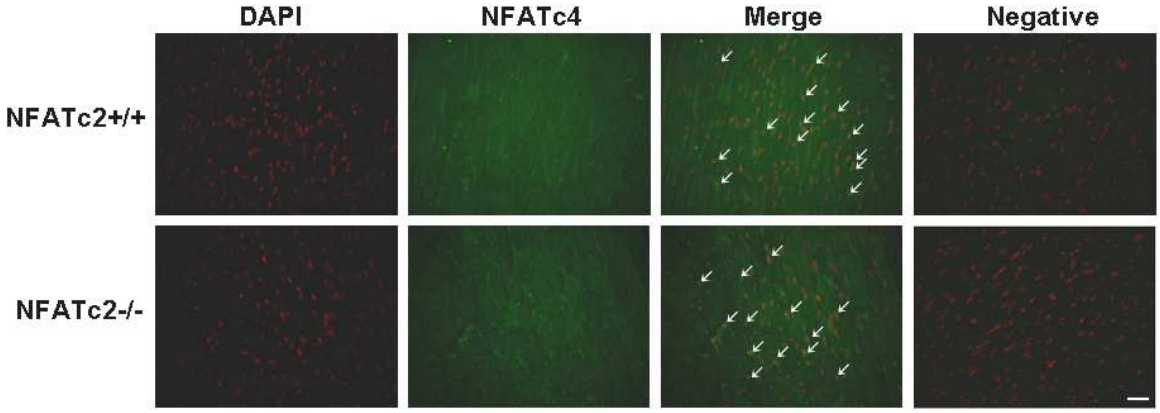

	NFATc1
	Positive Nuclei/Total Nuclei (%)
X8-1	13.9
N117-2	22.9
X8-2	14.3
N117-3	21.3
X7-1	14.9
N119-1	21.8

t-Test: Two-Sample Assuming Equal Variances

	Variable 1	*Variable 2*
Mean	14.36666667	22
Variance	0.253333333	0.67
Observations	3	3
Pooled Variance	0.461666667	
Hypothesized Mean Difference	0	
df	4	
t Stat	-13.75927649	
P(T<=t) one-tail	8.08348E-05	
t Critical one-tail	2.131846486	
P(T<=t) two-tail	0.00016167	
t Critical two-tail	2.776450856	

	NFATc2
	Positive Nuclei/Total Nuclei (%)
X8-1	7.16
N117-2	2.74
X8-2	8.72
N117-3	4.87
X7-1	8.54
N119-1	5.17

t-Test: Two-Sample Assuming Equal Variances

	Variable 1	*Variable 2*
Mean	8.14	4.26
Variance	0.7284	1.7553
Observations	3	3
Pooled Variance	1.24185	
Hypothesized Mean Difference	0	
df	4	
t Stat	4.264251239	
P(T<=t) one-tail	0.006504748	
t Critical one-tail	2.131846486	
P(T<=t) two-tail	0.013009496	
t Critical two-tail	2.776450856	

	NFATc3
	Positive Nuclei/Total Nuclei (%)
X8-1	10.5
N117-2	12.3
X8-2	9.46
N117-3	7.06
X7-1	10.4
N119-1	9.97

t-Test: Two-Sample Assuming Equal Variances

	Variable 1	*Variable 2*
Mean	10.12	9.776667
Variance	0.3292	6.892433
Observations	3	3
Pooled Variance	3.610816667	
Hypothesized Mean Difference	0	
df	4	
t Stat	0.221288518	
P(T<=t) one-tail	0.417852642	
t Critical one-tail	2.131846486	
P(T<=t) two-tail	0.835705284	
t Critical two-tail	2.776450856	

	NFATc4
	Positive Nuclei/Total Nuclei (%)
X8-1	13.4
N117-2	13.9
X8-2	9.5
N117-3	9.35
X7-1	9.03
N119-1	8.43

t-Test: Two-Sample Assuming Equal Variances

	Variable 1	*Variable 2*
Mean	10.64333333	10.56
Variance	5.754633333	8.5783
Observations	3	3
Pooled Variance	7.166466667	
Hypothesized Mean Difference	0	
df	4	
t Stat	0.038125175	
P(T<=t) one-tail	0.485707387	
t Critical one-tail	2.131846486	
P(T<=t) two-tail	0.971414775	
t Critical two-tail	2.776450856	

Appendix VI: Heart Histology Data

	Left Ventricle Inner Chamber Diameter: Total Heart Diameter
X8-1	0. 440678
N117-2	0. 62931
X8-2	0. 42029
N117-3	0. 555556
X7-1	0. 511278
N119-1	0. 575221

t-Test: Two-Sample Assuming Equal Variances

	Variable 1	*Variable 2*
Mean	0.457415	0.586696
Variance	0.00228	0.001459
Observations	3	3
Pooled Variance	0.001869	
Hypothesized Mean Difference	0	
df	4	
t Stat	-3.66221	
P(T<=t) one-tail	0.010769	
t Critical one-tail	2.131847	
P(T<=t) two-tail	0.021538	
t Critical two-tail	2.776445	

	Right Ventricular Wall Diameter: Total Heart Diameter
X8-1	0. 152542
N117-2	0. 068966
X8-2	0. 086957
N117-3	0. 083333
X7-1	0. 105263
N119-1	0. 106195

t-Test: Two-Sample Assuming Equal Variances

	Variable 1	*Variable 2*
Mean	0.114921	0.086165
Variance	0.001145	0.000353
Observations	3	3
Pooled Variance	0.000749	
Hypothesized Mean Difference	0	
df	4	
t Stat	1.286941	

P(T<=t) one-tail	0.13377
t Critical one-tail	2.131847
P(T<=t) two-tail	0.26754
t Critical two-tail	2.776445